

NATIONAL TAIWAN UNIVERSITY

&

UNIVERSITY OF PADOVA

DOUBLE MASTER'S THESIS

---

# Scheduling for MU-MIMO using Hybrid Beamforming based on DPC

---

*Candidate:*

Alessandro Traspadini

*Supervisors:*

Prof. Hsuan-Jung Su

Prof. Michele Zorzi

*Master of Science of the Graduate Institute of Communication Engineering (NTU)*

*Master of Science in ICT for Internet and Multimedia (UNIPD)*

ACADEMIC YEAR 2020 - 2021



國立臺灣大學碩士學位論文  
口試委員會審定書

Master Thesis Certification by Oral Defense Committee  
National Taiwan University

論文中文題目

基於驕紙編碼之多用戶多天線混合波束成形系統之排程設計

論文英文題目

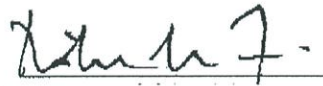
SCHEDULING FOR MU-MIMO USING HYBRID BEAMFORMING BASED ON DPC

本論文係 ALESSANDRO TRASPADINI 君 (學號 R09942152) 在國立臺灣大學電信工程學研究所完成之碩(博)士學位論文，於民國 110 年 08 月 26 日承下列考試委員審查通過及口試及格，特此證明

This is to certify that the Master thesis above is completed by ALESSANDRO TRASPADINI (ID R09942152) during his studying in Graduate Institute of Communication Engineering at National Taiwan University, and that the oral defense of this thesis is passed on 26/08/2021 in accordance with decision of following committee members:

口試委員 Committee members :





指導教授/Advisor(s)



系主任、所長(Department Chair/Program Director)





NATIONAL TAIWAN UNIVERSITY

# *Abstract*

College of Electrical Engineering & Computer Science  
Graduate Institute of Communication Engineering

Master of Science in the Graduate Institute of Communication Engineering

## **Scheduling for MU-MIMO using Hybrid Beamforming based on DPC**

by Alessandro Traspadini

Future wireless networks will require to transfer much greater amount of data at much higher speed. To deal with this fast-increasing demand of higher data rate and low latency, the carrier frequency needs to be increased in order to expand the bandwidth available for the transmissions. This is the reason why wireless communications are moving towards mmWave (5G) and even TeraHertz (6G) frequency bands.

Increasing the carrier frequency will provide a wider bandwidth, nevertheless an optimal PHY layer scheme is necessary to increase the spectral efficiency.

These promising technologies however come at a cost, the higher frequency yields limitations on the propagations of the signals in the environment.

To address this problem, highly directional beamforming is exploited to increase the antennas' gain.

This thesis will propose a solution for the scheduling of MU-MIMO system by employing Hybrid Beamforming based on Dirty Paper Coding.

The Hybrid precoder consists of a digital baseband precoder and an analog RF precoder, in this way it reduces the hardware complexity and the power consumption.



# Contents

<b>Abstract</b>	<b>iii</b>
<b>1 Introduction</b>	<b>1</b>
1.1 mmWave . . . . .	1
1.2 MU-MIMO . . . . .	2
<b>2 System Model</b>	<b>5</b>
2.1 MU-MIMO System . . . . .	5
2.2 mmWave Propagation . . . . .	6
2.3 Channel Model . . . . .	8
2.3.1 Uniform Spaced Linear Array . . . . .	9
2.3.2 Uniform Planar Array . . . . .	10
<b>3 MU-MIMO Scheduling</b>	<b>13</b>
3.1 Users's Scheduling procedure . . . . .	13
3.2 Zero-Forcing Coding . . . . .	15
3.2.1 Optimal power allocation . . . . .	18
3.2.2 ZF Algorithm . . . . .	19
3.2.3 Uniform Power allocation . . . . .	20
3.2.4 Comparison between optimal and uniform power allocation	23
3.2.5 Performance employing a users' set with different size . . . .	24
<b>4 Dirty Paper Coding</b>	<b>27</b>
4.1 ZF-DPC Scheme . . . . .	27
4.1.1 Inner Encoder . . . . .	29
Waterfilling . . . . .	30
4.1.2 Outer Encoder . . . . .	31
Tomlinson-Harashima Precoding . . . . .	33
4.2 Capacity of Broadcast Channel . . . . .	35
4.3 MU-DPC Algorithm . . . . .	39
4.4 Comparison between MU-DPC and MU-ZF . . . . .	40

<b>5</b>	<b>Hybrid Beamforming</b>	<b>47</b>
5.1	Analog Beamforming . . . . .	47
5.2	Digital Beamforming . . . . .	48
5.3	Hybrid Beamforming . . . . .	49
5.3.1	Analog Precoder Design . . . . .	52
	Initialization Phase . . . . .	53
	Stream Selection Phase . . . . .	54
5.4	Scheduling MU-DPC Hybrid . . . . .	55
5.4.1	Users' selection . . . . .	55
5.4.2	Analog Precoder Design . . . . .	56
5.4.3	Inner Precoder Design . . . . .	56
5.4.4	Outer Precoder Design . . . . .	57
5.5	MATLAB Code . . . . .	57
<b>6</b>	<b>Results and Simulations</b>	<b>63</b>
6.1	Comparison among different channels . . . . .	63
6.2	Comparison among different numbers of RF chains . . . . .	64
6.3	Comparison between HB and fully DB . . . . .	65
<b>7</b>	<b>Conclusions and Future Developments</b>	<b>73</b>
<b>A</b>	<b>Review of Algebra</b>	<b>75</b>
A.1	Determinant properties . . . . .	75
A.1.1	Basic properties . . . . .	75
A.2	Trace properties . . . . .	76
A.2.1	Basic properties . . . . .	76
	<b>Bibliography</b>	<b>79</b>



# List of Figures

1.1	Global mobile data traffic (EB per month), without including traffic generated by fixed wireless access (FWA) services [9] . . . . .	1
1.2	An illustration of MU-MIMO downlink [23] . . . . .	3
2.1	Comparison of distance-based path loss models [1] . . . . .	8
2.2	A uniform spaced linear array [27] . . . . .	9
2.3	Geometry of a planar array [27] . . . . .	11
3.1	Multi-user MIMO system [5] . . . . .	14
3.2	Comparison between optimal and uniform power allocation (Total-Rate) . . . . .	23
3.3	Comparison between optimal and uniform power allocation (Number of selected users) . . . . .	24
3.4	Comparison of total rate with different users' set . . . . .	25
3.5	Comparison of total number of selected users with different users' set . . . . .	25
4.1	DPC scheme of the outer encoder and the inner encoder [17] . . . . .	28
4.2	Optimal power allocation for problem 4.8a: Waterfilling scheme [10] . . . . .	32
4.3	Constellation of 16-QAM [5] . . . . .	34
4.4	The four channels, multiple access, broadcast, and their corresponding point-to-point channels, depicted along with the relationship between their capacities. [25] . . . . .	38
4.5	Comparison of the total achievable rate between DPC and ZF (64 available users and 64 antennas) . . . . .	42
4.6	Comparison of number of selected users between DPC and ZF (64 available users and 64 antennas) . . . . .	42
4.7	Comparison of the total achievable rate between DPC and ZF (100 available users and 64 antennas) . . . . .	43
4.8	Comparison of number of selected users between DPC and ZF (100 available users and 64 antennas) . . . . .	43
4.9	Comparison of the total achievable rate between DPC and ZF (1000 available users and 64 antennas) . . . . .	44

4.10	Comparison of number of selected users between DPC and ZF (1000 available users and 64 antennas) . . . . .	44
4.11	Comparison of the total achievable rate between DPC and ZF (100 available users and 32 antennas) . . . . .	45
4.12	Comparison of number of selected users between DPC and ZF (100 available users and 32 antennas) . . . . .	45
5.1	Analog Beamforming architecture [3] . . . . .	48
5.2	Digital Beamforming architecture [3] . . . . .	49
5.3	Hybrid Beamforming architecture [3] . . . . .	50
6.1	Comparison of the achievable rate between ZF and DPC in different scenarios using ULA ( $N_t^{RF} = 16, N_t = 64, N_u = 100$ ). . . . .	66
6.2	Comparison of the number of selected users between ZF and DPC in different scenarios using ULA ( $N_t^{RF} = 16, N_t = 64, N_u = 100$ ). . . . .	66
6.3	Comparison of the achievable rate between ZF and DPC in different scenarios using UPA ( $N_t^{RF} = 16, N_t = 64, N_u = 100$ ). . . . .	67
6.4	Comparison of the number of selected users between ZF and DPC in different scenarios using UPA ( $N_t^{RF} = 16, N_t = 64, N_u = 100$ ). . . . .	67
6.5	Comparison of the total achievable rate among DPC systems with a different number of RF chains using ULA ( $N_t = 64, N_u = 100$ ) . . . . .	68
6.6	Comparison of the number of selected users among DPC systems with a different number of RF chains using ULA ( $N_t = 64, N_u = 100$ ) . . . . .	68
6.7	Comparison of the total achievable rate between DPC and ZF with a different number of RF chains using ULA ( $N_t = 64, N_u = 100$ ) . . . . .	69
6.8	Comparison of the number of selected users between DPC and ZF with a different number of RF chains using ULA ( $N_t = 64, N_u = 100$ ) . . . . .	69
6.9	Comparison of the total achievable rate between digital and hybrid beamforming using ULA ( $N_t^{RF} = 8, N_u = 100$ ) . . . . .	70
6.10	Comparison of the number of selected users between digital and hybrid beamforming using ULA ( $N_t^{RF} = 8, N_u = 100$ ) . . . . .	70
6.11	Comparison of the total achievable rate between digital and hybrid beamforming using ULA ( $N_t^{RF} = 12, N_u = 100$ ) . . . . .	71
6.12	Comparison of the number of selected users between digital and hybrid beamforming using ULA ( $N_t^{RF} = 12, N_u = 100$ ) . . . . .	71
6.13	Comparison of the total achievable rate between digital and hybrid beamforming using ULA ( $N_t^{RF} = 20, N_u = 100$ ) . . . . .	72
6.14	Comparison of the number of selected users between digital and hybrid beamforming using ULA ( $N_t^{RF} = 20, N_u = 100$ ) . . . . .	72

# List of Abbreviations

<b>ULA</b>	<b>Uniform Linear Array</b>
<b>UPA</b>	<b>Uniform Planar Array</b>
<b>HB</b>	<b>Hybrid Beamforming</b>
<b>DB</b>	<b>Digital Beamforming</b>
<b>AB</b>	<b>Analog Beamforming</b>
<b>BS</b>	<b>Base Station</b>
<b>ZF</b>	<b>Zero Forcing</b>
<b>AoA</b>	<b>Angle of Arrival</b>
<b>AoD</b>	<b>Angle of Departure</b>
<b>CSI</b>	<b>Channel State Information</b>
<b>DPC</b>	<b>Dirty Paper Coding</b>
<b>SNR</b>	<b>Signal to Noise Ratio</b>
<b>SINR</b>	<b>Signal to Interference plus Noise Ratio</b>
<b>RF</b>	<b>Radio Frequency</b>
<b>DAC</b>	<b>Digital to Analog Converter</b>
<b>ADC</b>	<b>Analog to Digital Converter</b>
<b>MISO</b>	<b>Multiple Input Single Output</b>
<b>MISO</b>	<b>Multiple Input Multiple Output</b>
<b>MU-MIMO</b>	<b>Multiple Users Multiple Input Multiple Output</b>
<b>MU-DPC</b>	<b>Multiple Users Dirty Paper Coding</b>
<b>MU-ZF</b>	<b>Multiple Users Zero Forcing</b>
<b>ZF-DPC</b>	<b>Zero Forcing Dirty Paper Coding</b>
<b>gZF-DPC</b>	<b>greedy Zero Forcing Dirty Paper Coding</b>



# Chapter 1

## Introduction

### 1.1 mmWave

As described in the latest Ericsson's report [9], global total mobile data traffic is estimated to grow by a factor 4.5, to reach 226 EB (Exabyte) per month in 2026. Smartphones generate most of the mobile data traffic, around 95%.

To deal with this fast-increasing demand of higher data rate and low latency, the carrier frequency needs to be increased in order to expand the bandwidth available for the transmissions. This is the reason why next generation of wireless networks will adopt mmWave frequency.

The bandwidth's increase will offer high-capacity transmissions that eventually will lead to a data-rate greater than a Gbps indeed, in 2026, 5G will account for an estimated 54 percent of total mobile data, as shown in figure 1.1 [9].

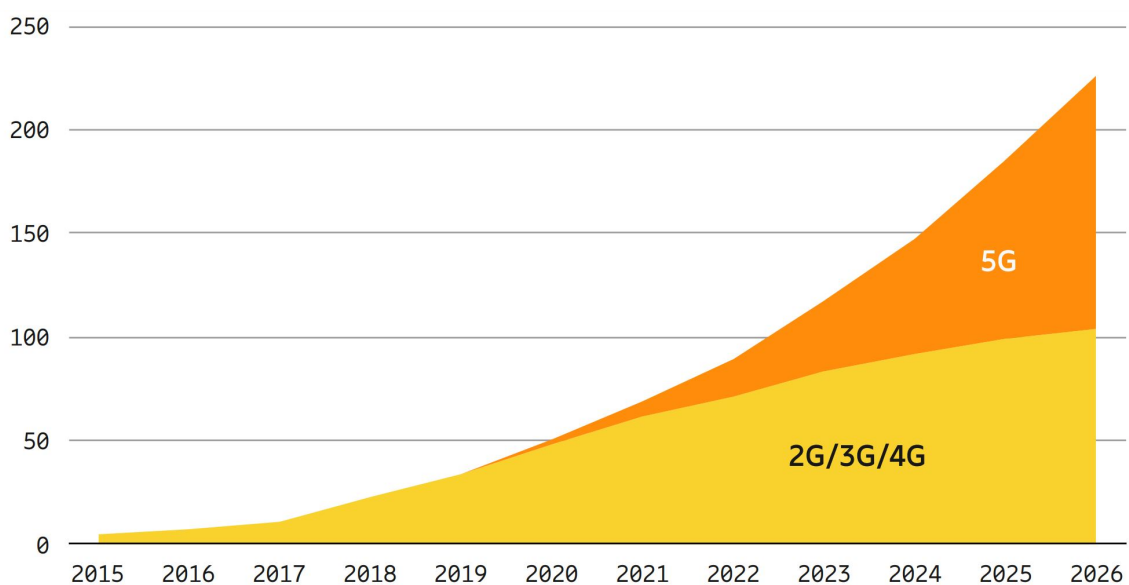


FIGURE 1.1: Global mobile data traffic (EB per month), without including traffic generated by fixed wireless access (FWA) services [9]

Despite the potential provided by a wider bandwidth, mmWave signals suffer from

many transmissions issue such as severe path loss and higher sensitivity to blockage due to the shorter wavelength.

This implies having harsh performance in term of SNR at the receiver. To overcome this problem, antennas with multiple active elements are required to increase the gain of the signal. The size of these antenna arrays can be tiny since the optimal antenna length decreases as the frequency increases.

Thus, it is possible to pack many antennas into small form factors (essential for user equipment).

Nowadays, within the global wireless mmWave band of 60 GHz, there is 7 GHz of bandwidth available, despite this wide bandwidth, data rates on the order of 100 Gbps can only be achieved with a spectral efficiency of at least 14 bit/s/Hz. [21]

Increasing the carrier frequency to mmWave will provide a larger bandwidth, nevertheless an optimal PHY layer scheme is necessary to increase the spectral efficiency. The higher frequency yields limitations on the propagations of the signals in the environment: the path-loss is higher (compared to sub 6GHz), and the number of scatterers is limited.

## 1.2 MU-MIMO

In a cellular network there are two communication problems to consider: the up-link, where a group of users transmits data to the same base station, and the down-link, where the base station transmits signals to multiple users. [23]

In this thesis the downlink's problem is investigated. Complete knowledge of the channel at the transmitter side is assumed, thus the base station is aware of the interference that is going to be observed by all the available users, hence efficient algorithms to optimally select the users can be analyzed.

Because of mmWave, the large number of antennas required to increase the gain of the transmission generates very narrow beams, hence spatial multiplexing can be exploited.

Nevertheless, it is also a hardware constraint that limits the use of fully digital precoding: many hardware components would be needed, including signal mixers, analog-to-digital/digital-to-analog converters (ADCs/DACs), and power amplifiers.

Having one RF chain for each antenna element means prohibitive cost and power consumption, and thus is not feasible.

A promising technology is the so-called Hybrid Beamforming: it consists of a digital baseband precoder and an analog RF precoder, in this way it reduces the hardware complexity and the power consumption. [12]

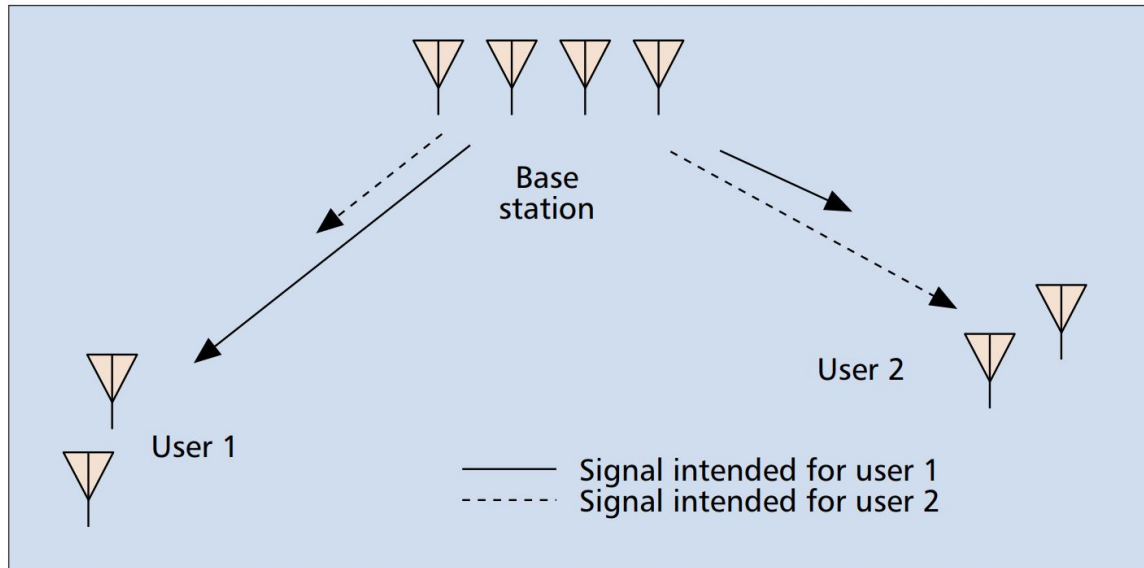


FIGURE 1.2: An illustration of MU-MIMO downlink [23]

This system limits the number of RF chains, nevertheless multiplexing beamforming is still exploited since it does not use only one RF chain as an analog precoder, hence many beams can be transmitted to point towards different directions.

The main scope of this thesis is to show the benefit of using Dirty Paper Coding for the Hybrid Beamforming and to evaluate the conditions in which it achieves higher capacity than the traditional Zero Forcing scheme.

In [4], the optimality of Dirty Paper Coding in achieving the sum capacity is shown, hence, by exploiting this precoding scheme, an algorithm for the users' scheduling with higher total achievable rate than the general rate-maximization algorithm based on ZF can be derived.

This thesis consists of the following chapters:

- Chapter 2 describes the mmWave MU-MIMO system model
- Chapter 3 introduces the problem of Scheduling
- Chapter 4 analyzes the idea of Dirty Paper Coding
- Chapter 5 describes the Hybrid Beamforming scheme and how it can be implemented using the Dirty Paper Coding approach
- Chapter 6 shows results of the simulations
- Chapter 7 defines the conclusions and explains possible future directions on this topic.





## Chapter 2

# System Model

### 2.1 MU-MIMO System

A MU-MIMO system refers to the system in which a base station communicates with many users at the same time.

The considered model consists of a transmitter with an array of  $N_t$  antennas and  $N_u$  users with only one antenna.

The baseband input-output relationship can be expressed as:

$$\mathbf{y} = \begin{bmatrix} y_1(t) \\ y_2(t) \\ \vdots \\ y_k(t) \\ \vdots \\ y_{N_u}(t) \end{bmatrix} = \mathbf{H}(t) * \mathbf{x}(t) + \mathbf{n}(t) \quad (2.1)$$

where  $y_k(t)$  is the received by signal by the k-th user,  $\mathbf{H}$  is the  $N_u \times N_t$  matrix that corresponds to the channel impulse response,  $\mathbf{x}$  is the transmitted vector,  $\mathbf{n}$  is the additive gaussian noise with zero mean and variance  $\sigma_w^2$  and the symbol  $*$  denotes the convolution.

For simplicity, in this thesis the frequency flat fading channel is considered and, therefore, the channel has the same response over the entire bandwidth, hence the input-output relationship becomes:

$$\begin{bmatrix} y_1 \\ y_2 \\ \vdots \\ y_{N_u} \end{bmatrix} = \begin{bmatrix} \cdots & \mathbf{h}_1 & \cdots \\ \cdots & \mathbf{h}_2 & \cdots \\ \vdots & \vdots & \vdots \\ \cdots & \mathbf{h}_{N_u} & \cdots \end{bmatrix} \begin{bmatrix} x_1 \\ x_2 \\ \vdots \\ x_{N_u} \end{bmatrix} + \begin{bmatrix} n_1 \\ n_2 \\ \vdots \\ n_{N_u} \end{bmatrix} \quad (2.2)$$

where  $\mathbf{h}_i$  denotes the narrowband MISO channel vector between the transmitter and the user  $i$ , thus the element  $h_{ij}$  represents the complex gain from the transmitter antenna  $i$  and the user  $j$ .

A digital precoder  $\mathbf{B}$  can be exploited to remove the interference received by users, the precoding matrix can be expressed as:

$$\mathbf{B} = \begin{bmatrix} \vdots & \vdots & \vdots & \vdots \\ \mathbf{B}_1 & \mathbf{B}_2 & \cdots & \mathbf{B}_{N_u} \\ \vdots & \vdots & \vdots & \vdots \end{bmatrix}$$

where the vector  $\mathbf{B}_i$  is the precoding signal for the user  $i$ , in this way, its received signal can be given as:

$$y_i = \mathbf{h}_i \mathbf{B}_i x_i + \sum_{k=1, k \neq i}^{N_u} \mathbf{h}_i \mathbf{B}_k x_k + n \quad (2.3)$$

The base station needs to find the best precoding matrix to maximize the capacity of the system, considering that the symbol vector has normalized power:  $E(\mathbf{x}\mathbf{x}^H) = \mathbf{I}$ , then in order to satisfy the total power constraint, the next inequality must hold:

$$\text{tr}(\mathbf{B}\mathbf{B}^H) \leq P_{TOT}$$

where  $P_{TOT}$  is the maximum available power at the transmitter.

The assumption of having the complete channel knowledge at the transmitter side enables precoding, indeed it depends on the channel matrix.

To estimate the channel, the base station usually transmits known pilot signals to the users, hence, they can estimate their own channel by comparing the received signal with the known transmitted pilot.

Then, this information is sent back to the transmitter. Since this procedure can be time-consuming and there could also be the problem of out-of-date of the CSIT, especially in fast time-varying scenarios, for instance the case of users in movement, hence it is better to use a different approach: assuming channel reciprocity, the estimation can be evaluated at the transmitter, using uplink pilots.

## 2.2 mmWave Propagation

Propagation's aspects of mmWave signals are extremely different compared to the Sub-6GHz band due to the small wavelength.

The relationship between the received power and the transmit power in free space

is given by the Friis' Law:

$$P_R = P_T G_T G_R \left( \frac{\lambda}{4\pi d} \right)^2 \quad (2.4)$$

where  $G_T$  and  $G_R$  refers respectively to the gain at the transmitter and at the receiver.  $d$  is the separation distance and the exponent 2 is related to the free space condition. Using isotropic antennas, the propagation of signals at higher frequency (shorter wavelength) will be worse compared to lower frequency signals, due to the path loss term.

The advantages is that because of the shorter wavelength, it is possible to pack much more antennas in the same space, providing higher directionality. Exploiting this property is necessary to overcome the severe path loss of mmWave.

As described in [12], the most common statistical model describes the average path loss via a linear model:

$$PL(d) = \alpha + 10\beta \log_{10}(d) + \zeta \quad (2.5)$$

the value is obtained in [dB],  $\alpha$  and  $\beta$  are linear model parameters, by considering the Friis' Law, the value  $\beta$  is equivalent to the exponent of the path loss term.  $\zeta$  is a lognormal term accounting for variances in shadowing.

Many studies, including measurements in New York City, has showed that for distances of up to 200m from a low power base station, the distance-based path loss in mmWave links is no worse than conventional cellular frequency after compensating for the beamforming gain. [12]

Those measurements in an urban scenario as NYC is a challenging condition because of the frequent lack of line-of-sight (LOS) connectivity, severe shadowing, as well as limitations on the height and placement of cells. [20]

In Figure 2.1, a comparison of the path loss at different frequencies, considering isotropic transmission. [1]

The standard 3GPP urban micro (UMi) path is given by:

$$PL(d) = 22.7 + 36.7 \log_{10}(d) + 26 \log_{10}(f_c)$$

where  $d$  is the distance between transmitter and receiver and  $f_c$  is the carrier frequency. [1]

Despite this beamforming solution, mmWave signals can be severely vulnerable to shadowing, resulting in outages and intermittent channel quality. [20]

For instance, materials such as brick can attenuate signals by as much as 40–80 dB and the human body itself can result in a 20–35-dB loss.

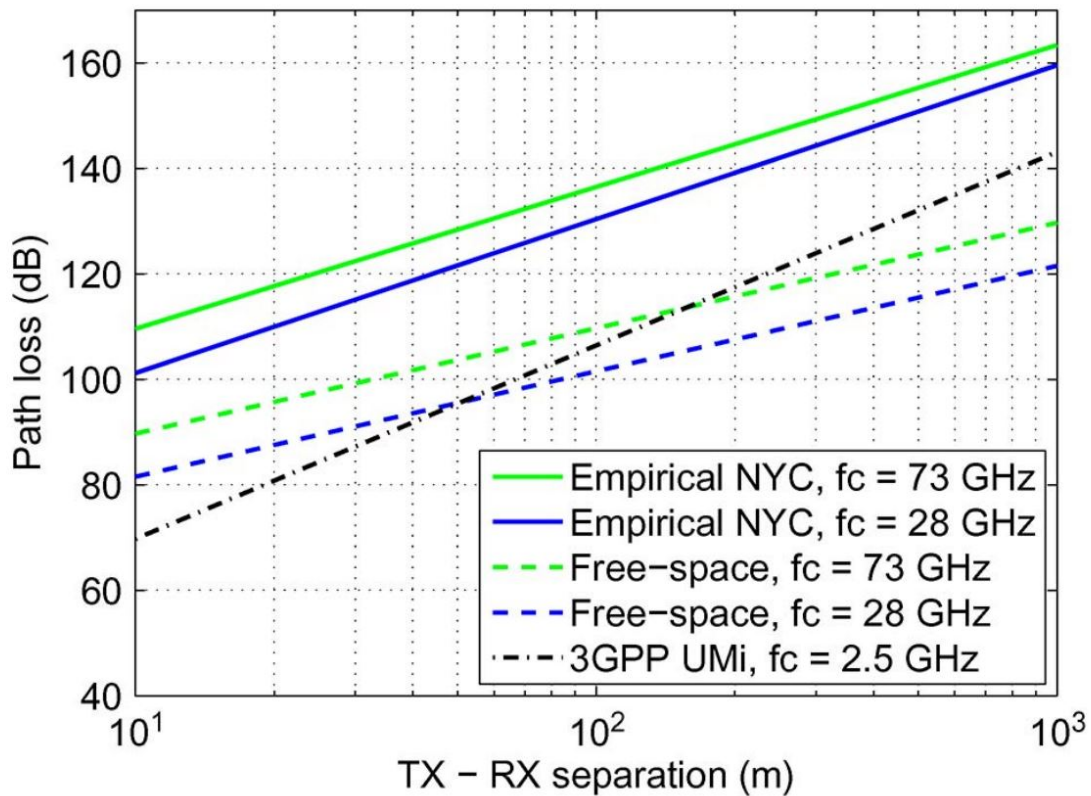


FIGURE 2.1: Comparison of distance-based path loss models [1]

On the other hand, humidity and rain fades (common problems for mmWave links) are not an issue in cellular systems, as shown in [19].

Also, the human body and many outdoor materials being very reflective allow them to be important scatterers for mmWave propagation, this enables coverage via NLOS paths for cellular systems.

To quantify the effect of blocking, a two-state probabilistic model (LOS and NLOS) or a three-state model (LOS, NLOS and signal outage) can be exploited.

The probability that a user is in one of those states depends on the distance. [12]

## 2.3 Channel Model

The mmWave MIMO system can be described using the standard multipath models used for lower frequencies. [12]

Path delays and Doppler shifts do not come into play due to the nonselective nature of the channel in time and frequency. [11]

### 2.3.1 Uniform Spaced Linear Array

A uniform linear array (ULA) is a set of  $N_t$  active elements along a unique direction. The space between two consecutive elements is uniform and it is denoted as  $d$ .

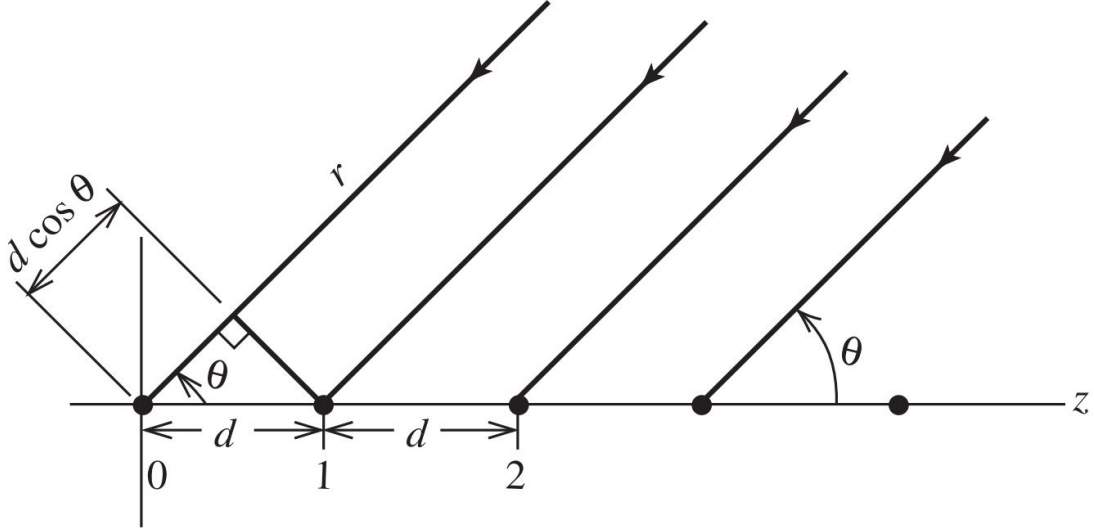


FIGURE 2.2: A uniform spaced linear array [27]

It enables 2D beamforming, the antenna arrays are described by their normalized antenna steering vectors that depends on the angle of arrival ( $\theta_R$ ) and the angle of departure ( $\theta_T$ ):

$$\begin{aligned} \mathbf{a}_T(\theta_T) &= \frac{1}{\sqrt{N_t}} \left[ 1, e^{j2\pi\phi_T}, e^{j4\pi\phi_T}, \dots, e^{j2\pi\phi_T(N_t-1)} \right]^T \\ \mathbf{a}_R(\theta_R) &= \frac{1}{\sqrt{N_r}} \left[ 1, e^{j2\pi\phi_R}, e^{j4\pi\phi_R}, \dots, e^{j2\pi\phi_R(N_r-1)} \right]^T \end{aligned} \quad (2.6)$$

where  $N_t$  and  $N_r$  are respectively the number of antennas at the transmitter and at the receiver. The normalized spatial angles  $\phi_T$  and  $\phi_R$  are related to the physical angle of arrival and departure [12] :

$$\begin{aligned} \phi_T &= \frac{d_T}{\lambda} \sin(\theta_T) \\ \phi_R &= \frac{d_R}{\lambda} \sin(\theta_R) \end{aligned}$$

$d_T$  and  $d_R$  denote the antenna spaces at the transmitter and receiver, respectively, and  $\lambda$  is the wavelength of propagation. [11]

The narrowband channel vector with the user  $k$  is given by:

$$\mathbf{h}_k = \sqrt{\frac{N_t N_r}{L_S \rho_k}} \sum_{i=1}^{L_S} \alpha_i \mathbf{a}_T(\theta_{T_i}) \mathbf{a}_R(\theta_{R_i}) \quad (2.7)$$

it represents the signal propagation over  $L_S$  paths, with different AoA and AoD.  $\alpha_i$  is the complex gain of the  $i$ -th multi-path component and  $\rho_k$  is the distance dependent path loss between the transmitter and the  $k$ -th receiver.

The considered system consists of users with only one antenna, thus the channel vector simplifies as:

$$\mathbf{h}_k = \sqrt{\frac{N_t}{L_S \rho_k}} \sum_{i=1}^{L_S} \alpha_i \mathbf{a}_T(\theta_{T_i}) \quad (2.8)$$

### 2.3.2 Uniform Planar Array

The linear arrays are limited because they cannot provide beamforming in the elevation domain (3D beamforming).

In this case, the normalized steering vectors are function of both the azimuth angle ( $\theta$ ) and the elevation angle ( $\phi$ ).

The uniform planar array (UPA) is the particular instance in which the space between consecutive antennas is the same in both directions.

If also the total number of antennas in one direction is the same as the other direction, that is the case of uniform square planar array described by Figure 2.3 with  $N = M$ .

The normalized steering vectors can be written as:

$$\begin{aligned} \mathbf{a}_T &= \frac{1}{\sqrt{N_t}} \text{vec}(\mathbf{a}'_T) \\ \mathbf{a}_R &= \frac{1}{\sqrt{N_r}} \text{vec}(\mathbf{a}'_R) \end{aligned} \quad (2.9)$$

where  $\mathbf{a}'_T$  and  $\mathbf{a}'_R$  are defined as:

$$\begin{aligned} \mathbf{a}'_T(\theta_T, \phi_T) &= \begin{bmatrix} 1 & e^{j\kappa \sin(\theta_T) \sin(\phi_T)} & \dots & e^{j(\sqrt{N_t}-1)\kappa \sin(\theta_T) \sin(\phi_T)} \\ 1 & e^{j\kappa(\sin(\theta_T) \sin(\phi_T) + \sin(\theta_T) \cos(\phi_T))} & \dots & e^{j\kappa((\sqrt{N_t}-1)\sin(\theta_T) \sin(\phi_T) + \sin(\theta_T) \cos(\phi_T))} \\ \vdots & \vdots & \dots & \vdots \end{bmatrix} \\ \mathbf{a}'_R(\theta_R, \phi_R) &= \begin{bmatrix} 1 & e^{j\kappa \sin(\theta_R) \sin(\phi_R)} & \dots & e^{j(\sqrt{N_r}-1)\kappa \sin(\theta_R) \sin(\phi_R)} \\ 1 & e^{j\kappa(\sin(\theta_R) \sin(\phi_R) + \sin(\theta_R) \cos(\phi_R))} & \dots & e^{j\kappa((\sqrt{N_r}-1)\sin(\theta_R) \sin(\phi_R) + \sin(\theta_R) \cos(\phi_R))} \\ \vdots & \vdots & \dots & \vdots \end{bmatrix} \end{aligned}$$

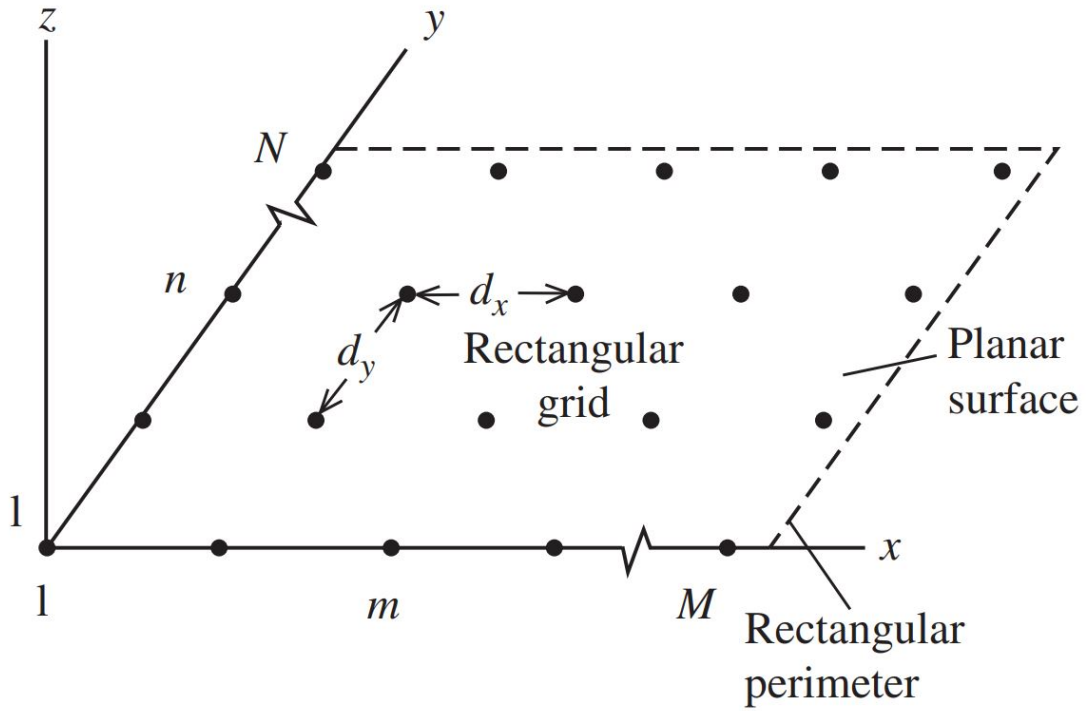


FIGURE 2.3: Geometry of a planar array [27]

the constant  $\kappa = \frac{2\pi d}{\lambda}$  and the function  $\text{vec}()$  refers to the transformation from matrix to column vector following the row order, for instance:

$$\text{vec} \left( \begin{bmatrix} \alpha & \beta \\ \gamma & \epsilon \end{bmatrix} \right) = [\alpha, \beta, \gamma, \epsilon]^T$$

The narrowband channel vector for user  $k$  is given by:

$$\mathbf{h}_k = \sqrt{\frac{N_t N_r}{L_S \rho_k}} \sum_{i=1}^{L_S} \alpha_i \mathbf{a}_T(\theta_{T_i}, \phi_{T_i}) \mathbf{a}_R(\theta_{R_i}, \phi_{R_i}) \quad (2.10)$$

which, in case of single antenna user equipment, simplifies to:

$$\mathbf{h}_k = \sqrt{\frac{N_t}{L_S \rho_k}} \sum_{i=1}^{L_S} \alpha_i \mathbf{a}_T(\theta_{T_i}, \phi_{T_i}) \quad (2.11)$$





## Chapter 3

# MU-MIMO Scheduling

In this chapter, various algorithms for the scheduling problem of a MU-MIMO system are investigated.

### 3.1 Users's Scheduling procedure

The users' scheduling algorithm is implemented at the base station to select the optimal set of users to increase the total achievable data rate.

The algorithm starts with a channel matrix  $\mathbf{H}$  defined as:

$$\mathbf{H} = \begin{bmatrix} h_{1,1} & h_{1,2} & \cdots & h_{1,N_t} \\ h_{2,1} & h_{2,2} & \cdots & h_{2,N_t} \\ \vdots & \vdots & \cdots & \vdots \\ h_{N_u,1} & h_{N_u,2} & \cdots & h_{N_u,N_t} \end{bmatrix}$$

without loss of generality the number of available users can be greater than the number of antennas at the transmitter side.

The scope of this algorithm is to reduce the total number of users, selecting only some of them, in order to maximize the total capacity.

The total number of selected users must be smaller than the number of antennas at the base station, since each user requires a different stream of data.

A basic idea of the user selection problem is given by Figure 3.1, in this case the fourth user is not selected for the transmission because otherwise the total achievable rate will be lower, thus it means that the fourth channel is the worst in a relative sense. [5]

Thus, the selection is based on the total available power, on the number of antennas and on the full channel knowledge of the user, at the base station.

Because of the spatial multiplexing, channel state information (CSI) at the transmitter is necessary for beamforming.

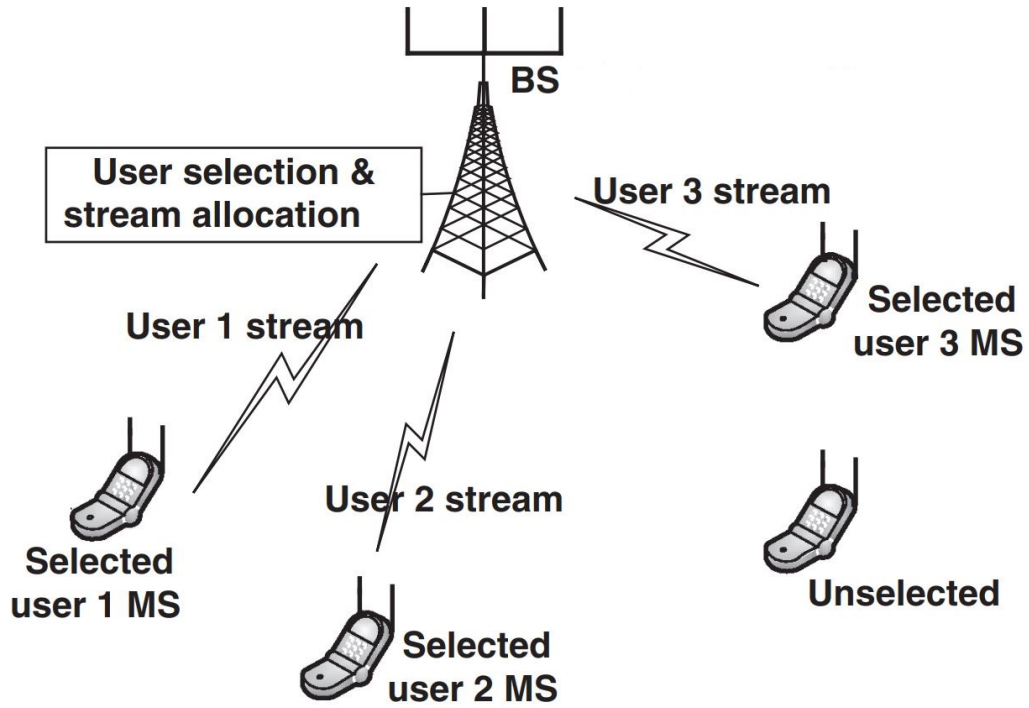


FIGURE 3.1: Multi-user MIMO system [5]

The general optimization problem that has to be solved for the user scheduling is:

$$\max_{\mathbf{B}, \Omega} \sum_{i \in \Omega} \log_2 \left( 1 + \frac{\mathbf{h}_i \mathbf{B}_i (\mathbf{h}_i \mathbf{B}_i)^H E_s}{\sum_{k \in \Omega, k \neq i} \mathbf{h}_i \mathbf{B}_k (\mathbf{h}_i \mathbf{B}_k)^H E_s + \sigma_w^2} \right) \quad (3.1a)$$

$$\text{subject to } \Omega \subseteq \Psi, \quad (3.1b)$$

$$\text{Tr}(\mathbf{B} \mathbf{B}^H E_s) \leq P_T. \quad (3.1c)$$

The maximization of the spectral efficiency over all the selected users is given by 3.1a, where  $\Omega$  is the set of selected users and  $\Psi$  is the set of all the available users for the downlink transmission; indeed  $\Omega \subseteq \Psi$ .

The maximization depends on the precoder matrix, denoted by  $\mathbf{B}$ , and on the users set.

The inequality 3.1c is for the power constraint, where  $P_T$  is the total power available at the base station. The constant  $E_s$  refers to the symbols' energy and the subscript  $()^H$  denotes the Hermitian transpose transformation.

Different algorithms can be implemented based on the selected precoding scheme.

## 3.2 Zero-Forcing Coding

Zero forcing beamforming is a simple technique that allows orthogonal transmissions, without multiuser interference, by inverting the channel matrix at the transmitter.

If the number of antennas  $N_t$  is greater than the number of available users  $N_u$ , the beamforming matrix consists of the Moore-Penrose pseudoinverse of the channel matrix:

$$\mathbf{B} = \mathbf{H}^H (\mathbf{H}\mathbf{H}^H)^{-1} \quad (3.2)$$

In this way, the received signal by user  $i$  is:

$$y_i = \mathbf{h}_i \mathbf{B}_i x_i + \sum_{k=1, k \neq i}^{N_u} \mathbf{h}_i \mathbf{B}_k x_k + n = \mathbf{h}_i \mathbf{B}_i x_i + n = x_i + n \quad (3.3)$$

Because the product of the channel matrix by the precoding matrix is the identity:

$$\mathbf{H}\mathbf{B} = \mathbf{H}\mathbf{H}^H (\mathbf{H}\mathbf{H}^H)^{-1} = \mathbf{I} \quad (3.4)$$

ZF beamforming at the transmitter does not enhance noise at the receiver and each user terminal receives only its own data.

To keep the used power under a certain threshold, the power constraint inequality need to be satisfied, thus a power allocation matrix,  $\mathbf{P}$ , is multiplied by the precoding matrix to complete the description of the beamforming.

$$\mathbf{B} = \mathbf{H}^H (\mathbf{H}\mathbf{H}^H)^{-1} \mathbf{P} \quad (3.5)$$

The power constraint is illustrated by the following inequality:

$$\text{Tr} (\mathbf{B}\mathbf{B}^H E_s) = \text{Tr} \left( \mathbf{H}^H (\mathbf{H}\mathbf{H}^H)^{-1} \mathbf{P} \left( \mathbf{H}^H (\mathbf{H}\mathbf{H}^H)^{-1} \mathbf{P} \right)^H E_s \right) \leq P_T \quad (3.6)$$

Using the following property about the trace function that is proved in the Appendix A:

$$\text{Tr} (\mathbf{B}\mathbf{B}^H) = \text{Tr} (\mathbf{B}^H \mathbf{B})^* = \text{Tr} (\mathbf{B}^H \mathbf{B})$$

where the last equality comes from the fact that in this case the trace is real because the diagonal elements are square of the rows' modulus of the matrix  $\mathbf{B}$ ; the power

allocation inequality can be simplified to:

$$\text{Tr}(\mathbf{B}\mathbf{B}^H E_s) = \text{Tr}\left(\left(\mathbf{P}^H (\mathbf{H}\mathbf{H}^H)^{-H} \mathbf{P}\right) E_s\right) \leq P_T \quad (3.7)$$

where the subscript  $()^{-H}$  denotes the Hermitian transpose transformation of the inverse matrix.

The power allocation matrix is real and diagonal. The entry  $P_{ii}$  refers to the power for the  $i$ -th user:

$$\mathbf{P} = \begin{bmatrix} P_{1,1} & 0 & \cdots & 0 \\ 0 & P_{2,2} & \cdots & 0 \\ \vdots & \vdots & \cdots & \vdots \\ 0 & 0 & \cdots & P_{N_u, N_u} \end{bmatrix}$$

Thus the optimization problem for the user scheduling using Zero-Forcing is:

$$\max_{\mathbf{P}, \Omega} \sum_{i \in \Omega} \log_2 \left( 1 + \frac{P_{i,i}^2 E_s}{\sigma_w^2} \right) \quad (3.8a)$$

$$\text{subject to } \Omega \subseteq \Psi, \quad (3.8b)$$

$$\text{Tr}(\mathbf{P}^H \mathbf{H}_p \mathbf{P} E_s) \leq P_T. \quad (3.8c)$$

where the matrix  $\mathbf{H}_p$  is a constant factor in the used power expression that depends only on the channel matrix:  $\mathbf{H}_p = (\mathbf{H}\mathbf{H}^H)^{-1}$ .

Due to the fact that the matrix  $\mathbf{P}$  is diagonal and real, its Hermitian transpose has the same values:  $\mathbf{P} = \mathbf{P}^H$ .

The energy of the symbols,  $E_s$ , without loss of generality, can be considered equal to 1.

In this way, the power constraint 3.8c becomes:

$$\text{Tr}(\mathbf{P}\mathbf{H}_p\mathbf{P}) = \text{Tr} \left( \begin{bmatrix} P_{1,1} & 0 & \cdots & 0 \\ 0 & P_{2,2} & \cdots & 0 \\ \vdots & \vdots & \cdots & \vdots \\ 0 & 0 & \cdots & P_{N_u, N_u} \end{bmatrix} \mathbf{H}_p \begin{bmatrix} P_{1,1} & 0 & \cdots & 0 \\ 0 & P_{2,2} & \cdots & 0 \\ \vdots & \vdots & \cdots & \vdots \\ 0 & 0 & \cdots & P_{N_u, N_u} \end{bmatrix} \right) \leq P_T \quad (3.9)$$

This expression can be further simplified, because of the diagonality of  $\mathbf{P}$ . As it will be shown next, that trace depends only on the diagonal elements of  $\mathbf{H}_P$ .

$$\begin{aligned}
\text{Tr}(\mathbf{P}\mathbf{H}_P\mathbf{P}) &= \text{Tr} \left( \begin{bmatrix} P_{1,1} & 0 & \cdots & 0 \\ 0 & P_{2,2} & \cdots & 0 \\ \vdots & \vdots & \cdots & \vdots \\ 0 & 0 & \cdots & P_{N_u, N_u} \end{bmatrix} \mathbf{H}_P \begin{bmatrix} P_{1,1} & 0 & \cdots & 0 \\ 0 & P_{2,2} & \cdots & 0 \\ \vdots & \vdots & \cdots & \vdots \\ 0 & 0 & \cdots & P_{N_u, N_u} \end{bmatrix} \right) \\
&= \text{Tr} \left( \begin{bmatrix} P_{1,1}\mathbf{H}_{P_1} \\ P_{2,2}\mathbf{H}_{P_2} \\ \vdots \\ P_{N_u, N_u}\mathbf{H}_{P_{N_u}} \end{bmatrix} \begin{bmatrix} P_{1,1} & 0 & \cdots & 0 \\ 0 & P_{2,2} & \cdots & 0 \\ \vdots & \vdots & \cdots & \vdots \\ 0 & 0 & \cdots & P_{N_u, N_u} \end{bmatrix} \right) \\
&= \text{Tr} \left( \begin{bmatrix} P_{1,1}^2 H_{P_{1,1}} & P_{1,1} P_{2,2} H_{P_{1,2}} & \cdots & P_{1,1} P_{N_u, N_u} H_{P_{1, N_u}} \\ P_{2,2} P_{1,1} H_{P_{2,1}} & P_{2,2}^2 H_{P_{2,2}} & \cdots & P_{2,2} P_{N_u, N_u} H_{P_{2, N_u}} \\ \vdots & \vdots & \cdots & \vdots \\ P_{N_u, N_u} P_{1,1} H_{P_{N_u, 1}} & P_{N_u, N_u} P_{2,2} H_{P_{N_u, 2}} & \cdots & P_{N_u, N_u}^2 H_{P_{N_u, N_u}} \end{bmatrix} \right) \\
&= \sum_{i=1}^{N_u} P_{i,i}^2 H_{P_{i,i}}
\end{aligned}$$

where  $\mathbf{H}_{P_i}$  and  $H_{P_{j,k}}$  are respectively the row  $i$  and the element in position  $(j, k)$  of the matrix  $\mathbf{H}_P$ .

This problem can be solved by exhaustive search over all the possible subsets: for all  $n \in (1, N_u)$ , find all the possible subsets with  $n$  users, in order to select the subset with the higher rate.

Doing this procedure for all the values of  $n$  and then choose the value of  $n$  that allows maximization of the rate, thus this is a solution for the analyzed problem.

Nevertheless, due to the massive number of combinations when the number of available antennas is high (for instance, with 64 antennas and 100 available users, the number of subsets with 64 users is:  $\binom{100}{64} \simeq 2 \times 10^{27}$ ) such an algorithm has prohibitive complexity.

In [7] a suboptimal algorithm is proposed:

it starts with an empty set and the first selected user is the one such that:

$$s_1 = \underset{i \in \Psi}{\text{argmax}} \mathbf{h}_i \mathbf{h}_i^H \quad (3.10)$$

Then, this algorithm follows an iterative procedure in which the user that maximizes the rate is added to the set. It stops either when the number of users in the set is equal to the number of antennas or when, at a certain iteration, all the users left do not increase the total rate.

At each iteration the user set ( $\Omega$ ) is defined and its channel matrix is known, thus the zero forcing precoder can be computed.

To find the maximum total rate the best power allocation matrix is necessary, hence the following optimization problem needs to be solved:

$$\max_{\mathbf{P}} \quad \sum_{i \in \Omega} \log_2 \left( 1 + \frac{P_{i,i}^2}{\sigma_w^2} \right) \quad (3.11a)$$

$$\text{subject to} \quad \sum_{i \in \Omega} P_{i,i}^2 H_{P_{i,i}} \leq P_T \quad (3.11b)$$

### 3.2.1 Optimal power allocation

Denoting the square of the  $i$ -th elements of the power allocation matrix as  $p_i$ .

$$p_i = P_{i,i}^2 \quad (3.12)$$

The optimization problem can be rewritten as:

$$\max_{\mathbf{P}} \quad \sum_{i \in \Omega} \log_2 \left( 1 + \frac{P_i}{\sigma_w^2} \right) \quad (3.13a)$$

$$\text{subject to} \quad \sum_{i \in \Omega} p_i H_{P_{i,i}} \leq P_T \quad (3.13b)$$

$$p_i \geq 0 \quad (3.13c)$$

The solution of this problem, the optimal values of the matrix  $\mathbf{P}$ , can be obtained employing the Lagrangian method.

The Lagrangian function is :

$$\mathcal{L}(\mathbf{p}_i, \boldsymbol{\lambda}, \pi) = \sum_{i \in \Omega} \log_2 \left( 1 + \frac{P_i}{\sigma_w^2} \right) - \sum_{i \in \Omega} \lambda_i p_i - \pi \left( \sum_{i \in \Omega} p_i H_{P_{i,i}} - P_T \right) \quad (3.14)$$

where the vector  $\boldsymbol{\lambda}$  and the variable  $\pi$  are Lagrangian multipliers. The  $i$ -th element of the vector  $\boldsymbol{\lambda}$  is denoted by  $\lambda_i$ .

Setting to zero the derivative of the Lagrangian function with respect to  $p_k$  is necessary to obtain the Lagrangian dual function.

$$\frac{\partial \mathcal{L}}{\partial p_k} = \frac{1}{\ln(2)\sigma_w^2} \left( \frac{1}{1 + \frac{P_k}{\sigma_w^2}} \right) - \lambda_k - \pi H_{P_{k,k}} = 0$$

The result of this equation is:

$$P_k = \frac{1}{(\lambda_k + \pi H_{P_{k,k}}) \ln(2)} - \sigma_w^2$$

The constraint 3.13c requires the elements of the power matrix to be positive. Hence, a compact result can be found by forcing it to be positive without the Lagrangian multiplier  $\lambda$ .

$$P_k = \left( \frac{1}{\pi H_{P_{k,k}} \ln(2)} - \sigma_w^2 \right)^+ \quad (3.15)$$

where the function  $()^+$  is described as:

$$x^+ = \max(0, x)$$

in order to keep only positive values for the power, in case of negatives, they are set to zero.

This solution is similar to the water-filling scheme studied in 4.1.1, where the Lagrangian multiplier  $\pi$  is a positive constant such that power constraint 3.13b is satisfied.

The values of optimal power allocation have to be computed at each iteration with a different subset of users.

To compute the power matrix,  $\mathbf{P}$ , the square root of the elements obtained with 3.15 are the diagonal entries of the final matrix, because of 3.12.

### 3.2.2 ZF Algorithm

This users' scheduling algorithm [7] is fully outlined as follows:

#### Initialization:

- Set  $n=1$
- Find the first selected user,  $s_1$ , such that:

$$s_1 = \operatorname{argmax}_{i \in \Psi} \mathbf{h}_i \mathbf{h}_i^H$$

- Set  $S_1 = \{s_1\}$  and denotes the max achieved rate  $R_{zf}(S_1)_{\max}$

#### Iterative step:

**While**  $n < N_u$

- Increase  $n$  by 1
- Find the  $n$ -th selected user,  $s_n$ , such that:

$$s_n = \arg \max_{i \in \Psi \setminus S_{n-1}} R_{zf}(S_{n-1} \cup \{i\})$$

- Set  $S_n = S_{n-1} \cup \{s_n\}$  and denotes the max achieved rate  $R_{zf}(S_n)_{\max}$
- If  $R_{zf}(S_n)_{\max} \leq R_{zf}(S_{n-1})$  decrease  $n$  by 1 and **break**

where the maximum achieved rate  $R_{zf}(S_n)_{\max}$  with the set of users  $S_n$  is computed as follows:

$$R_{zf}(S_n)_{\max} = \sum_{i \in S_n} \log_2 \left( 1 + \frac{P_i}{\sigma_w^2} \right) \quad (3.16)$$

where the optimal power allocation for the user  $i$ ,  $p_i$ , is given by the Equation 3.15. The algorithm stops when by adding none of the remaining users (which have not been selected yet) can increase the total rate.

At the end, the best set of users is  $S_n$  and the maximum achievable rate is  $R_{zf}(S_n)_{\max}$ . The best set of users is related to the best channel matrix, that is necessary to compute the beamformer.

By denoting the channel matrix  $\mathbf{H}$  as the matrix in which the  $i$ -th row is the channel vector of the  $i$ -th selected user, the beamformer,  $\mathbf{B}$ , is obtained as described in 3.5:

$$\mathbf{B} = \mathbf{H}^H (\mathbf{H}\mathbf{H}^H)^{-1} \mathbf{P}$$

### 3.2.3 Uniform Power allocation

To limit the computational complexity of the algorithm, another suboptimal solution is introduced.

In the previous algorithm the solution of the optimal power allocation problem needs to be computed for a number of times equal to the remaining users in the set for each iteration.

Due to the orthogonality of the channels, a uniform power allocation can lead to sub-optimal performance in terms of total rate, keeping the complexity of the algorithm as low as possible. It means that the power associated for the  $i$ -th user depends only on the channel of that user and on the total available power.

In this way, from the channel matrix, with a single operation, is possible to obtain the sub-optimal power matrix without solving the optimization problem previously described.



The allocated power for the  $i$ -th user is equal to:

$$P_i = \frac{P_T}{N_u H_{P_{i,i}}} \quad (3.17)$$

To be sure that these values of the power allocation can be used in this sense, they need to satisfy the constraints 3.13b and 3.13c.

To prove that the condition 3.13c holds, the elements need to be positive regardless of the channel matrix  $\mathbf{H}$ .

The total available power at the transmitter and the number of users are certainly positive values and also the diagonal elements of  $\mathbf{H}_P = (\mathbf{H}\mathbf{H}^H)^{-1}$  are positive as shown in the next theorem for the special case of square channel matrix.

**Theorem 3.2.1.** *Let  $\mathbf{H}$  be a full rank  $N \times N$  matrix, the diagonal elements of the matrix  $(\mathbf{H}\mathbf{H}^H)^{-1}$  are positive.*

*Proof.* The diagonal elements of the matrix  $\mathbf{H}\mathbf{H}^H$  are positive because they are nothing but the square of the module of each row vector,  $\mathbf{h}_i$ , of the matrix  $\mathbf{H}$ :

$$\mathbf{H}\mathbf{H}^H = \begin{bmatrix} \|\mathbf{h}_1\|^2 & \star & \cdots & \star \\ \star & \|\mathbf{h}_2\|^2 & \cdots & \star \\ \vdots & \vdots & \cdots & \vdots \\ \star & \star & \cdots & \|\mathbf{h}_N\|^2 \end{bmatrix}$$

The determinant of the matrix  $\mathbf{H}\mathbf{H}^H$  is positive due to Binet's theorem (Appendix A):

$$\det(\mathbf{H}\mathbf{H}^H) = \det(\mathbf{H}) \det(\mathbf{H}^H)$$

The determinant of the transpose of a matrix is equal to the determinant of the matrix itself, thus:

$$\det(\mathbf{H}\mathbf{H}^H) = \|\det(\mathbf{H})\|^2 > 0$$

The case of null determinant happens when at least two rows or columns of the matrix  $\mathbf{H}$  are linearly dependent.

The hypothesis of full rank channel matrix is consistent because the probability that two random channel vectors are not linearly independent is negligible.

Given that both the determinant and the elements on the main diagonal are positive, also the diagonal elements of the inverse matrix are positive.  $\square$

By exploiting this theorem, a general result can be obtained:

**Lemma 3.2.2.** Let  $\mathbf{H}$  be a full rank  $N \times N$  matrix, the matrix  $\mathbf{H}\mathbf{H}^H$  is positive-definite.

*Proof.* As stated previously, the determinant of the matrix  $\mathbf{H}\mathbf{H}^H$  is positive.

By iterative removing the last row of the matrix  $\mathbf{H}$  and denoting the considered matrix at the  $i$ -th iteration as  $\hat{\mathbf{H}}(i)$ , the property of positive determinant for  $\hat{\mathbf{H}}(i)\hat{\mathbf{H}}(i)^H$  is still satisfied.

The determinant of the matrix  $\hat{\mathbf{H}}(i)\hat{\mathbf{H}}(i)^H$  is the  $i$ -th principal minor of the matrix  $\mathbf{H}\mathbf{H}^H$ , it is positive, thus for Sylvester's criterion  $\mathbf{H}\mathbf{H}^H$  is positive definite.  $\square$

The second step is to prove that the solution proposed in 3.17 satisfies the condition 3.13b.

It can be easily shown as follows:

$$\sum_{i \in \Omega} P_i H_{P_i,i} = \sum_{i \in \Omega} \frac{P_T}{N_u H_{P_i,i}} H_{P_i,i} \stackrel{(1)}{=} \sum_{i \in \Omega} \frac{P_T}{N_u} = P_T$$

Where in (1) the fact that the set  $\Omega$  contains  $N_u$  users is employed to prove the condition of the inequality in 3.13b.

Using the power allocation in 3.17, the algorithm to obtain the  $n$ -th selected user is described:

**For all**  $K$  available users not selected yet:  $i \leq K$

- Add to the selected channel matrix  $\mathbf{H}$ , the channel vector of the  $i$ -th remaining user as new row.
- Compute the matrix  $\mathbf{H}_P = (\mathbf{H}\mathbf{H}^H)^{-1}$ .
- Obtain the vector of powers using the diagonal elements of  $\mathbf{H}_P$ :

$$P_j = \frac{P_T}{N_u H_{P_j,j}}$$

- Calculate the value of the total rate using the  $i$ -th user:

$$R(i) = \sum_j \log_2 \left( 1 + \frac{P_j}{\sigma_w^2} \right)$$

In this way the vector  $R$  contains in position  $i$  the value of the total achievable rate by adding the  $i$ -th not selected user.

To get the index of the best user, this last instruction is necessary after the for cycle is concluded:

- Acquire the best user,  $i^*$ , by seeking the maximum value of the rate over all the remaining users:

$$i^* = \operatorname{argmax}_i R(i)$$

### 3.2.4 Comparison between optimal and uniform power allocation

As described in the previous section, uniform power allocation, described with the Equation 3.17, is a valid solution for the entries of the power matrix.

The meaning of this method is to allocate more power to the users with a better channel.

Indeed, if a certain user has the best channel condition compared to other users, the square of the module of its channel vector:  $\mathbf{h}_i \mathbf{h}_i^H$  is the highest, thus its diagonal element of the matrix  $\mathbf{H}_p$  results to be the lowest, hence more power is allocated for its transmission due to Equation 3.17.

In order to understand if uniform power allocation is a good solution in terms of total rate, despite its low complexity, a comparison between optimal and uniform power allocation is shown in Figure 3.2 and 3.3.

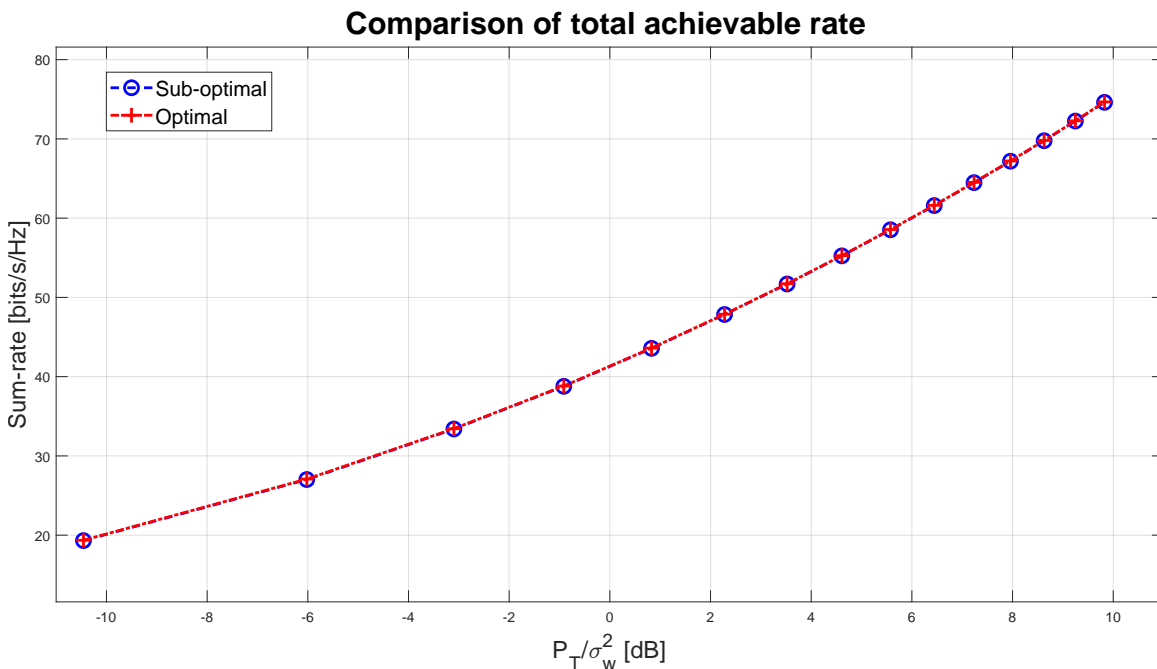


FIGURE 3.2: Comparison between optimal and uniform power allocation (Total-Rate)

In this simulation, the whole set contains 100 available users and the antenna at the transmitter is a Uniform Planar Array with 64 active elements.

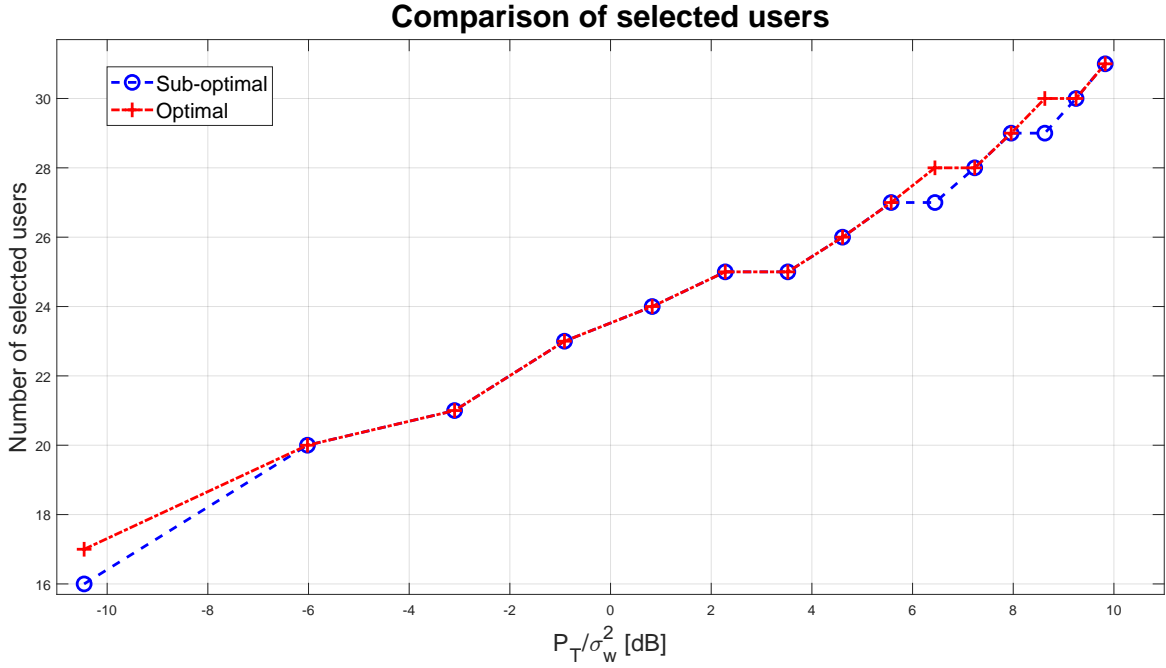


FIGURE 3.3: Comparison between optimal and uniform power allocation (Number of selected users)

The comparison between the different allocation methods is shown as functions of the ratio  $\frac{P_T}{\sigma_w^2}$ .

In Figure 3.3, the comparison is based on the number of selected users: the optimal algorithm sometimes selects one more user for the transmission, however, as shown in Figure 3.2, despite the total achievable rate of the optimal method is larger than the uniform power allocation, the difference, in these conditions, is negligible.

### 3.2.5 Performance employing a users' set with different size

Using uniform power allocation to obtain the power matrix, a comparison of the performance employing a users' set with different cardinality is shown in Figure 3.4 and 3.5.

In this simulation, the transmitted antenna is a Uniform Planar Array with 64 active element and the cardinality of the users set goes from 64 (equal to the number of antennas) to 1000.

Using the same power, by increasing the number of available users, this scheduling algorithm can select more users and increase the total achievable rate.

This is due to the fact that with a higher cardinality of the users set is more likely to have more users with a good channel.

A total rate dependence on the users set is more relevant with higher SNR conditions: as shown in Figure 3.4, when the ratio  $\frac{P_T}{\sigma_w^2}$  is equal to 10dB, the difference of the total rate between 64 users and 1000 users is more than  $25 \frac{\text{bits/s}}{\text{Hz}}$ , whereas when the ratio  $\frac{P_T}{\sigma_w^2}$  is equal to  $-10\text{dB}$ , the difference is less than  $10 \frac{\text{bits/s}}{\text{Hz}}$ .

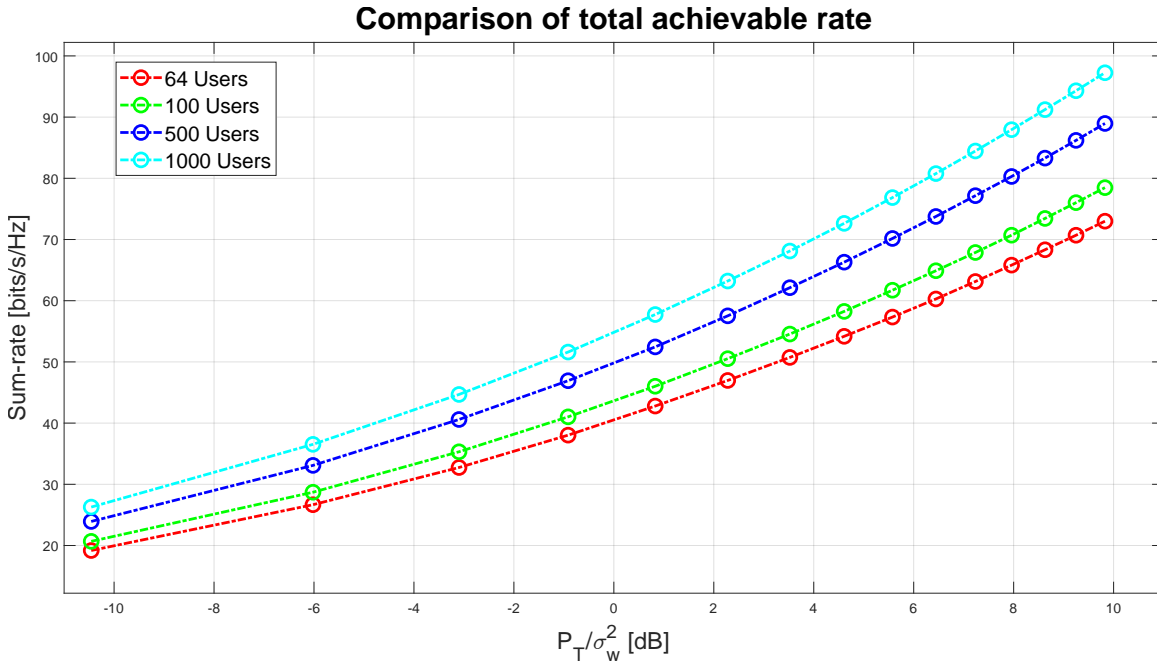


FIGURE 3.4: Comparison of total rate with different users' set

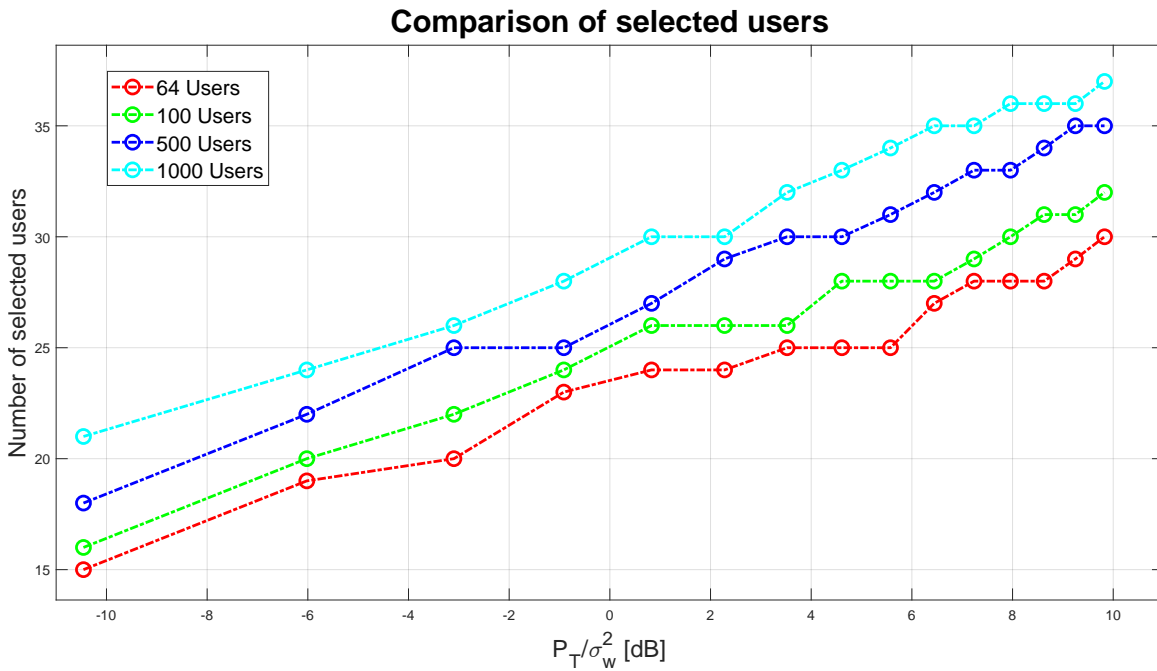


FIGURE 3.5: Comparison of total number of selected users with different users' set



## Chapter 4

# Dirty Paper Coding

Dirty Paper Coding is introduced by Max Costa in [6].

It is a method of precoding the data such that the effect of the interference can be canceled subject to some interference that is known to the transmitter. [5]

The title of Costa's work came by making an analogy to the problem of writing on dirty paper, where the reader cannot nominally distinguish dirt from ink. [18]

In a single-user memoryless channel, with transmitted signal  $\mathbf{x}$ , unknown Gaussian noise  $\mathbf{n}$  and additive interference  $s$  known to the transmitter but not to the receiver, the received signal is equal to:

$$\mathbf{y} = \mathbf{x} + \mathbf{s} + \mathbf{n} \quad (4.1)$$

By definition, the capacity of this system is defined as:

$$C = \max_{p(\mathbf{u}, \mathbf{x} | \mathbf{s})} \{I(\mathbf{u}; \mathbf{y}) - I(\mathbf{u}; \mathbf{s})\} \quad (4.2)$$

where the vector  $\mathbf{u}$  is an auxiliary random variable and  $I(\mathbf{x}; \mathbf{y})$  is the mutual information of  $\mathbf{x}$  and  $\mathbf{y}$ .

The idea of Costa [6] is that with Dirty Paper Coding (DPC), it is possible to reach a channel capacity  $C$  that is the same even if the known interference  $\mathbf{s}$  is not present. This precoding technique can be extended to multi-users broadcast channels so that the known interference  $\mathbf{s}$  is the undesired signal designated to other users.

### 4.1 ZF-DPC Scheme

In [4], the sum capacity of a Gaussian MIMO broadcast channel with two users is derived and it is shown to be achieved using Dirty Paper Coding (DPC), then a suboptimal but simpler scheme is proposed for any number of users, the so called Zero-Forcing - Dirty Paper Coding (ZF-DPC).

This precoding method is based on the LQ-decomposition: the channel matrix  $\mathbf{H}$

of size  $N_u \times N_t$  can be written as product of 2 matrices.

$$\mathbf{H} = \begin{bmatrix} \mathbf{L} & \mathbf{0} \end{bmatrix} \mathbf{Q}_t = \begin{bmatrix} \mathbf{L} & \mathbf{0} \end{bmatrix} \begin{bmatrix} \mathbf{Q} \\ \mathbf{Q}_r \end{bmatrix} = \mathbf{LQ} \quad (4.3)$$

where  $\mathbf{L}$  is lower-triangular of dimension  $N_u \times N_u$  and  $\mathbf{Q}_t$  is orthonormal. The matrix  $\mathbf{Q}$  consists of the first  $m$  rows of the matrix  $\mathbf{Q}_t$ .

The received signal by a user  $i$  of a general MU-MIMO system is described in 2.3, that equation can be rewritten as:

$$y_i = \mathbf{h}_i \mathbf{B}_i x_i + \underbrace{\sum_{k=1}^{i-1} \mathbf{h}_i \mathbf{B}_k x_k}_{\text{Int}(k < i)} + \underbrace{\sum_{k=i+1}^{N_u} \mathbf{h}_i \mathbf{B}_k x_k}_{\text{Int}(k > i)} + n \quad (4.4)$$

where  $\text{Int}(k < i)$  is the interference caused by signals for users with index lower than  $i$ , whereas  $\text{Int}(k > i)$  is the interference due to signals for users with index greater than  $i$ .

This scheme removes the interference caused by users in two different part implemented at the transmitter side: outer encoder and inner encoder.

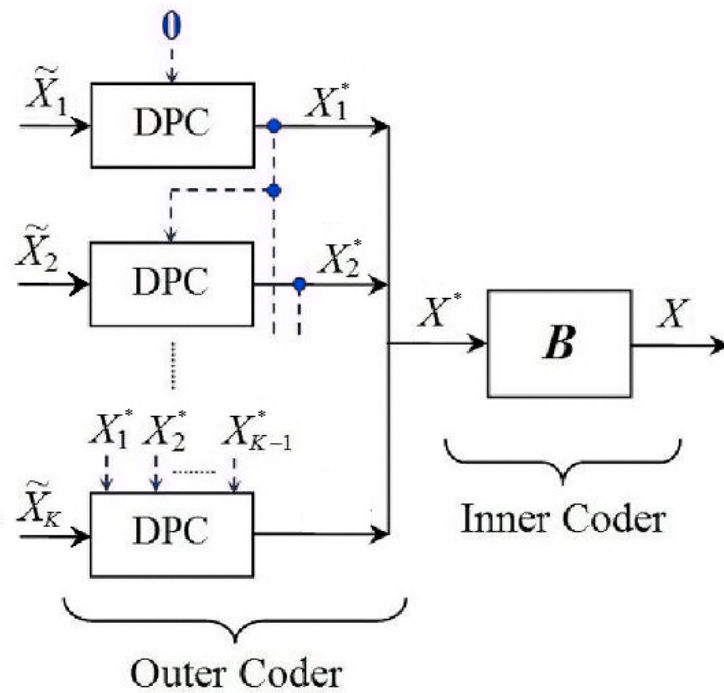


FIGURE 4.1: DPC scheme of the outer encoder and the inner encoder [17]



### 4.1.1 Inner Encoder

The scope of the inner encoder is to cancel  $\text{Int}(k > i)$ , this can be done by transmitting  $\mathbf{x} = \mathbf{Q}^H \mathbf{x}^*$ , where  $\mathbf{x}^*$  is the signal processed by the outer encoder and  $\mathbf{x}$  is the signal transmitted by the antennas.

By applying this precoder, the received vector  $\mathbf{y}$  is as follows:

$$\mathbf{y} = \mathbf{H}\mathbf{x} + \mathbf{n} = \mathbf{H}\mathbf{Q}^H \mathbf{x}^* + \mathbf{n}$$

The channel matrix can be written as product of 2 matrices because of the LQ-decomposition, thus:

$$\mathbf{y} = \mathbf{L}\mathbf{Q}\mathbf{Q}^H \mathbf{x}^* + \mathbf{n} = \mathbf{L}\mathbf{x}^* + \mathbf{n} \quad (4.5)$$

The matrix  $\mathbf{L}$  is lower-triangular, hence the signal received by the first user is not affected by interference; the second user receives its own signal and as additive noise the signal of the first user. Generically the user  $k$  receives as interference the signal transmitted for users 1 to  $k - 1$ , therefore it is possible to completely cancel  $\text{Int}(k > i)$  using this precoder. Moreover, this scheme does not increase the power consumption because  $\mathbf{Q}$  is orthonormal:

$$\text{Tr}(\mathbf{x}^H \mathbf{x}) = \text{Tr}(\mathbf{x}^{*H} \mathbf{Q}\mathbf{Q}^H \mathbf{x}^*) = \text{Tr}(\mathbf{x}^{*H} \mathbf{x}^*) \quad (4.6)$$

Since the energy of the symbols,  $E_s$ , is considered equal to 1, the achievable rate with power constraint equal to 1 can be written as:

$$R = \sum_{i=1}^{N_u} \log_2 \left( 1 + \frac{l_{i,i}^2}{\sigma_w^2} \right) \quad (4.7)$$

where  $l_{i,i}$  is the  $i$  th diagonal entry of the matrix  $\mathbf{L}$ .

This expression considers  $\text{Int}(k < i) = 0$  (reachable employing the outer encoder), more in general, in order to maximize the total achievable rate, a power allocation matrix  $\mathbf{P}$  is required. Hence, the ZF-DPC precoder is set to  $\mathbf{B} = \mathbf{Q}^H \mathbf{P}$  where  $\mathbf{P}$  is a  $N_u \times N_u$  diagonal matrix, whose  $n$ -th element,  $P_{n,n}$ , represents the power allocated for the  $n$  th user.

Entries of this matrix are the solutions of the sum-rate maximization problem, formulated as:

$$\max_{\mathbf{P}} \quad \sum_{i \in \Omega} \log_2 \left( 1 + \frac{P_{i,i}^2 l_{i,i}^2}{\sigma_w^2} \right) \quad (4.8a)$$

$$\text{subject to} \quad \text{Tr}(\mathbf{B}^H \mathbf{B}) \leq P_T \quad (4.8b)$$

the power constraint 4.8b, can be simplified due to the orthonormal property of  $\mathbf{Q}$ :

$$\text{Tr}(\mathbf{B}^H \mathbf{B}) = \text{Tr}\left(\left(\mathbf{Q}^H \mathbf{P}\right)^H \mathbf{Q}^H \mathbf{P}\right) = \text{Tr}(\mathbf{P}^H \mathbf{P}) \leq P_T \quad (4.9)$$

The power matrix is diagonal, thus:

$$\text{Tr}(\mathbf{P}^H \mathbf{P}) = \sum_{i \in \Omega} P_{i,i}^2 \leq P_T \quad (4.10)$$

The solution of this problem is the classical waterfilling result.

### Waterfilling

To obtain a simpler expression, the substitution  $p_i = P_{i,i}^2$ , as in Equation 3.12 is applied. Thus, the optimization problem can be rewritten as:

$$\max_{\mathbf{P}} \quad \sum_{i \in \Omega} \log_2 \left( 1 + \frac{P_i l_{i,i}^2}{\sigma_w^2} \right) \quad (4.11a)$$

$$\text{subject to} \quad \sum_{i \in \Omega} p_i \leq P_T \quad (4.11b)$$

$$p_i \geq 0 \quad (4.11c)$$

The solution can be obtained employing the Lagrangian method.

The Lagrangian function is:

$$\mathcal{L}(\mathbf{p}_i, \boldsymbol{\lambda}, \pi) = \sum_{i \in \Omega} \log_2 \left( 1 + \frac{p_i l_{i,i}^2}{\sigma_w^2} \right) - \sum_{i \in \Omega} \lambda_i p_i - \pi \left( \sum_{i \in \Omega} p_i - P_T \right) \quad (4.12)$$

where the vector  $\boldsymbol{\lambda}$  and the variable  $\pi$  are Lagrangian multipliers. The  $i$ -th element of the vector  $\boldsymbol{\lambda}$  is denoted by  $\lambda_i$ .

Setting to zero the derivative of the Lagrangian function with respect to  $p_k$  is necessary to obtain the Lagrangian dual function.

$$\frac{\partial \mathcal{L}}{\partial p_k} = \frac{1}{\ln(2)} \left( \frac{1}{p_k + \frac{\sigma_w^2}{l_{k,k}^2}} \right) - \lambda_k - \pi = 0$$

The result of this equation is:

$$p_k = \frac{1}{(\lambda_k + \pi) \ln(2)} - \frac{\sigma_w^2}{l_{k,k}^2}$$

The constraint 4.11c requires the elements of the power matrix to be positive. Hence, a compact result can be found by forcing it to be positive without the Lagrangian multiplier  $\lambda$ .

$$P_k = \left( \frac{1}{\ln(2)\pi} - \frac{\sigma_w^2}{l_{k,k}^2} \right)^+ \quad (4.13)$$

where the function  $()^+$  is described as:

$$x^+ = \max(0, x)$$

Considering the ratio of the allocated power over the total available power, the expression can be written as:

$$\frac{P_k}{P_T} = \left( \frac{1}{\ln(2)\pi P_T} - \frac{\sigma_w^2}{l_{k,k}^2 P_T} \right)^+ \quad (4.14a)$$

$$= \left( \frac{1}{\gamma_0} - \frac{1}{\gamma_k} \right)^+ \quad (4.14b)$$

This expression is required to be positive, thus if power is allocated for user  $k$ , then:  $\gamma_0 < \gamma_k$ .

The constant  $\frac{1}{\gamma_0}$  does not depend on the channel and it sets the "water level". Therefore, the power allocated for user  $k$  can be summarized as:

$$\frac{P_k}{P_T} = \begin{cases} \frac{1}{\gamma_0} - \frac{1}{\gamma_k} & \text{if } \gamma_k > \gamma_0 \\ 0 & \text{if } \gamma_k \leq \gamma_0 \end{cases} \quad (4.15)$$

This scheme is described in Figure 4.2.

### 4.1.2 Outer Encoder

To implement the DPC scheme, also  $\text{Int}(k < i)$  needs to be removed. This procedure can be done with successive coding based on DPC.

By employing the inner encoder, the received signal can be written as function of the transmitted vector and the elements of the matrix  $\mathbf{L}$ .

From Equation 3.2 and by exploiting the waterfilling optimal result, the vector received by users is:

$$\mathbf{y} = \mathbf{L}\mathbf{p}\mathbf{x}^* + \mathbf{n} \quad (4.16)$$

Due to the shape of  $\mathbf{L}$ , the product  $\mathbf{L}\mathbf{P}$  is again a lower-triangular matrix, for clarity denoted as  $\mathbf{G}$ :

$$\mathbf{G} = \mathbf{L}\mathbf{P} \quad (4.17)$$

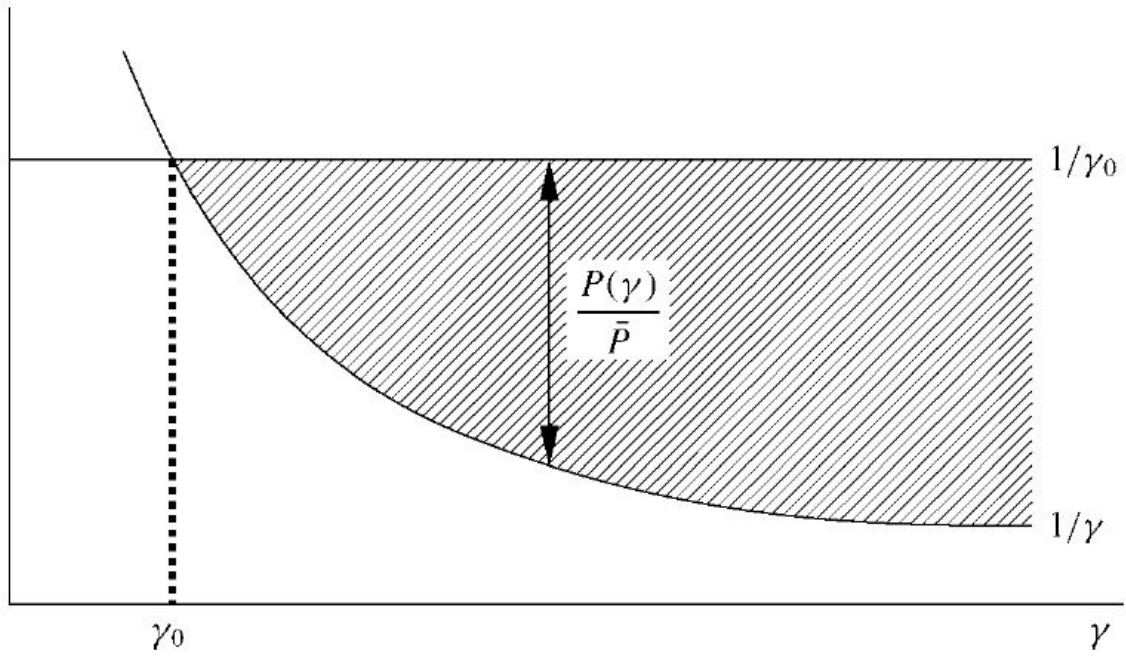


FIGURE 4.2: Optimal power allocation for problem 4.8a: Waterfilling scheme [10]

Therefore, the received signal of the first user is:

$$y_1 = g_{1,1}x_1^* + n \quad (4.18)$$

There is not interference caused by other users hence its signal can be directly forwarded to the inner encoder:

$$x_1^* = \tilde{x}_1 \quad (4.19)$$

where  $\tilde{x}^*$  denotes the signal to transmit to the users, as described in Figure 4.1.

The received signal of the second user is given as:

$$\begin{aligned} y_2 &= g_{2,1}x_1^* + g_{2,2}x_2^* + n \\ &= g_{2,1}\tilde{x}_1 + g_{2,2}x_2^* + n \end{aligned} \quad (4.20)$$

This signal is corrupted by the interference caused by the first user, to remove it, a precoded signal  $x_2^*$  is computed.

The necessary expression, without interference, is:

$$y_2 = g_{2,2}\tilde{x}_2 + n$$

then,

$$\begin{aligned} g_{2,2}\tilde{x}_2 &= g_{2,1}\tilde{x}_1 + g_{2,2}x_2^* \\ \Downarrow \\ x_2^* &= \tilde{x}_2 - \frac{g_{2,1}}{g_{2,2}}\tilde{x}_1 \end{aligned} \quad (4.21)$$

where the precoded signal  $x_2^*$  is composed of the known user signals  $\tilde{x}_1$  and  $\tilde{x}_2$ . For a general user  $k$ , the received signal is:

$$\begin{aligned} y_k &= \sum_{i=1}^k g_{k,i}x_i^* + n \\ &= g_{k,1}x_1^* + g_{k,2}x_2^* + \sum_{i=3}^{k-1} g_{k,i}x_i^* + g_{k,k}x_k^* + n \end{aligned} \quad (4.22)$$

The required expression for the general user is:

$$y_k = g_{k,k}\tilde{x}_k + n \quad (4.23)$$

hence,

$$g_{k,k}\tilde{x}_k = g_{k,1}\tilde{x}_1 + g_{k,2}x_2^* + \sum_{i=3}^{k-1} g_{k,i}x_i^* + g_{k,k}x_k^*$$

The final expression of the precoded signal is given as:

$$x_k^* = \tilde{x}_k - \sum_{i=1}^{k-1} \frac{g_{k,i}}{g_{k,k}}x_i^* \quad (4.24)$$

where it depends on the precoded signal of the previous users.

The energy of the precoded symbol  $x^*$  is greater than the original one  $\tilde{x}$ , thus a modulo operation needs to be applied, for instance the so called Tomlinson-Harashima precoding.

### Tomlinson-Harashima Precoding

Consider a M-ary QAM with a square constellation, the real and imaginary parts are bounded by  $[-A, A)$ , with  $A = \sqrt{M}$  as shown in Figure for the case of  $A = 4$ . [5]

As described in [5], the symmetric modulo operation of a M-ary QAM symbol is

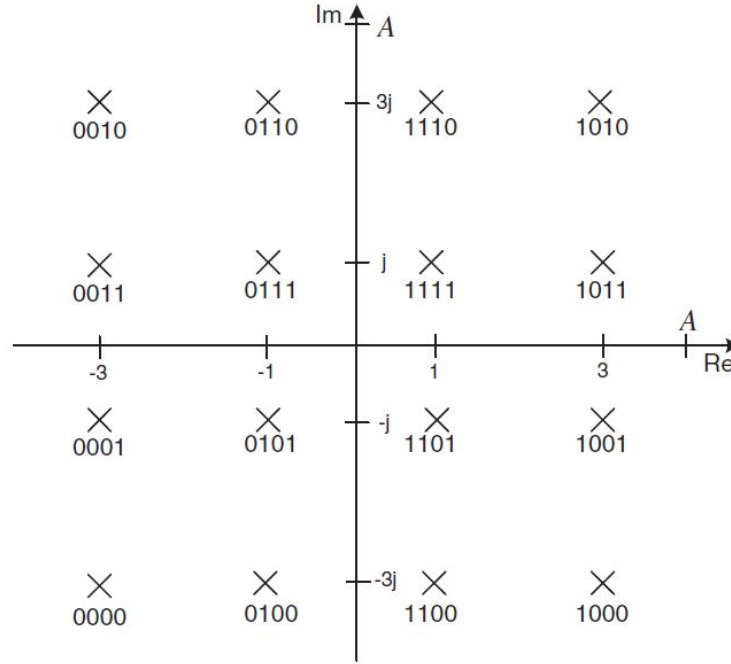


FIGURE 4.3: Constellation of 16-QAM [5]

defined as:

$$\text{mod}_A(x) = x - 2A \left\lfloor \frac{x + A + jA}{2A} \right\rfloor \quad (4.25)$$

This modulo operation can be interpreted as a method to find integer values,  $m$  and  $r$ , such that the following inequality is satisfied:

$$\text{mod}_A(x) = x + 2A \cdot m + j2A \cdot r \quad (4.26)$$

The final precoded symbols are represented as the modular operation of  $\mathbf{x}^*$  computed in the previous section (Equation 4.24):

$$x_k^* = \text{mod}_A \left( \tilde{x}_k - \sum_{i=1}^{k-1} \frac{g_{k,i}}{g_{k,k}} x_i^* \right) \quad (4.27)$$

Equation 4.26 leads to the following expression:

$$x_k^* = \tilde{x}_k - \sum_{i=1}^{k-1} \frac{g_{k,i}}{g_{k,k}} x_i^* + 2A \cdot m_k + j2A \cdot r_k \quad (4.28)$$

For instance, by considering the second user, the precoded signal is:

$$x_2^* = \tilde{x}_2 - \frac{g_{2,1}}{g_{2,2}} \tilde{x}_1 + 2A \cdot m_2 + j2A \cdot r_2 \quad (4.29)$$

Using Equation 4.20, its received signal is:

$$y_2 = g_{2,1}x_1^* + g_{2,2}x_2^* + n$$

thus,

$$\begin{aligned} y_2 &= g_{2,1}\tilde{x}_1 + g_{2,2} \left( \tilde{x}_2 - \frac{g_{2,1}}{g_{2,2}}\tilde{x}_1 + 2A \cdot m_2 + j2A \cdot r_2 \right) + n \\ &= g_{2,2} (\tilde{x}_2 + 2A \cdot m_2 + j2A \cdot r_2) \end{aligned} \quad (4.30)$$

In order to retrieve the original data  $\tilde{x}_2$ , the second user can apply a modular operation of the scaled version of the received signal:

$$\tilde{y}_2 = \text{mod}_A \left( \frac{y_2}{g_{2,2}} \right) \quad (4.31)$$

where  $\tilde{y}_2$  is the processed signal at the receiver side, estimation of  $\tilde{x}_2$ . If the noise  $n$  is small enough such that this inequality is satisfied:

$$-A - jA < \tilde{x}_2 + \frac{n}{g_{2,2}} < A + jA \quad (4.32)$$

the processed signal can be written as:

$$\tilde{y}_2 = \frac{y_2}{g_{2,2}} - 2A \left\lfloor \frac{\frac{y_2}{g_{2,2}} + A + jA}{2A} \right\rfloor = \frac{y_2}{g_{2,2}} - 2A(m_2 + jr_2) + n \quad (4.33)$$

Employing the following expression:

$$\frac{y_2}{g_{2,2}} = \tilde{x}_2 + 2A \cdot m_2 + j2A \cdot r_2 + \frac{n}{g_{2,2}} \quad (4.34)$$

the final expression of the processed signal for the second user is:

$$\tilde{y}_2 = \tilde{x}_2 + \frac{n}{g_{2,2}} \quad (4.35)$$

Other implementations of the outer encoder are based on Lattice precoding as studied in [8].

## 4.2 Capacity of Broadcast Channel

A solution to obtain an achievable downlink channel capacity for the case of 2 users with a single antenna and 2 antennas at the transmitter is described in [5].

The received signal by the users can be derived by Equation 2.2:

$$\begin{bmatrix} y_1 \\ y_2 \end{bmatrix} = \begin{bmatrix} \mathbf{h}_1 \\ \mathbf{h}_2 \end{bmatrix} \begin{bmatrix} x_1 \\ x_2 \end{bmatrix} + \begin{bmatrix} n_1 \\ n_2 \end{bmatrix} \quad (4.36)$$

where  $\mathbf{h}_1$  and  $\mathbf{h}_2$  denote the channel vectors between the BS and the users.

$x_i$  is the signal transmitted by the  $i$  th antenna, whereas  $\tilde{x}_i$  is the signal addressed to the  $i$  th user.

The channel matrix can be LQ-decomposed:

$$\begin{bmatrix} \mathbf{h}_1 \\ \mathbf{h}_2 \end{bmatrix} = \underbrace{\begin{bmatrix} l_{1,1} & 0 \\ l_{2,1} & l_{2,2} \end{bmatrix}}_{\mathbf{L}} \begin{bmatrix} \mathbf{q}_1 \\ \mathbf{q}_2 \end{bmatrix} \quad (4.37)$$

where the matrix  $\mathbf{L}$  is lower-triangular and the row vectors  $\mathbf{q}_1$  and  $\mathbf{q}_2$  are orthonormal:

$$\begin{aligned} \|\mathbf{q}_1\| &= \|\mathbf{q}_2\| = 1 \\ \mathbf{q}_1 (\mathbf{q}_2)^H &= 0 \end{aligned}$$

The values of the decomposition can be obtain through the channel vectors as follows:

$$\begin{aligned} l_{1,1} &= \|\mathbf{h}_1\|, & \mathbf{q}_1 &= \frac{\mathbf{h}_1}{l_{1,1}} \\ l_{2,1} &= \mathbf{q}_1 (\mathbf{h}_2)^H, & \mathbf{q}_2 &= \frac{\mathbf{h}_2 - l_{2,1}\mathbf{q}_1}{l_{2,2}} \\ l_{2,2} &= \|\mathbf{h}_2 - l_{2,1}\mathbf{q}_1\| \end{aligned}$$

The signal can be precoded at the transmitter side, by exploiting the LQ-decomposition, in order to obtain two interference-free channels:

$$\begin{bmatrix} x_1 \\ x_2 \end{bmatrix} = \mathbf{Q}^H \begin{bmatrix} \tilde{x}_1 \\ \tilde{x}_2 - \frac{l_{2,1}}{l_{2,2}} \tilde{x}_1 \end{bmatrix} \quad (4.38)$$

where

$$\mathbf{Q} = \begin{bmatrix} \mathbf{q}_1 \\ \mathbf{q}_2 \end{bmatrix}$$



Transmitting the precoded vector  $\mathbf{x}$ , the signals received by users is given by Equation 2.2:

$$\begin{aligned} \mathbf{y} &= \mathbf{H}\mathbf{x} + \mathbf{n} \\ &= \begin{bmatrix} l_{1,1} & 0 \\ l_{2,1} & l_{2,2} \end{bmatrix} \begin{bmatrix} \mathbf{q}_1 \\ \mathbf{q}_2 \end{bmatrix} \mathbf{Q}^H \begin{bmatrix} \tilde{x}_1 \\ \tilde{x}_2 - \frac{l_{2,1}}{l_{2,2}}\tilde{x}_1 \end{bmatrix} + \mathbf{n} \\ &= \begin{bmatrix} l_{1,1} & 0 \\ l_{2,1} & l_{2,2} \end{bmatrix} \begin{bmatrix} \mathbf{q}_1 \\ \mathbf{q}_2 \end{bmatrix} \begin{bmatrix} \mathbf{q}_1^* & \mathbf{q}_2^* \end{bmatrix} \begin{bmatrix} \tilde{x}_1 \\ \tilde{x}_2 - \frac{l_{2,1}}{l_{2,2}}\tilde{x}_1 \end{bmatrix} + \mathbf{n} \end{aligned}$$

Due to the orthogonal property of matrix  $\mathbf{Q}$ , this expression can be simplified:

$$\begin{aligned} \mathbf{y} &= \mathbf{H}\mathbf{x} + \mathbf{n} \\ &= \begin{bmatrix} l_{1,1} & 0 \\ l_{2,1} & l_{2,2} \end{bmatrix} \begin{bmatrix} \tilde{x}_1 \\ \tilde{x}_2 - \frac{l_{2,1}}{l_{2,2}}\tilde{x}_1 \end{bmatrix} + \mathbf{n} \\ &= \begin{bmatrix} l_{1,1}\tilde{x}_1 \\ l_{2,2}\tilde{x}_2 \end{bmatrix} + \mathbf{n} \\ &= \begin{bmatrix} \|\mathbf{h}_1\|\tilde{x}_1 \\ \|\mathbf{h}_2 - l_{2,1}\mathbf{q}_1\|\tilde{x}_2 \end{bmatrix} + \mathbf{n} \end{aligned} \tag{4.39}$$

Processing of the signals allows users to be not affected by inter-users' interference. They receive only a scaled version of their own signal with additive white Gaussian noise (AWGN).

The total available power  $P_T$  is split into  $\alpha P_T$  and  $(1 - \alpha)P_T$  for the different antennas:

$$\begin{aligned} E(\|x_1\|^2) &= E(\|\tilde{x}_1\|^2) = \alpha P_T \\ E(\|x_2\|^2) &= E\left(\left\|\tilde{x}_2 - \frac{l_{2,1}}{l_{2,2}}\tilde{x}_1\right\|^2\right) = (1 - \alpha)P_T \end{aligned}$$

The capacity of the first user is given as:

$$R_1 = \log_2 \left( 1 + \|\mathbf{h}_1\|^2 \frac{\alpha P_T}{\sigma_w^2} \right)$$

whereas the capacity of the second user is:

$$R_2 = \log_2 \left( 1 + \|\mathbf{h}_2 - l_{2,1}\mathbf{q}_1\|^2 \frac{(1 - \alpha)P_T}{\sigma_w^2} \right)$$

The maximum total achievable rate of this system is found in [4]:

$$\begin{cases} \log_2(1 + \|\mathbf{h}_1\|^2 P_T) & \text{if } P_T \leq P^* \\ \log_2\left(\frac{(P_T \det(\mathbf{H}\mathbf{H}^H) + \text{Tr}(\mathbf{H}\mathbf{H}^H))^2 - 4\|\mathbf{h}_2\mathbf{h}_1^H\|^2}{4 \det(\mathbf{H}\mathbf{H}^H)}\right) & \text{if } P_T > P^* \end{cases} \quad (4.40)$$

where, without loss of generality, the fact that  $\|\mathbf{h}_1\| \geq \|\mathbf{h}_2\|$  is assumed. The constant  $P^*$  depends on the channel matrix and it is defined as:

$$P^* = \frac{\|\mathbf{h}_1\|^2 - \|\mathbf{h}_2\|^2}{\det(\mathbf{H}\mathbf{H}^H)}$$

For the case of two users, Caire and Shamai [4] showed that Dirty Paper Coding is optimal in achieving the sum capacity, by demonstrating that the achievable rate meets the Sato's upper bound [22], which is the capacity of a point-to-point channel where the receivers in the downlink can cooperate as a single user with multiple antennas.

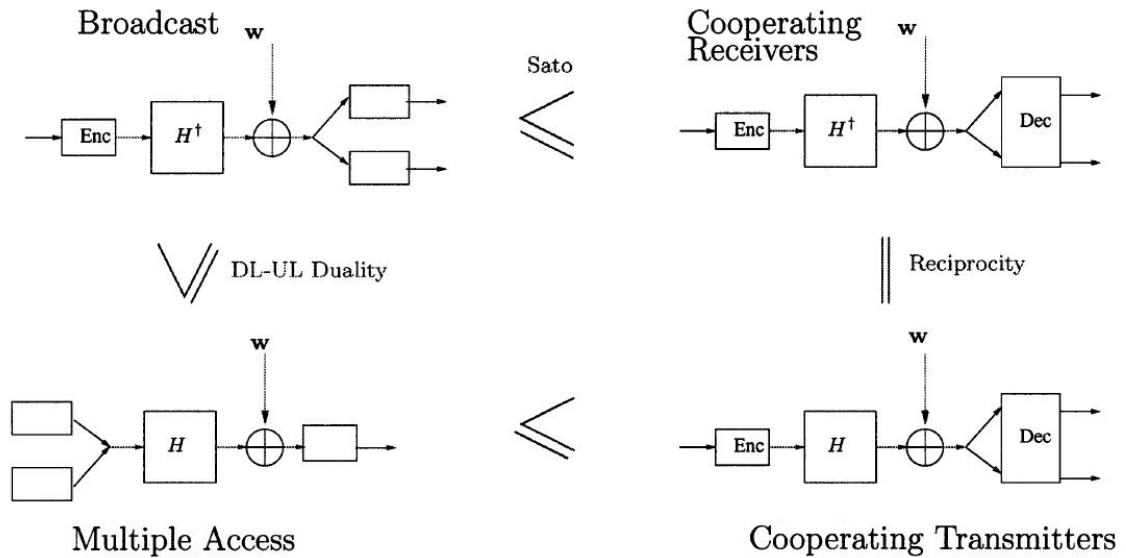


FIGURE 4.4: The four channels, multiple access, broadcast, and their corresponding point-to-point channels, depicted along with the relationship between their capacities. [25]

By exploiting the uplink-downlink duality described in Figure 4.1, thus between Gaussian multiple-access channels (MACs) and Gaussian broadcast channels (BCs) studied in [13] and [25], it has been proved that the capacity regions of the BC and the MAC with the same channel gains (i.e., the channel gain of receiver in the BC equals the channel gain of transmitter in the MAC) and the same noise power at every receiver are closely related.

Thus, it is possible to find the capacity region of the BC if the capacity region of only the MAC is known.

Using this property, in [25] the optimality of DPC is generalized for an arbitrary number of users.

### 4.3 MU-DPC Algorithm

As studied for Zero-Forcing in 3.2.2, in this section an algorithm based on DPC to solve the optimization problem for multi-user selection is described.

In [24] a greedy algorithm for the selection of  $N_t$  users out of  $N_u$  is proposed.

The initialization is as in 3.2.2, where the first selected user is the one such that:

$$s_1 = \operatorname{argmax}_{i \in \Psi} \mathbf{h}_i \mathbf{h}_i^H \quad (4.41)$$

Then, it follows an iterative procedure in which the user that maximizes the rate is added to the set.

It projects all the channel vectors of the non-selected users onto the orthogonal complement of the subspace spanned by the channels of the selected users ( $\Omega$ ).

At each iteration, the selected user is one that has the greatest 2-norm of its projection.

This algorithm is outlined as follows:

#### Initialization:

- Set  $n=1$
- Find the first selected user,  $s_1$ , such that:

$$s_1 = \operatorname{argmax}_{i \in \Psi} \mathbf{h}_i \mathbf{h}_i^H$$

- Set  $\Omega_1 = \{s_1\}$

#### Iterative step:

**While**  $n < N_t$

- Increase  $n$  by 1
- Compute the projector matrix:

$$\mathbf{P}_n^\perp = \mathbf{I}_{N_t} - \mathbf{H}(\Omega_{n-1})^H \left( \mathbf{H}(\Omega_{n-1}) \mathbf{H}(\Omega_{n-1})^H \right)^{-1} \mathbf{H}(\Omega_{n-1}) \quad (4.42)$$

- Find the  $n$ -th selected user,  $s_n$ , such that:

$$s_n = \arg \max_{i \in \Psi \setminus \Omega_{n-1}} \mathbf{h}_i \mathbf{P}_n^\perp \mathbf{h}_i^H \quad (4.43)$$

- Set  $\Omega_n = \Omega_{n-1} \cup \{s_n\}$

where  $\mathbf{H}(\Omega_{n-1})$  is the channel matrix of the set  $\Omega_{n-1}$ , namely the selected users at the end of the  $n - 1$  iteration:

$$\mathbf{H}(\Omega_{n-1}) = \begin{bmatrix} \mathbf{h}_{s_1}^H & \mathbf{h}_{s_2}^H & \dots & \mathbf{h}_{s_{n-1}}^H \end{bmatrix}^H \quad (4.44)$$

At the last iteration, the algorithm selects the  $N_t$ -th user for the transmission hence the final channel matrix is  $\mathbf{H}(\Omega_{N_t})$ .

The next step is to set the digital beamformer of the inner encoder.

From 4.16, the matrices  $\mathbf{L}$  and  $\mathbf{Q}$  are obtained through the LQ-decomposition of  $\mathbf{H}(\Omega_{N_t})$ .

The inner precoder is:

$$\mathbf{B} = \mathbf{Q}^H \mathbf{P} \quad (4.45)$$

To maximize the total achievable rate, the elements of the power matrix  $\mathbf{P}$  are computed by employing the waterfilling algorithm described in 4.1.1.

The last step is to set the outer encoder because it depends on the interference observed by the users, that is a function of the elements of the matrix  $\mathbf{L}\mathbf{P} = \mathbf{G}$ , as shown in 4.1.2.

As proved in [7], this algorithm has significantly lower computational complexity than the sum power iterative water-filling algorithm if the number of available users is greater than the number of antennas of the transmitter.

## 4.4 Comparison between MU-DPC and MU-ZF

In this section, the results of simulations to compare Zero-Forcing (ZF) and Dirty Paper Coding (DPC) algorithms for users' scheduling are shown.

In Figure 4.5 and 4.6, three algorithms are compared: ZF with uniform power allocation described in 3.2.3, Greedy ZF-DPC (gZF-DPC) studied in 4.3 and ZF-DPC that is the sum power iterative waterfilling algorithm, analogous to 3.2.2 but employing DPC.

As shown in these plots, the total sum-rate achieved by Greedy ZF-DPC (gZF-DPC) is overlaid with that of the sum power iterative waterfilling algorithm (ZF-DPC), hence it means that they share the same performances in terms of total rate.

The difference is in the total number of selected users, gZF-DPC has a fixed number of selected users that is equal to the number of antennas, whereas ZF-DPC stops when by adding another user to the set, the total rate is not increased; thus ZF-DPC selects the smallest set of users capable of achieving that rate.

This means that more users (the maximum number of users) are involved in the transmission with gZF-DPC, thus the average single rate is lower than the average single rate of ZF-DPC, due to the difference in the total number of selected users; however, the scope of this algorithm is to maximize the total sum rate and, for this condition, both obtain the same result.

The computational complexity of ZF-DPC is much greater than gZF-DPC but the total achievable rate is very similar, thus in the next simulations only gZF-DPC and ZF are compared.

Also in different conditions, ZF-DPC is expected to obtain the same rate of gZF-DPC with a lower number of selected users.

In the simulation of Figure 4.5 and 4.6, the number of available users is equal to the number of antennas (64), hence in gZF-DPC all the users are selected for the transmission, however, even in this case, the same procedure is required because different ordering of users' selection leads to different result.

In Figure 4.7 and 4.8 the number of available users is 100, whereas in Figure 4.9 and 4.10, 1000 users are available for the transmission.

It is shown that DPC achieves a greater rate than ZF and this gap is more significant when the ratio  $\frac{P_T}{\sigma_w^2}$  is higher. By increasing the number of users, the total rate is greater and ZF selects more of them. This is due to the fact that with a higher cardinality of the users set is more likely to have more users with a good channel. However, with more users both DPC and ZF obtain a constant gain of the capacity, thus the difference in the total achievable rate between these two methods does not depend on the number of available users.

In Figure 4.11 and 4.12 a ULA with 32 active elements is used. This difference leads to a lower number of selected users and a strong reduction in the total achievable rate for both ZF and DPC.

Nevertheless, especially at high-SNR, the loss of the total rate is higher for DPC, hence the advantage of this method over ZF is more substantial when more antennas are exploited and in high-SNR condition.

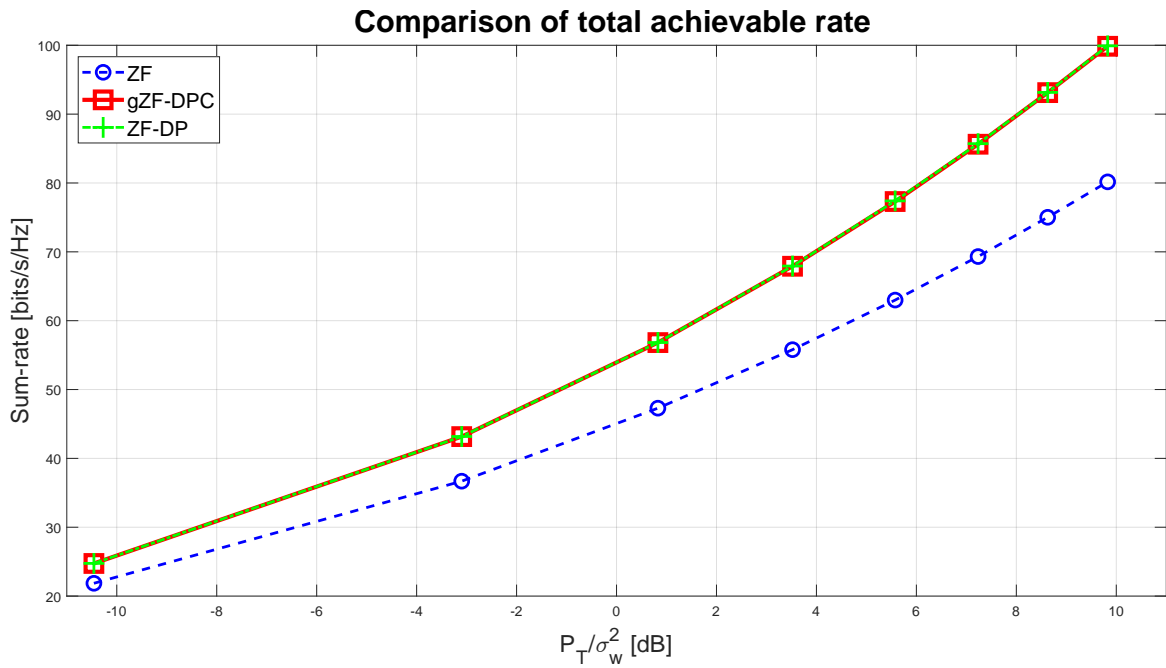


FIGURE 4.5: Comparison of the total achievable rate between DPC and ZF (64 available users and 64 antennas)

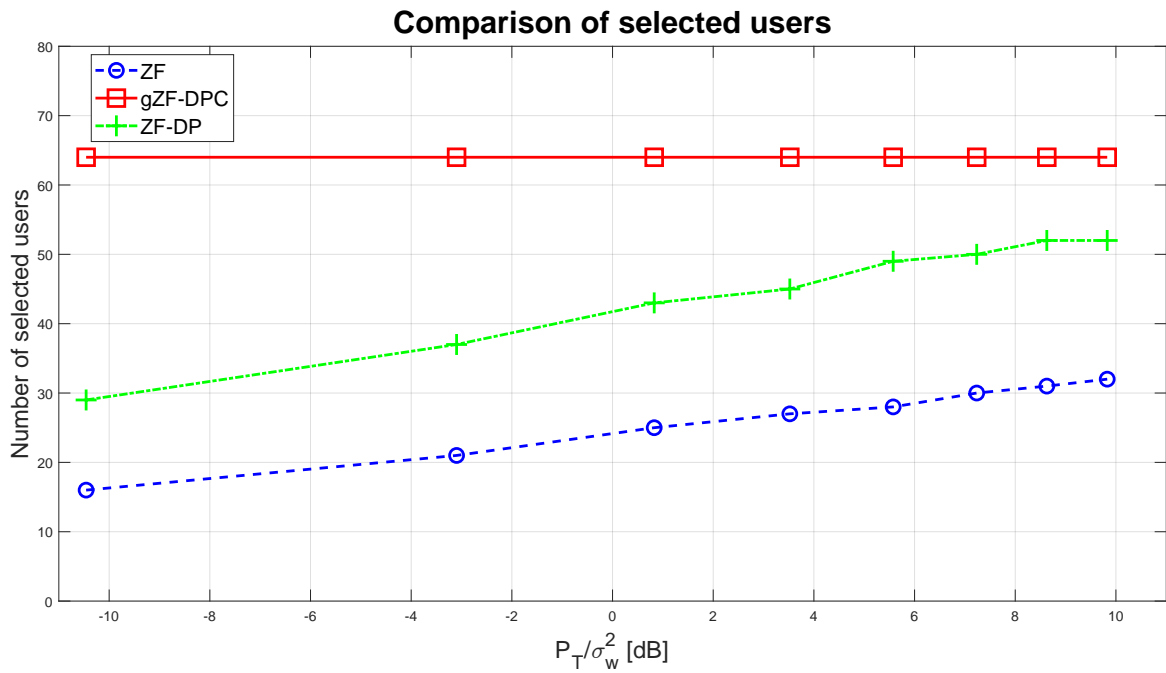


FIGURE 4.6: Comparison of number of selected users between DPC and ZF (64 available users and 64 antennas)

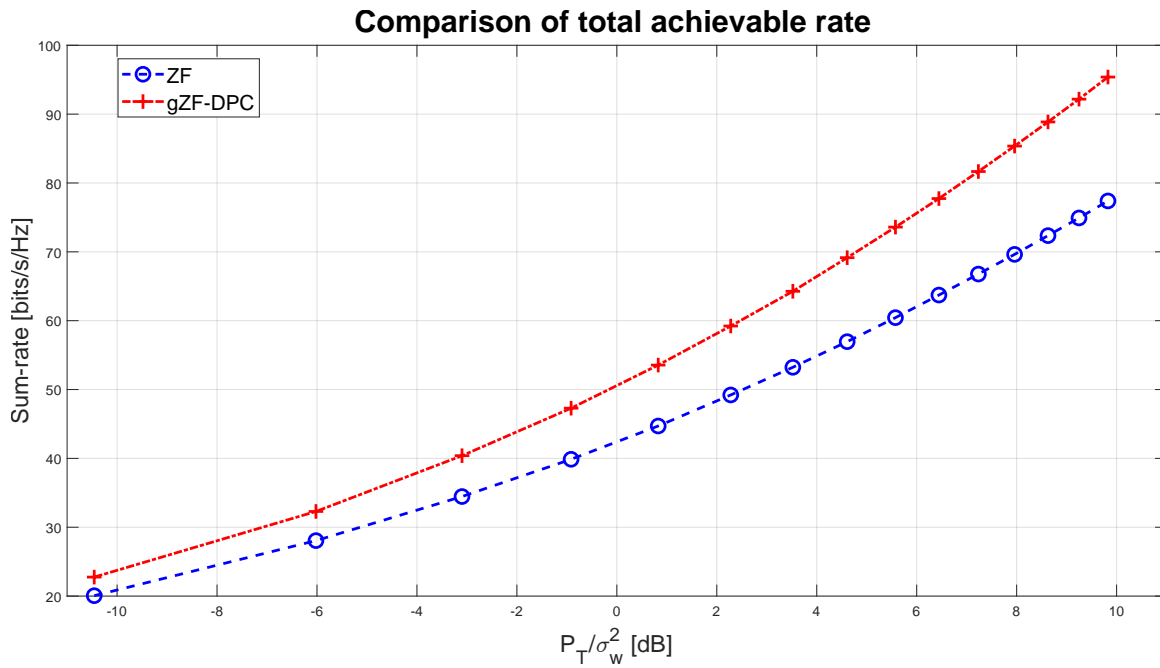


FIGURE 4.7: Comparison of the total achievable rate between DPC and ZF (100 available users and 64 antennas)

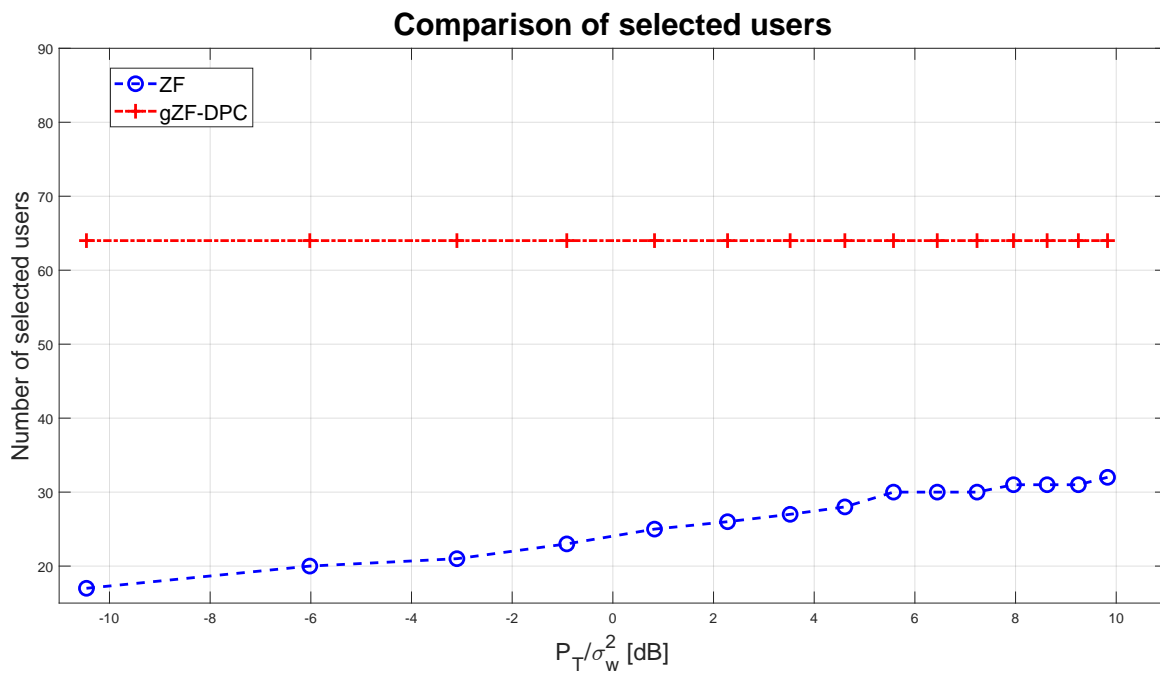


FIGURE 4.8: Comparison of number of selected users between DPC and ZF (100 available users and 64 antennas)

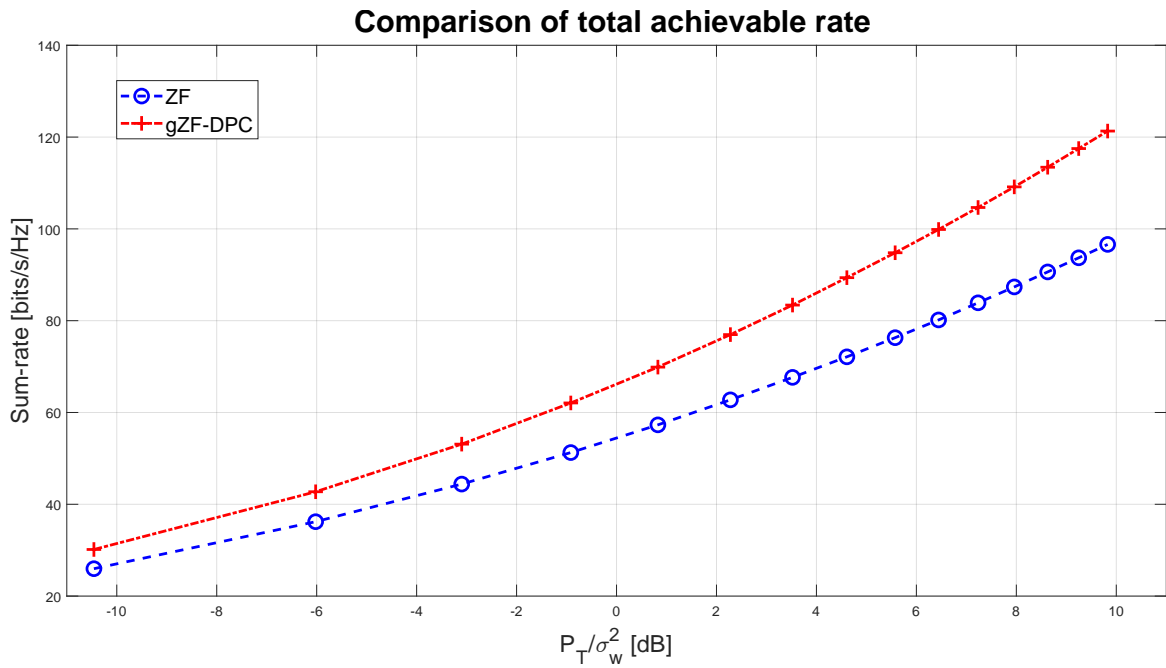


FIGURE 4.9: Comparison of the total achievable rate between DPC and ZF (1000 available users and 64 antennas)

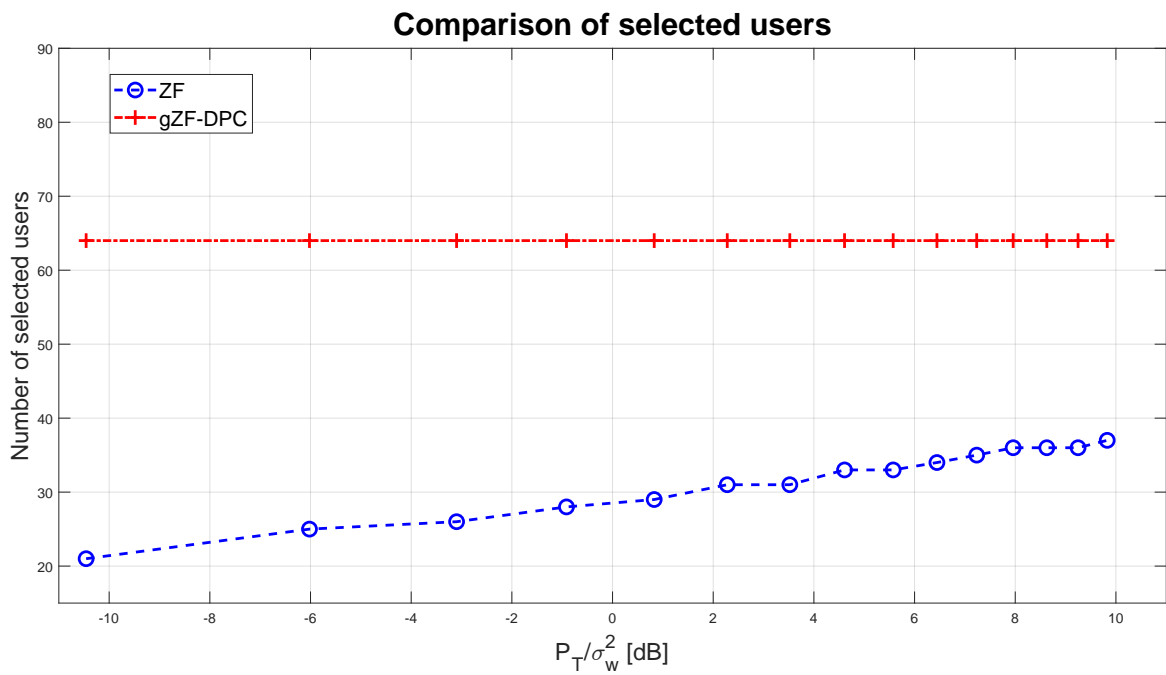


FIGURE 4.10: Comparison of number of selected users between DPC and ZF (1000 available users and 64 antennas)



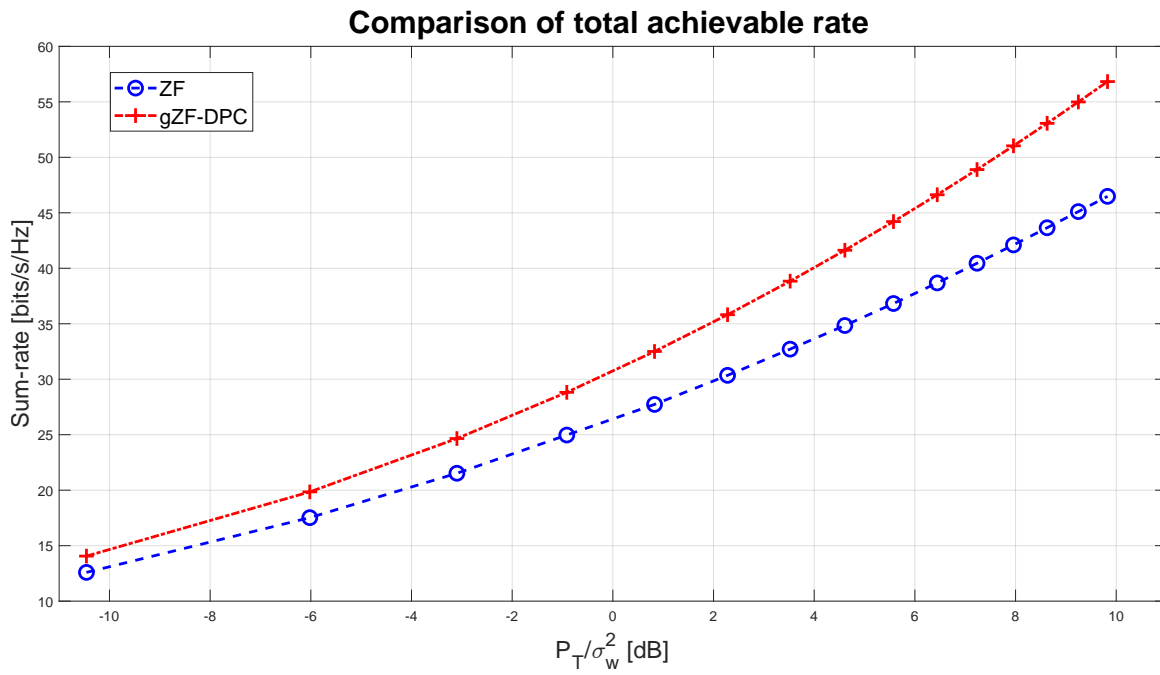


FIGURE 4.11: Comparison of the total achievable rate between DPC and ZF (100 available users and 32 antennas)

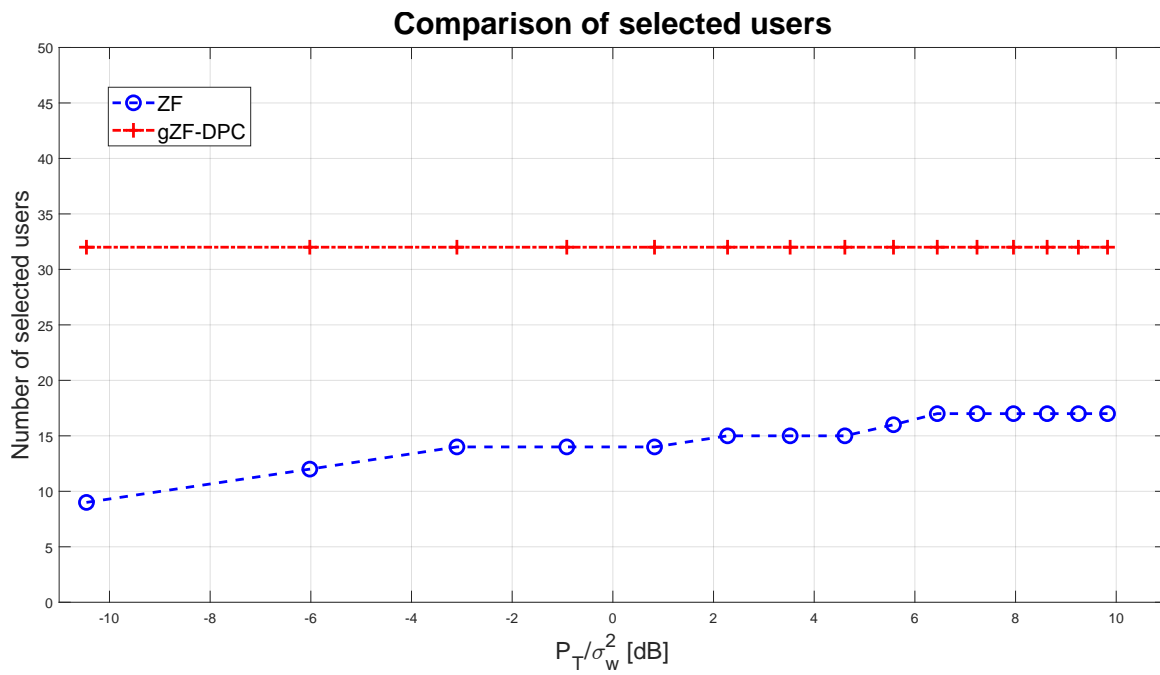


FIGURE 4.12: Comparison of number of selected users between DPC and ZF (100 available users and 32 antennas)



## Chapter 5

# Hybrid Beamforming

To deal with the fast-increasing demand of higher data rate and low latency, the carrier frequency need to be increased in order to expand the bandwidth available for the transmissions. This is the reason why next generation of wireless networks will adopt mmWave frequency.

As described in 2.2, the propagation of signals at higher frequency leads to worse performance due to the frequency-dependence of the path loss term and more significant loss of energy caused by various phenomena of wave's propagation (reflection, scattering, ...).

An advantage of mmWave is that the shorter wavelength enables more antennas to be packed in the same space, which allows high-directional transmissions, necessary to overcome the problem of worse physical propagation.

There are three basic architectures: analog beamforming, digital beamforming and hybrid beamforming.

### 5.1 Analog Beamforming

This system is implemented by a phased array with only one RF chain driven by a digital-to-analog converter (DAC), as shown in Figure 5.1.

Employing analog beamforming, the same signal is fed to each antenna and analog phase-shifters are used to steer the signal emitted by the array.

The phase shifter weights are adaptively adjusted using digital signal processing to steer the beam in order, for instance, to maximize the total achievable rate. [12]

The resulting beam consists of constructive and destructive interference based on the direction.

RF phase shifters can be either active or passive: the former category introduces performance degradation due to phase-shifter loss, noise and non-linearity, whereas the latter category has a lower consumption without non-linear distortion, nevertheless it occupies a larger area. [12]

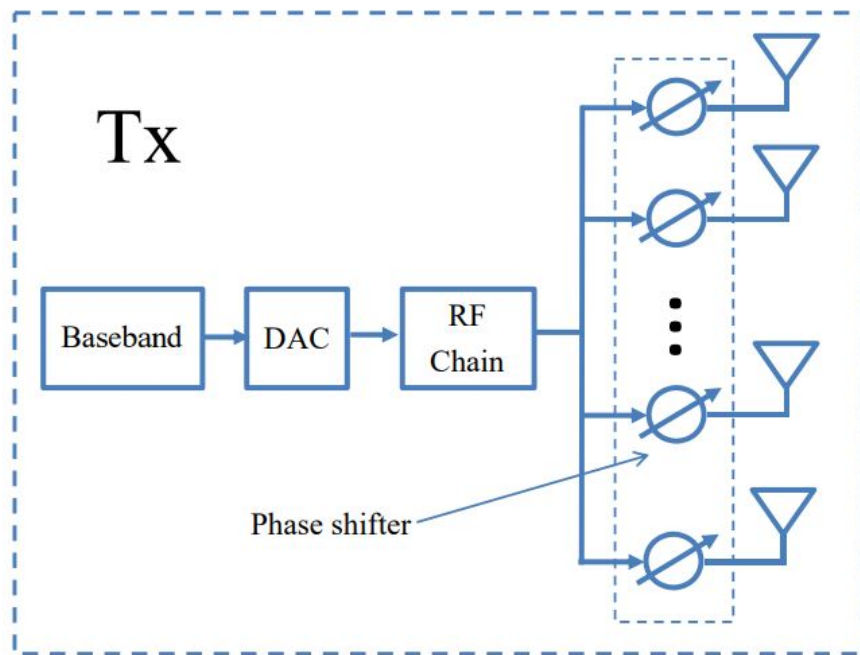


FIGURE 5.1: Analog Beamforming architecture [3]

Analog Beamforming cannot be used for Multi-User MIMO systems, because having only one RF chain, it only supports single-stream transmission.

## 5.2 Digital Beamforming

In Digital Beamforming the number of RF chains is equal to the number of antennas.

As shown in Figure 5.2, each antenna is connected to its own RF chain and DAC; in this way independent signals can be transmitted to different users.

This precoding scheme is the optimal solution for the scheduling problem, studied with the Algorithms 4.3 and 3.2.2, this is due to its higher flexibility in terms of signal processing.

Nevertheless, using a conventional fully Digital Beamforming is not viable in practice: many hardware components would be needed, including signal mixers, analog-to-digital/digital-to-analog converters (ADCs/DACs), and power amplifiers.

These devices would have to be packed behind each antenna, and all the antenna elements are placed very close to each other to avoid grating lobes; hence it is a problem due to the space limitation. [12]

Thus, having one RF chain for each antenna element means prohibitive cost and power consumption.

Indeed, the increase of energy consumption in wireless communication systems

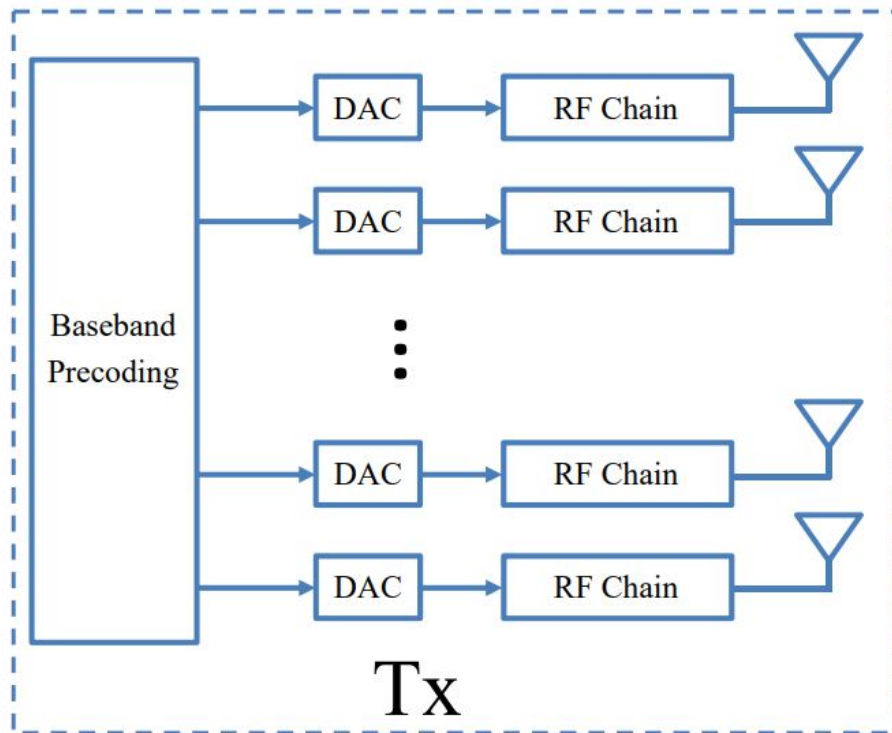


FIGURE 5.2: Digital Beamforming architecture [3]

causes an increase of CO<sub>2</sub> emission indirectly, which currently is considered as a major threat for the environment. [26]

### 5.3 Hybrid Beamforming

Hybrid Analog and Digital Beamforming limits the number of RF chains and DAC, reducing energy consumption and system design complexity.

It employs a combination of analog beamformer in the RF domain and digital beamformer in the baseband domain. That leads to fewer RF chains compared to the number of active elements as shown in Figure 5.3.

Compared with analog beamforming, hybrid beamforming supports multistream transmission with spatial multiplexing because it has not only one RF chain, thus this architecture can be exploited to solve the scheduling problem of a MU-MIMO system.

The target is to optimally design both digital and analog precoders, to solve the scheduling of users.

The system is described by  $N_u$  selected users,  $N_t$  antennas and the number of RF chains is denoted as  $N_t^{RF}$ .

The final beamformer can be written as product of the digital precoder  $\mathbf{F}_{BB}$  and the

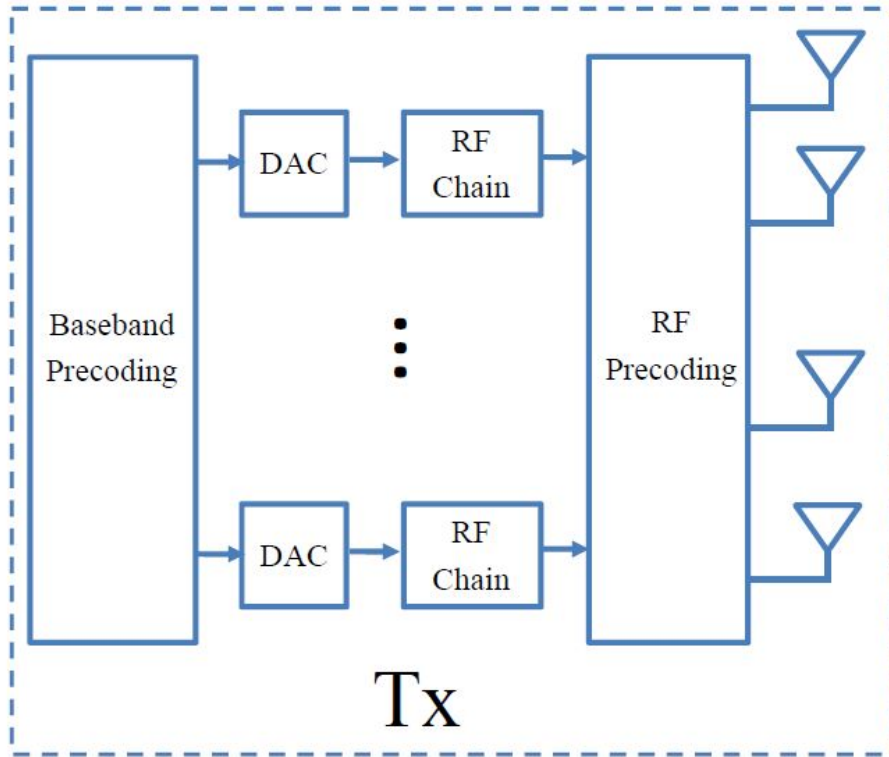


FIGURE 5.3: Hybrid Beamforming architecture [3]

analog precoder  $\mathbf{F}_{RF}$ :

$$\mathbf{B} = \mathbf{F}_{RF}\mathbf{F}_{BB} \quad (5.1)$$

where  $\mathbf{F}_{BB}$  is a matrix of size  $N_t^{RF} \times N_u$  and  $\mathbf{F}_{RF}$  is a matrix of size  $N_t \times N_t^{RF}$ .

The number of RF chains is a steady feature of the system since it counts the number of independent hardware blocks to up-convert the processed signals to the carrier frequency.

Thus, once the system is defined, the dimensions of the matrices  $\mathbf{F}_{RF}$  and  $\mathbf{F}_{BB}$  are fixed.

Moreover, since the analog precoder is implemented using analog phase shifters, all its elements have equal norm.

Starting from the digital precoder, denoted as  $\mathbf{F}_{opt}$  because it is the optimal solution for the MU-MIMO system, its closer hybrid beamformer can be obtained by solving the following problem:

$$\left(\mathbf{F}_{RF}^{opt}, \mathbf{F}_{BB}^{opt}\right) = \operatorname{argmin} \quad \|\mathbf{F}_{opt} - \mathbf{F}_{RF}\mathbf{F}_{BB}\|_F \quad (5.2a)$$

$$\text{subject to } \mathbf{F}_{RF} \in \mathcal{F}_{RF} \quad (5.2b)$$

where  $\mathcal{F}_{RF}$  is the set of feasible RF precoders, based on phase shifters, and  $\|\cdot\|_F$  denotes the Frobenius norm.

The number of RF chains  $N_t^{RF}$  sets a limitation in the maximum number of users for the transmission, indeed it is necessary that  $N_t^{RF}$  is greater than or equal to the number of users:

$$N_t^{RF} \geq N_u \quad (5.3)$$

*Proof.* Due to the dimensions of the analog and digital precoder, these inequalities can be written:  $\text{rank}(\mathbf{F}_{RF}\mathbf{F}_{BB}) \leq N_t^{RF}$  and  $\text{rank}(\mathbf{F}_{opt}) = N_u$ .

Therefore, hybrid beamforming structure requires at least  $N_t^{RF} \geq N_u$  RF chains to implement the precoder.  $\square$

The complex non-convex nature of the feasible set  $\mathcal{F}_{RF}$  makes it impossible to solve the problem 5.2 in closed form.

In [2] a near-optimal solution is proposed, exploiting Orthogonal Matching Pursuit.

This method requires a set of possible feasible vectors and selects the vector along which the optimal precoder  $\mathbf{F}_{opt}$  has the maximum projection as a column of  $\mathbf{F}_{RF}$ .

To obtain the digital precoder, this algorithm solves the least-squares (LS) problem that minimizes the norm of the error and then computes the residual as the difference between the optimal matrix and its result.

It iteratively proceeds by seeking the vector of the set along which the residual has the largest projection and then updates the residual matrix.

The process continues until all the columns of  $\mathbf{F}_{RF}$  are selected.

The precoder studied in [2] is based on the singular value decomposition of the channel.

It is shown that the columns of this precoder are related to the array response vectors  $\mathbf{a}_T(\theta_T)$  through a linear combination.

Since  $\mathbf{a}_T(\theta_T)$  are constant-magnitude vectors, they can be applied at RF using an analog phase shifter.

Therefore, the transmitter selects  $N_t^{RF}$  vectors of  $\mathbf{a}_T(\theta_T)$  via the RF precoder, and forms arbitrary linear combinations of them using the digital precoder  $\mathbf{F}_{BB}$ .

Due to this property, the initial set in [2] is a matrix of array response vectors  $\mathbf{a}_T(\theta_T)$ . However, this method cannot be applied to DPC because its precoder is not a linear combination of the array response vectors.

Besides, the precoder does not show sparsity property, thus it does not seem possible to obtain a set of vectors for the analog beamformer in order to employ Orthogonal Matching Pursuit.

Given the set of selected users  $\Omega$ , the complete problem to design the Hybrid Beamformer is as follows:

$$\max_{\mathbf{F}_{RF}\mathbf{F}_{BB}} \sum_{i \in \Omega} \log_2 \left( 1 + \frac{\mathbf{h}_i (\mathbf{F}_{RF}\mathbf{F}_{BB})_i (\mathbf{h}_i (\mathbf{F}_{RF}\mathbf{F}_{BB})_i)^H E_s}{\sum_{k \in \Omega, k \neq i} \mathbf{h}_i (\mathbf{F}_{RF}\mathbf{F}_{BB})_k (\mathbf{h}_i (\mathbf{F}_{RF}\mathbf{F}_{BB})_k)^H + \sigma_w^2} \right) \quad (5.4a)$$

$$\text{subject to} \quad \text{Tr}((\mathbf{F}_{RF}\mathbf{F}_{BB}) (\mathbf{F}_{RF}\mathbf{F}_{BB})^H) \leq P_T, \quad (5.4b)$$

$$\|\mathbf{F}_{RF}(l, m)\| = 1 \quad \forall l, \forall m \quad (5.4c)$$

The constant-magnitude phase shifter constraint 5.4c makes the sum-rate maximization problem nonconvex and NP-hard, thus it is hard to find a globally optimal solution.

In [14], a different approach to obtain an approximated solution is proposed.

In the first step, the analog precoder is computed with fixed  $\mathbf{F}_{BB}$ . This problem is still nonconvex because of the constraint 5.4c, nevertheless a low complexity is proposed to find a sub-optimal solution of this problem.

In the second step, the digital precoder is computed. With the analog precoder obtained in the previous step, the effective channel matrix becomes:

$$\mathbf{H}_{eff} = \mathbf{H}\mathbf{F}_{RF} \quad (5.5)$$

Hence, the optimization problem for the digital precoder is:

$$\max_{\mathbf{F}_{BB}} \sum_{i \in \Omega} \log_2 \left( 1 + \frac{\mathbf{h}_{eff_i} \mathbf{F}_{BB_i} (\mathbf{h}_{eff_i} \mathbf{F}_{BB_i})^H}{\sum_{k \in \Omega, k \neq i} \mathbf{h}_{eff_i} \mathbf{F}_{BB_k} (\mathbf{h}_{eff_i} \mathbf{F}_{BB_k})^H + \sigma_w^2} \right) \quad (5.6a)$$

$$\text{subject to} \quad \text{Tr}((\mathbf{F}_{RF}\mathbf{F}_{BB}) (\mathbf{F}_{RF}\mathbf{F}_{BB})^H) \leq P_T \quad (5.6b)$$

This problem is akin to those studied in the previous chapters using ZF and DPC, with an effective channel matrix instead of the original one.

### 5.3.1 Analog Precoder Design

The algorithm proposed in [14] consists of two phases, namely, the initialization phase and the stream section phase.

In the initialization phase, a sub-optimal solution for the first  $N_u$  RF chains is obtained, whereas in the last phase the additional RF chains are allocated.



### Initialization Phase

The downlink-uplink duality is exploited to develop this low-complexity algorithm.

The digital beamformer is set to the identity matrix:  $\mathbf{F}_{BB} = \mathbf{I}$ .

For simplicity, equal power allocation is applied:

$$\gamma = \frac{P_t}{N_t^{RF}} \quad (5.7)$$

thus, in the uplink system, the received signal of user  $k$  is equal to:

$$y_k^{UL} = \mathbf{F}_{RF,k}^H \left( \gamma \sum_{i=1}^{N_u} \mathbf{h}_i^H \mathbf{x}_i^{UL} + \mathbf{n}^{UL} \right) \quad (5.8)$$

where  $\mathbf{x}_i^{UL}$  is the transmit signal of user  $i$ .

Therefore, the SINR of user  $k$  in the uplink system, is given as:

$$SINR_k^{UL} = \frac{\text{Tr} \left( \mathbf{F}_{RF,k}^H \mathbf{G}_k \mathbf{F}_{RF,k} \right)}{\text{Tr} \left( \mathbf{F}_{RF,k}^H \mathbf{Q}_k \mathbf{F}_{RF,k} \right)} \quad (5.9)$$

where  $\mathbf{G}_k = \gamma^2 \mathbf{h}_k^H \mathbf{h}_k$  and  $\mathbf{Q}_k = \sum_{i=1, i \neq k}^{N_u} \gamma^2 \mathbf{h}_i^H \mathbf{h}_i + \sigma_w^2 \mathbf{I}$ .

The sum-rate maximization problem can be described as the maximization of the SINR for each user:

$$\max_{\mathbf{F}_{RF,k}} \quad SINR_k^{UL} \quad (5.10a)$$

$$\text{subject to} \quad \|\mathbf{F}_{RF,k}(l, m)\| = 1 \quad \forall l, \forall m \quad (5.10b)$$

This problem is still nonconvex due to the constant-magnitude constraint.

To solve it, in [14] the unconstrained problem is considered to obtain a preliminary precoder,  $\tilde{\mathbf{F}}_{RF,k}$ .

The result obtained in [14] is to compute the generalized eigenvalues of  $\mathbf{G}_k$  and  $\mathbf{Q}_k$ . The generalized eigenvector corresponding to the largest generalized eigenvalue is the preliminary solution for the user:

$$\tilde{\mathbf{F}}_{RF,k} = \text{eig}(\mathbf{G}_k, \mathbf{Q}_k) \quad (5.11)$$

The globally optimal unconstrained precoder is expressed as:

$$\tilde{\mathbf{F}}_{RF} = \left[ \tilde{\mathbf{F}}_{RF,1} \quad \dots \quad \tilde{\mathbf{F}}_{RF,N_u} \right] \quad (5.12)$$

A general solution, for the case of multi-stream required by users, is to use the eigenvector associated to the  $d$ -th largest generalized eigenvalue for the  $d$ -th stream of each user. In this case, the total number of RF chains allocated in this phase is equal to the total number of streams: assume that each user requests  $D$  streams, at each transmission the base station transmits  $N_s = N_u D$  data streams to all users.

The final step of this phase is to obtain the solution of the constrained problem, adding 5.10b.

It is described as the projection of  $\tilde{\mathbf{F}}_{RF}$  onto the feasible region, thus it can be found by solving the following optimization problem:

$$\hat{\mathbf{F}}_{RF} = \underset{\mathbf{F}_{RF}}{\operatorname{argmin}} \quad \|\tilde{\mathbf{F}}_{RF} - \mathbf{F}_{RF}\|_F^2 \quad (5.13a)$$

$$\text{subject to } \|\mathbf{F}_{RF}(l, m)\| = 1 \quad \forall l, \forall m \quad (5.13b)$$

The globally optimal solution studied in [14] is:

$$\hat{\mathbf{F}}_{RF} = e^{j\arg(\tilde{\mathbf{F}}_{RF})} \quad (5.14)$$

where  $\arg(\cdot)$  is the element-wise argument operator.

### Stream Selection Phase

This phase is necessary when the total number of users is not equal to the number of RF chains, therefore employing the first phase is not possible to obtain the whole analog precoder, since  $N_t^{RF} - N_u$  RF chains are not allocated.

The generalized eigenvalue of each user can be written as:

$$\lambda_k = \frac{(\tilde{\mathbf{F}}_{RF,k})^H \mathbf{G}_k \tilde{\mathbf{F}}_{RF,k}}{(\tilde{\mathbf{F}}_{RF,k})^H \mathbf{Q}_k \tilde{\mathbf{F}}_{RF,k}} \quad (5.15)$$

it describes the maximum SINR that can be achieved by user  $k$ . Using the projection of  $\tilde{\mathbf{F}}_{RF}$  onto the feasible region, a SINR loss is introduced.

For user  $k$ , it is denoted as  $\Delta\lambda_k$ :

$$\Delta\lambda_k = \lambda_k - \frac{(\hat{\mathbf{F}}_{RF,k})^H \mathbf{G}_k \hat{\mathbf{F}}_{RF,k}}{(\hat{\mathbf{F}}_{RF,k})^H \mathbf{Q}_k \hat{\mathbf{F}}_{RF,k}} \quad (5.16)$$

In this phase, this algorithm allocated the additional  $N_t^{RF} - N_u$  RF chains to the users corresponding to the highest loss  $\Delta\lambda_k$ .

As described in [16], a complex number  $c = \rho e^{j\alpha}$  with  $0 \leq \rho \leq 2$  can be expressed

as sum of two complex number with unitary magnitude:

$$c = e^{j\theta} + e^{j\phi} \quad (5.17)$$

where,

$$\theta = \alpha + \cos^{-1} \left( \frac{\rho}{2} \right) \quad (5.18)$$

$$\phi = \alpha - \cos^{-1} \left( \frac{\rho}{2} \right) \quad (5.19)$$

When  $\rho > 2$ , this decomposition can still be applied by introducing a normalization factor.

Thus, the unconstrained precoder can be decomposed into the sum of two analog beams satisfying the constant magnitude constraint.

Using this procedure other  $N_t^{RF} - N_u$  RF chains can be allocated.

## 5.4 Scheduling MU-DPC Hybrid

The base station receives, as feedback from the users, the channel vector of all the available users for the transmission.

The whole algorithm to obtain the precoder for the transmission consists of 4 steps, namely the users' selection, the design of the analog precoder, the inner precoder and, as last phase, the outer precoder.

### 5.4.1 Users' selection

The objective of the first step is to select a subset of users  $\Omega$  to maximize the total rate of the downlink transmission.

If the number of available users is greater than the number of RF chains, the maximum number of selected users is equal to the number of RF chains using the optimal digital precoder based on DPC.

The greedy algorithm, for this purpose, is described in 4.3, but with a stronger limitation in the number of users for the selected set.

Otherwise, if the number of available users is lower than the number of RF chains, the procedure follows a sum power iterative waterfilling algorithm, analogous to 3.2.2 but employing DPC.

Although the computational complexity is much higher, the number of iterations is limited to the number of available users (lower than the number of RF chains), hence it is acceptable.

The total achievable rate of these algorithms is the same, as described in 4.4. Starting from the complete channel matrix with a set of users  $\Psi$ , employing this algorithm, the subset  $\Omega$  and the channel matrix  $\mathbf{H}$  of these users are obtained.

### 5.4.2 Analog Precoder Design

The analog precoder implemented for hybrid beamforming is described in the Initialization Phase of 5.3.1. If the number of available users is greater than the number of RF chains, the stream selection phase is not required because the number of users selected is equal to the number of RF chains.

The analog precoder is implemented using phase shifter, whose values are given by the matrix  $\mathbf{F}_{RF}$ .

### 5.4.3 Inner Precoder Design

With the analog precoder  $\mathbf{F}_{RF}$ , obtained in the previous step, it is possible to define an effective channel matrix:

$$\mathbf{H}_{eff} = \mathbf{H}\mathbf{F}_{RF}$$

Then, the LQ-decomposition is applied:

$$\mathbf{H}_{eff} = \mathbf{L}\mathbf{Q}$$

The inner precoder is set to:  $\mathbf{B} = \mathbf{Q}^H\mathbf{P}$ . To get the entries of the diagonal matrix  $\mathbf{P}$ , the waterfilling algorithm described in 4.1.1 is employed.

This algorithm needs to take into account the difference in the total available power introduced by the analog precoder  $\mathbf{F}_{RF}$ , the power constraint is:

$$\text{Tr}((\mathbf{F}_{RF}\mathbf{F}_{BB})(\mathbf{F}_{RF}\mathbf{F}_{BB})^H) \leq P_T \quad (5.20)$$

that can be written as:

$$\begin{aligned} \text{Tr}((\mathbf{F}_{RF}\mathbf{F}_{BB})(\mathbf{F}_{RF}\mathbf{F}_{BB})^H) &= \text{Tr}((\mathbf{F}_{RF}\mathbf{F}_{BB})^H(\mathbf{F}_{RF}\mathbf{F}_{BB}))^* \\ &= \text{Tr}(\mathbf{F}_{BB}^H\mathbf{F}_{RF}^H\mathbf{F}_{RF}\mathbf{F}_{BB})^* \\ &= \text{Tr}(\mathbf{P}^H\mathbf{Q}\mathbf{F}_{RF}^H\mathbf{F}_{RF}\mathbf{Q}^H\mathbf{P}) \leq P_T \end{aligned}$$

As described in Chapter 3, this trace depends only on the diagonal elements of  $\mathbf{Q}\mathbf{F}_{RF}^H\mathbf{F}_{RF}\mathbf{Q}^H$ , because the power matrix  $\mathbf{P}$  is diagonal.

These diagonal entries are used as multiplicative factor in the power constraint of the waterfilling procedure.

#### 5.4.4 Outer Precoder Design

The outer encoder is implemented through a successive coding process based on DPC.

A complete description of the interference observed by users can be written as function of the elements of the matrices  $\mathbf{L}$  and  $\mathbf{P}$  computed in the previous step.

As described in 4.1.2, this procedure allows  $\text{Int}(k < i)$  to be removed.

### 5.5 MATLAB Code

The MATLAB code of the users' selection algorithm described in 5.4 is shown below.

```

1 %% Initialization of the variables
2
3 N_users = 100; % Number of available users
4 N_antennas = 64; % Number of antennas at the transmitter
5 Power = 1; % Available power of the transmitter
6 Es = 1; % Energy of the symbols
7 Np = 10; % Number of paths (scatterers)
8 Sigma_w2 = 1; % Variance of the noise
9 Nt_RF = 12; % Number of RF chains
10
11 %% Channel matrix initialization
12
13 [H,steering_vector] = Channel_model([N_users,N_antennas],Np,'ULA');
14
15 %% Users' selection
16
17 [H_best,~] = greedy_DPC(H,Nt_RF,Power,Es,Sigma_w2);
18 Users = size(H_best,1);
19
20 %% Analog Precoder Design
21
22 % Hybrid beamforming
23 V_RF = Analog_Precoder(H_best,Nt_RF,Users,N_antennas,Sigma_w2);
24
25 % Effective channel
26 H_best_eff = H_best*V_RF;
27

```

```

28 % Inner precoder design
29 [Q,P,Capacity] = DPC2(H_best_eff, Power, Es, Sigma_w2,V_RF);
30
31 %% Results
32
33 disp(['This algorithm based on DPC selects ',num2str(Users),' users
    and the achieved total rate is',num2str(Capacity)]);
34
35
36 %% Channel Model function
37
38 % This function returns the channel matrix H
39
40 function [H,array_steering_vector_tx] = Channel_model(size,Np,type)
41
42 % size is a vector that consists of the size of the channel matrix:
    size(1) is the number of users and size(2) is the number of
    antennas of the base station. Np denotes the number of scatterers
    . The type of the antenna can be either ULA or UPA.
43
44 path_loss = 1;
45 H = zeros(size);
46 N = size(2);
47
48 % ULA case
49 if isequal(type,'ULA')
50     for i=1:size(1)
51
52         % randomly select the angle of departure
53         phi = rand(Np,1).*2*pi;
54
55         % define the normalized spatial angle
56         nsa = sin(phi)/2;
57         array_steering_vector_tx = 1/sqrt(N).*exp(1j*2*pi*nsa*(0:(N
    -1)))';
58         channel_coeff = sqrt(N/(Np*path_loss)).*(randn(Np,1)+1j*randn
    (Np,1)).*(sqrt(2)/2);
59         H(i,:) = array_steering_vector_tx*channel_coeff;
60     end
61 end
62
63 %UPA case
64 if isequal(type,'UPA')
65     array_steering_vector_tx = zeros(N,Np);
66     N=sqrt(N);
67     for i=1:size(1)

```

```

68     for j=1:Np
69         % randomly select the angles of departure
70         phi = rand(1).*2*pi;
71         theta = rand(1).*pi - pi/2;
72         ni = pi*sin(phi).*sin(theta);
73         mu = pi*cos(phi).*sin(theta);
74         array_row = exp(1j*mu.*(0:N-1));
75         array_col = exp(1j*ni.*(0:N-1));
76         matrix_steering = array_row'*array_col;
77         array_steering_vector_tx(:,j) = (1/N).*reshape(
matrix_steering.',1,[]);
78     end
79     channel_coeff = (N/sqrt((Np*path_loss))).*(randn(Np,1)+1j*
randn(Np,1)).*(sqrt(2)/2);
80     H(i,:) = array_steering_vector_tx*channel_coeff;
81     end
82 end
83
84 % approximate the channel matrix
85 H=floor(H*100)/100;
86 end
87
88 %% Algorithm for the users' selection
89
90 % This function obtains the sub optimal set of users H_best in order
to maximize the total achievable rate. max_users is the maximum
number of users that can be selected, using hybrid beamforming
this value is equal to the number of RF chains.
91
92 function [H_best,C] = greedy_DPC(H,max_users,Power,Es,Sigma_w2)
93 N = size(H,2);
94 R = diag(H*H');
95 [~,I] = max(R);
96 H_best = H(I,:);
97 n = 1;
98 while n<max_users
99     n=n+1;
100     P = eye(N) - H_best'*inv(H_best*H_best')*H_best;
101     R = diag(H*P*H');
102     [~,I] = max(R);
103     H_best = [H_best;H(I,:)];
104 end
105
106 % H_best is the optimal channel matrix, selected during the first
phase of the algorithm
107

```

```

108 % To obtain the optimal precoder, waterfilling is used
109 [L,~] = LQ(H_best);
110 L_diag = diag(L);
111 B = modified_waterfilling(L_diag,Power);
112
113 % Evaluate the Capacity
114 C = sum((log2(1+(L_diag.^2.*B)*Es/Sigma_w2)));
115 end
116
117 %% Analog Precoder Design
118
119 % Algorithm for the design of the analog precoder V_RF as described
    in 5.3.1. This algorithm is proposed in [14].
120
121 function [V_RF] = Analog_Precoder(H,Nt_RF,N_selected_users,N_antennas
    ,Sigma_w2)
122
123 % First we design an analog precoder for the first N_selected_users
    RF chains
124
125 gamma = 1/80;
126 Gk = zeros(N_antennas,N_antennas,N_selected_users);
127 Qk = zeros(N_antennas,N_antennas);
128 for i = 1:N_selected_users
129     Qk = Qk + gamma.*H(i,:)'*H(i,:);
130 end
131 Qk = Qk + eye(N_antennas).*Sigma_w2;
132 Qk = repmat(Qk, 1, 1, N_selected_users);
133 for i = 1:N_selected_users
134     Gk(:,:,i) = gamma.*H(i,:)'*H(i,:);
135     Qk(:,:,i) = Qk(:,:,i) - Gk(:,:,i);
136 end
137
138 V_tilda_RF = zeros(N_antennas,N_selected_users);
139 eigen = zeros(N_selected_users,1);
140 for j = 1:N_selected_users
141     [V,D] = eig(Gk(:,:,j),Qk(:,:,j));
142     [a,I] = max(diag(D));
143     eigen(j) = a;
144     V_tilda_RF(:,j) = V(:,I);
145 end
146 V_RF =exp(1j*angle(V_tilda_RF));
147
148 % Now we allocate more Nt_RF - N_selected_users RF chains, if
    necessary.
149 if Nt_RF ~= N_selected_users

```



```

150     delta_eigenvalues = zeros(size(eigen));
151     for j = 1:N_selected_users
152         delta_eigenvalues(j) = eigen(j)-(V_RF(:,1) '*Gk(:, :, 1)*V_RF
153         (:,1))/(V_RF(:,1) '*Qk(:, :, 1)*V_RF(:,1));
154     end
155     V_RF = [V_RF, zeros(N_antennas, Nt_RF-N_selected_users)];
156     [~, I] = sort(delta_eigenvalues);
157     I = I(1:Nt_RF-N_selected_users);
158     for i = 1:size(I,1)
159         d = I(i);
160         module = abs(V_tilda_RF(:,d));
161         phase = angle(V_tilda_RF(:,d));
162         theta = phase + acos(module./2);
163         phi = phase - acos(module./2);
164         V_RF(:,d) = exp(1j*theta);
165         V_RF(:, N_selected_users + i) = exp(1j*phi);
166     end
167 end
168
169 %% DPC Algorithm
170
171 % Algorithm to compute the digital precoder based on DPC.
172
173 function [Q,P,C]=DPC2(H, Power_constraint, Es, Sigma_w2, V_RF )
174
175 % Compute the LQ decomposition of the channel matrix H
176 [L,Q] = LQ(H);
177 L_diag = diag(L);
178 power_diag = real(diag(Q*(V_RF')*V_RF*Q'));
179
180 %Waterfilling is used to obtain the optimal power matrix P
181 P = modified_waterfilling(L_diag, Power_constraint, power_diag);
182
183 % Compute the capacity
184 C = sum((log2(1+(L_diag.^2.*B)*Es/Sigma_w2)));
185 end
186
187 %% Waterfilling Algorithm
188
189 % Algorithm to obtain the optimal power distribution among the
190     different antennas.
191
192 function [Pn_opt2] = modified_waterfilling(varargin)
193 switch nargin

```

```

194     case 2
195         % Case of standard waterfilling, solution of the digital
196         beamforming optimization problem.
197
198         SNR_0 = varargin{1};
199         P_total = varargin{2};
200         options = optimset('Display','off');
201         fun = @(Pn_opt) -sum(log2(1+Pn_opt.*(SNR_0.^2)));
202         x = ones(size(SNR_0))*P_total/size(SNR_0,1);
203         Pn_opt2 = fmincon(fun,x,ones(size(x')),P_total,[],[],zeros(
204         size(x)),[],[],options);
205
206     case 3
207         % Case in which the power constraint consists of the scalar
208         product between the power vector and P_diag, solution of the
209         hybrid beamforming optimization problem
210
211         SNR_0 = varargin{1};
212         P_total = varargin{2};
213         P_diag = varargin{3};
214         options = optimset('Display','off');
215         fun = @(Pn_opt) -sum(log2(1+Pn_opt.*(SNR_0.^2)));
216         x = ones(size(SNR_0))*P_total/size(SNR_0,1);
217         Pn_opt2 = fmincon(fun,x,P_diag',P_total,[],[],zeros(size(x))
218         ,[],[],options);
219     end
220 end
221
222 %% LQ decomposition
223
224 % Given that the matrix H has size NxM, this decomposition allows the
225 output matrices to have sizes NxN and NxM respectively. N has to
226 be smaller than M.  $H = r*q$ 
227
228 function [r,q]=LQ(H)
229 N=size(H,1);
230 H=H';
231 [q,r]=qr(H);
232 q=q';
233 r=r';
234 r=r(:,1:N);
235 q=q(1:N,:);
236 end

```

## Chapter 6

# Results and Simulations

In this chapter various results are shown, the studied parameters consist of the total achievable rate of the downlink transmission and the number of selected users, in different simulations.

The comparison is between the algorithm described in 5.4 based on DPC and an analogous one based on ZF.

### 6.1 Comparison among different channels

The first simulation, described in Figure 6.1 and 6.2, is among different distributions of users using a ULA. This kind of antenna enables 2D beamforming, indeed the array steering vector only depends on the angle of arrival  $\theta_T$ .

For each user 10 scatterers arrive from different directions and define the channel vector.

The distribution of users is modified by varying the range of the angle of departure, assumed to be uniformly distributed:

$$\text{Channel 1} \longrightarrow \theta_T \sim \mathcal{U}(0, 2\pi)$$

$$\text{Channel 2} \longrightarrow \theta_T \sim \mathcal{U}(0, \pi)$$

$$\text{Channel 3} \longrightarrow \theta_T \sim \mathcal{U}\left(0, \frac{\pi}{2}\right)$$

Employing the same channel, the algorithm based on DPC shows a higher total rate than that based on ZF.

The worst scenario, for this scheme, is represented by channel 3, when the range of the angle of departure is tighter.

In this condition, however, the loss of ZF compared to the best-case scenario (channel 1) is higher than the same comparison of DPC.

Thus, the gap of the total rate between the algorithms is more relevant when the paths are not uniformly distributed over  $2\pi$ .

This condition represents a more practical scenario, where the angles of departure can be close to each other, because of the environment, also for different users.

This property is shown in 6.3 as well, where a UPA is utilized.

The smaller antenna size, exploiting both dimensions, and the 3D beamforming are the main advantages of this kind of antenna, however the total achievable rate is comparable.

Also in this simulation, 3 different scenarios are studied:

$$\begin{aligned} \text{Channel 1} &\longrightarrow \theta_T \sim \mathcal{U}(0, 2\pi), & \phi_T &\sim \mathcal{U}\left(-\frac{\pi}{2}, \frac{\pi}{2}\right) \\ \text{Channel 2} &\longrightarrow \theta_T \sim \mathcal{U}(0, \pi), & \phi_T &\sim \mathcal{U}\left(-\frac{\pi}{2}, \frac{\pi}{2}\right) \\ \text{Channel 3} &\longrightarrow \theta_T \sim \mathcal{U}\left(0, \frac{\pi}{2}\right), & \phi_T &\sim \mathcal{U}\left(-\frac{\pi}{2}, -\frac{\pi}{4}\right) \end{aligned}$$

where  $\theta_T$  is the azimuth angle of departure and  $\phi_T$  is the elevation angle of departure.

When the ratio  $\frac{P_T}{\sigma_w^2}$  is equal to 9.54dB, with Channel 1 the total rate of DPC is  $63.8 \frac{\text{bits/s}}{\text{Hz}}$  and the total rate of ZF is  $62.2 \frac{\text{bits/s}}{\text{Hz}}$ , leading to a difference of  $1.6 \frac{\text{bits/s}}{\text{Hz}}$ . Whereas with Channel 3 the total rate of DPC is  $58.2 \frac{\text{bits/s}}{\text{Hz}}$  and that of ZF is  $51.5 \frac{\text{bits/s}}{\text{Hz}}$ , thus the gap is  $6.7 \frac{\text{bits/s}}{\text{Hz}}$ .

As shown in Figure 6.1 for ULA, in Figure 6.3 DPC achieves a much higher total rate than ZF when the paths are not uniformly distributed over  $360^\circ$ .

In these simulations, the number of available users is 100 and the antenna consists of 64 active elements.

16 RF chains are employed in the hybrid architecture, indeed this is the maximum number of selected users as shown in Figure 6.2 and 6.4.

## 6.2 Comparison among different numbers of RF chains

A comparison of the performance among hybrid beamforming architectures based on DPC with a different number of RF chains is shown in Figure 6.5.

Increasing the number of RF chains leads to higher total rate, more users can be scheduled for the transmission, whereas the drawback is the larger number of hardware components and power consumption.

Hybrid beamforming structure limits the number of RF chains still supporting multistream transmission.

The total rate achieved by HB-DPC with 20 RF chains is close to the rate of fully digital structure using ZF, especially at low SNR. As shown in Figure 6.6, more users are scheduled with 20 RF chains than DB-ZF when  $\frac{P_T}{\sigma_w^2}$  is below  $-5\text{dB}$ .

In Figure 6.7, the comparison is between DPC and ZF with different number of RF chains, the distribution used for this simulation is Channel 1 of a ULA, thus with the lowest gap between the total rate of the algorithms.

The result provided in this simulation is that, using the same channel, the advantage of DPC is more relevant if an higher number of RF chains is employed.

### 6.3 Comparison between HB and fully DB

The last comparison is among systems of the same hardware complexity: hybrid beamformers with  $N_t^{RF}$  RF chains and fully digital precoders with only  $N_t^{RF}$  antennas for both DPC and ZF. In these simulations the considered channel is Channel 1 of a ULA with 64 antennas.

The hardware complexity is the same because in both architectures the number of signal mixers, ADCs and power amplifiers is equal to  $N_t^{RF}$ . The fully digital scheme directly connects an antenna to one RF chain, whereas in the hybrid beamforming a network of phase shifter is attached to increase the number of employed antenna, nevertheless this does not increase the power consumption because both the hardware complexity and the total power constraint are the same.

As described by Figure 6.7, there is not much difference in the total achievable rate between hybrid DPC and hybrid ZF with only 8 RF chains.

This result is shown also by Figure 6.9, however the overall rate of the hybrid architecture is more than double compared to the fully digital scheme with only 8 antennas, hence from this plot it is possible to observe the value of hybrid beamforming. In Figure 6.11 and 6.13 the same comparison is shown with respectively 12 RF chains and 20 RF chains.

Increasing the number of RF chains, the gap between fully digital beamforming and hybrid beamforming is reduced and the difference in the total rate between DPC and ZF is increased, as described in 6.2.

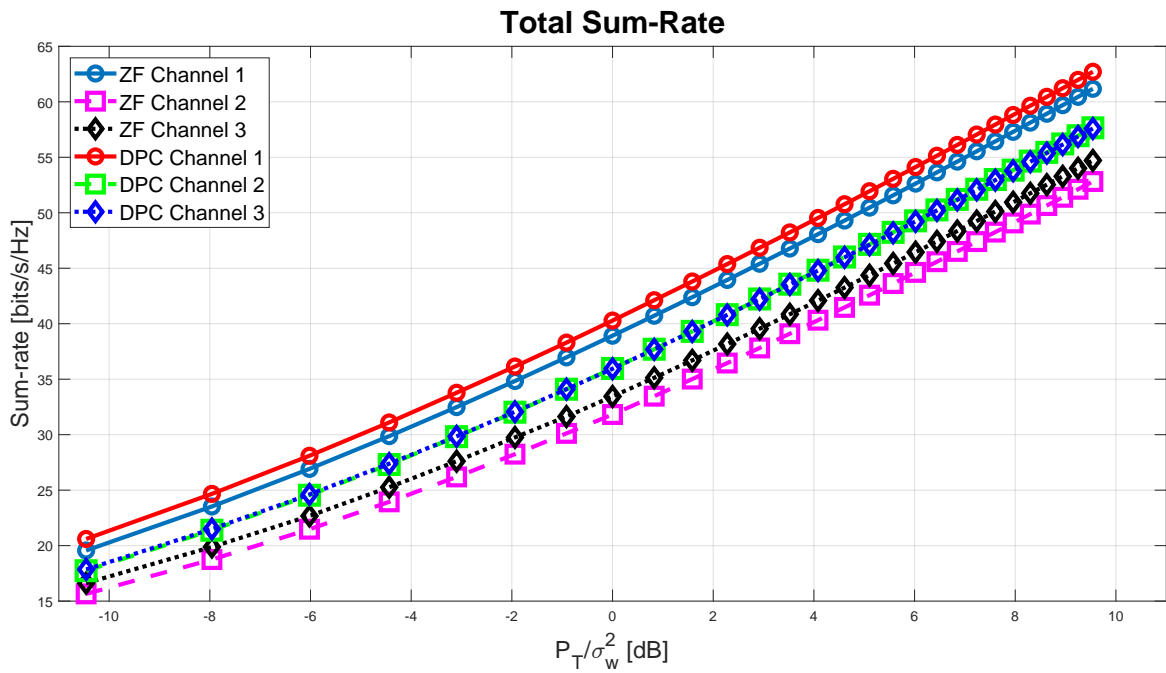


FIGURE 6.1: Comparison of the achievable rate between ZF and DPC in different scenarios using ULA ( $N_t^{RF} = 16$ ,  $N_t = 64$ ,  $N_u = 100$ ).

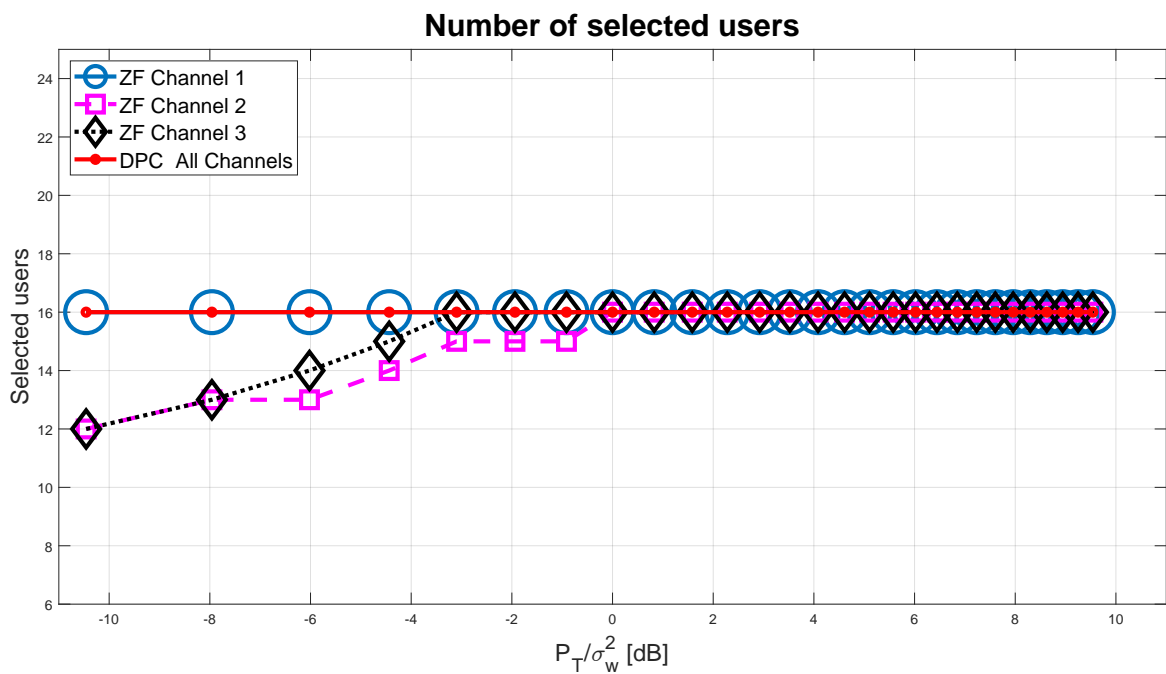


FIGURE 6.2: Comparison of the number of selected users between ZF and DPC in different scenarios using ULA ( $N_t^{RF} = 16$ ,  $N_t = 64$ ,  $N_u = 100$ ).

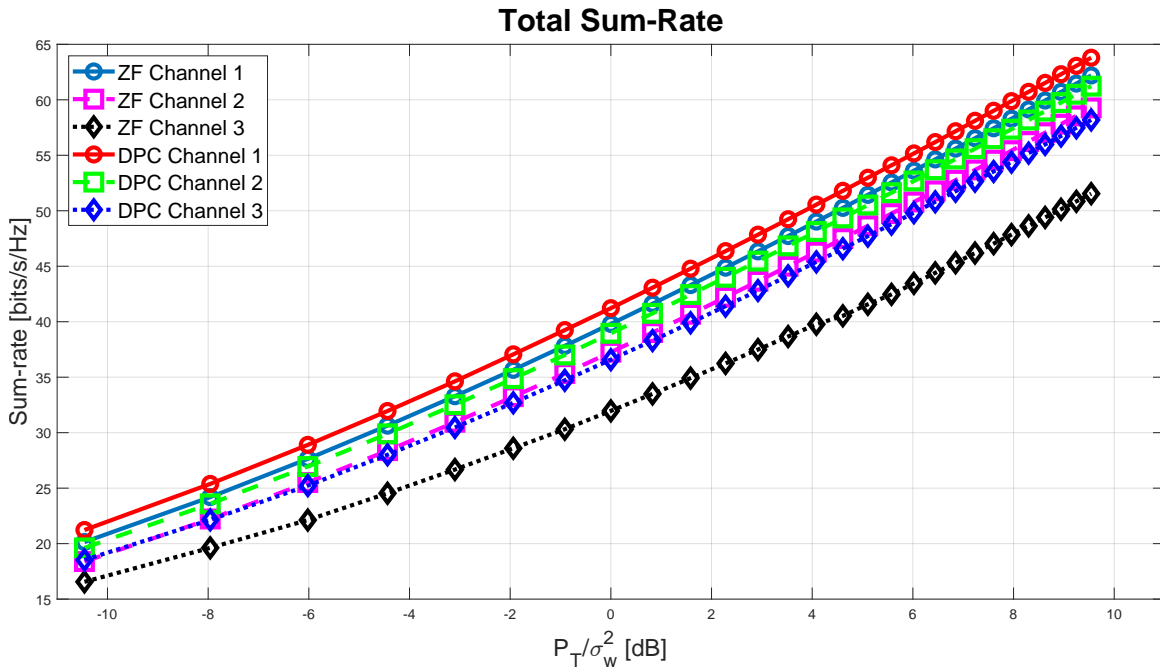


FIGURE 6.3: Comparison of the achievable rate between ZF and DPC in different scenarios using UPA ( $N_t^{RF} = 16$ ,  $N_t = 64$ ,  $N_u = 100$ ).

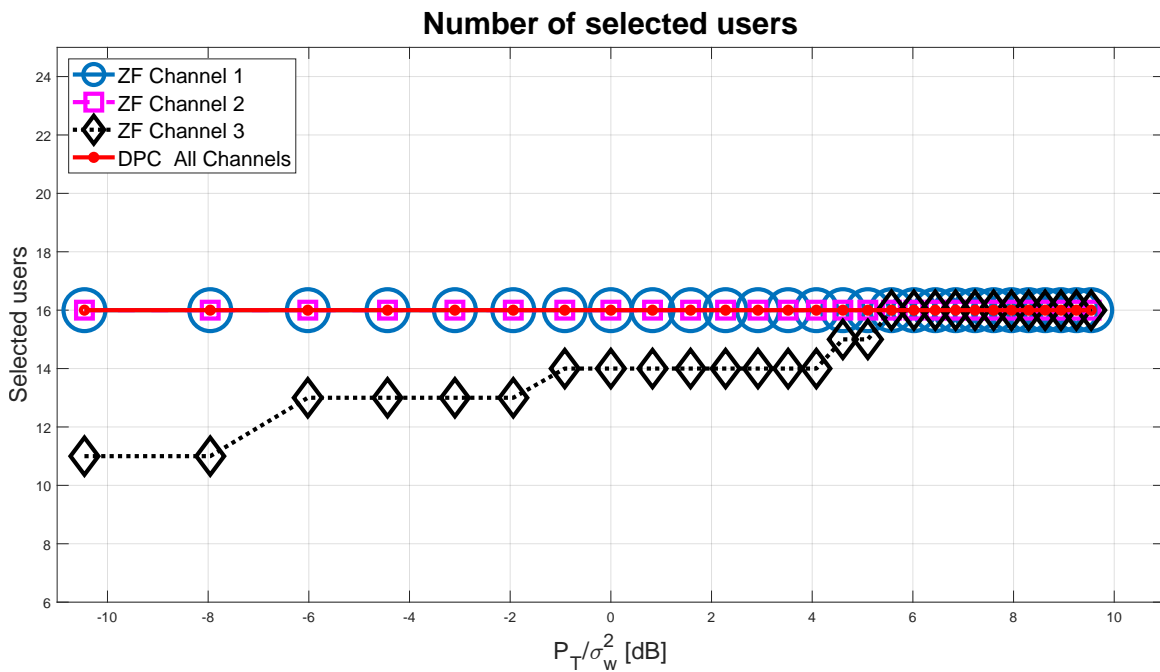


FIGURE 6.4: Comparison of the number of selected users between ZF and DPC in different scenarios using UPA ( $N_t^{RF} = 16$ ,  $N_t = 64$ ,  $N_u = 100$ ).

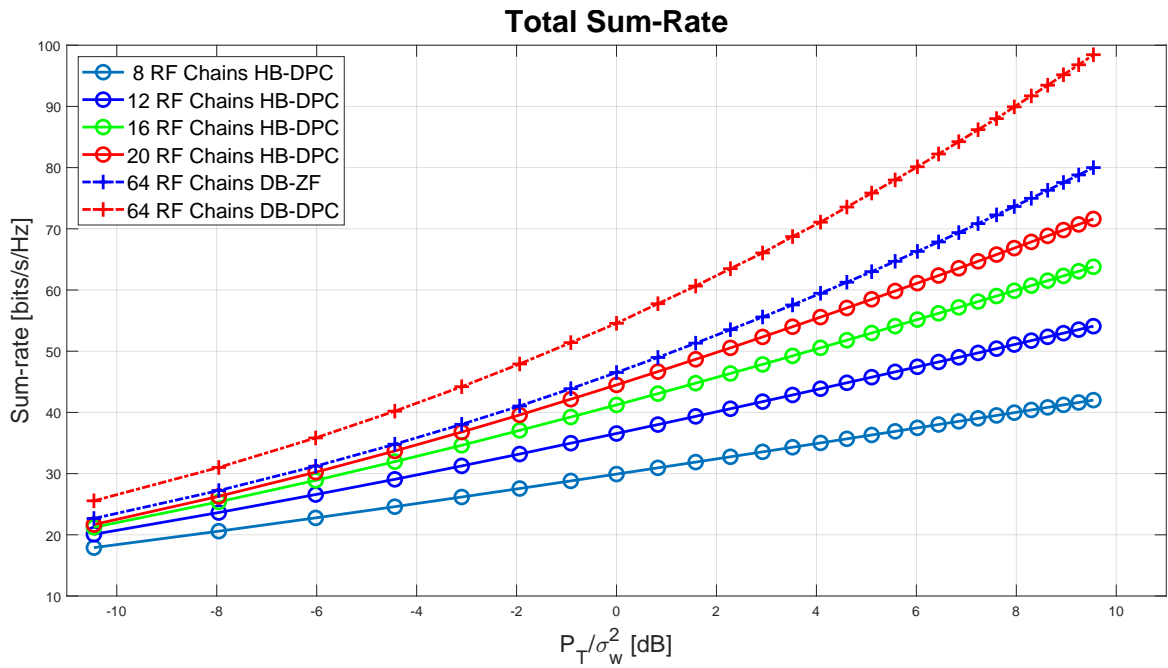


FIGURE 6.5: Comparison of the total achievable rate among DPC systems with a different number of RF chains using ULA ( $N_t = 64$ ,  $N_u = 100$ )

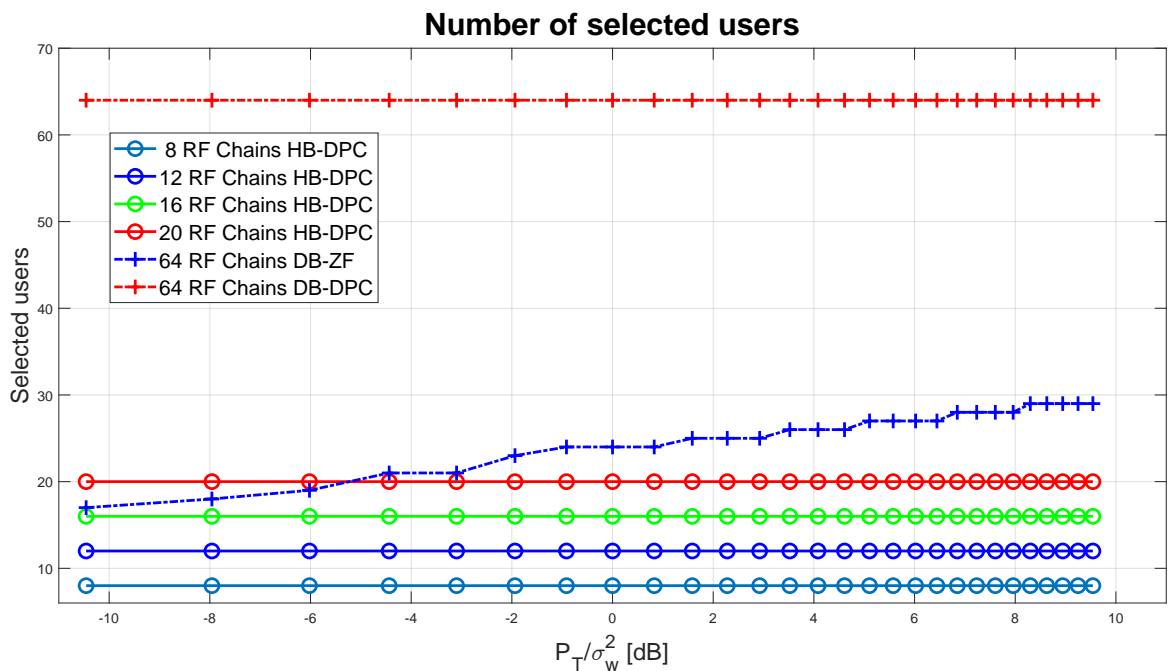


FIGURE 6.6: Comparison of the number of selected users among DPC systems with a different number of RF chains using ULA ( $N_t = 64$ ,  $N_u = 100$ )



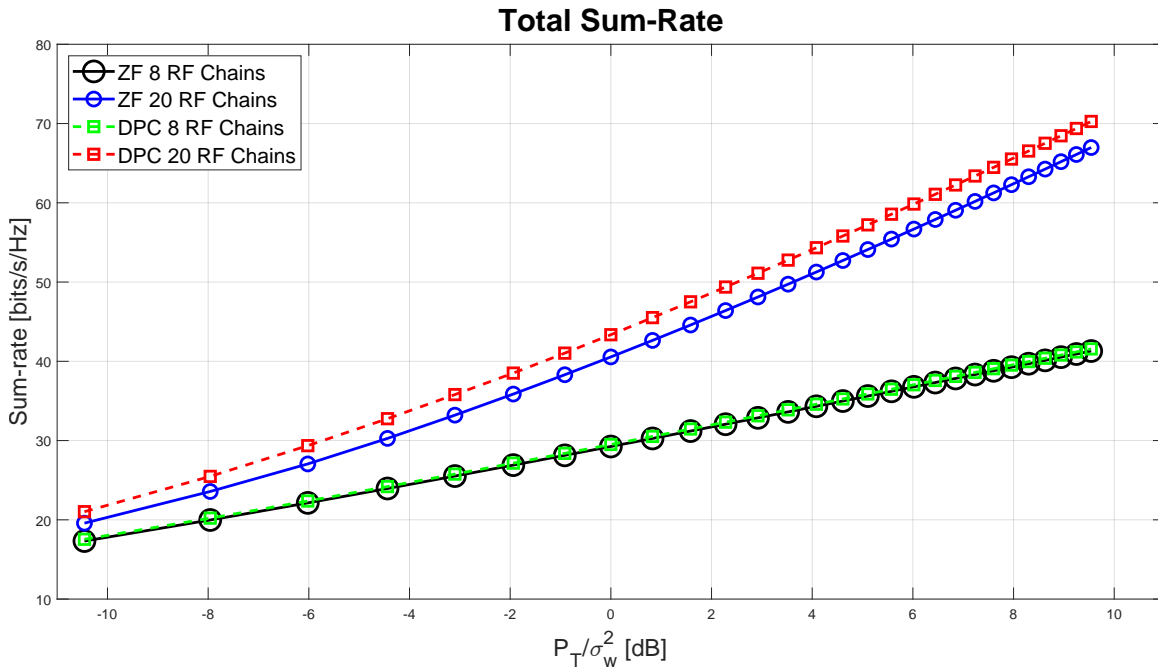


FIGURE 6.7: Comparison of the total achievable rate between DPC and ZF with a different number of RF chains using ULA ( $N_t = 64$ ,  $N_u = 100$ )

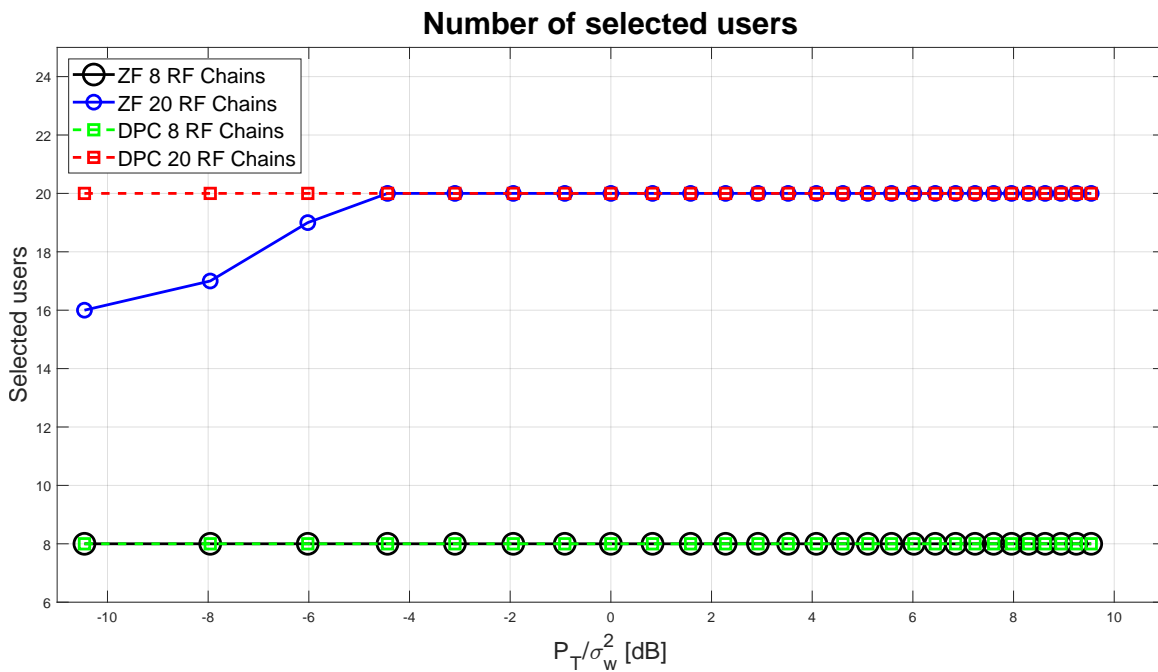


FIGURE 6.8: Comparison of the number of selected users between DPC and ZF with a different number of RF chains using ULA ( $N_t = 64$ ,  $N_u = 100$ )

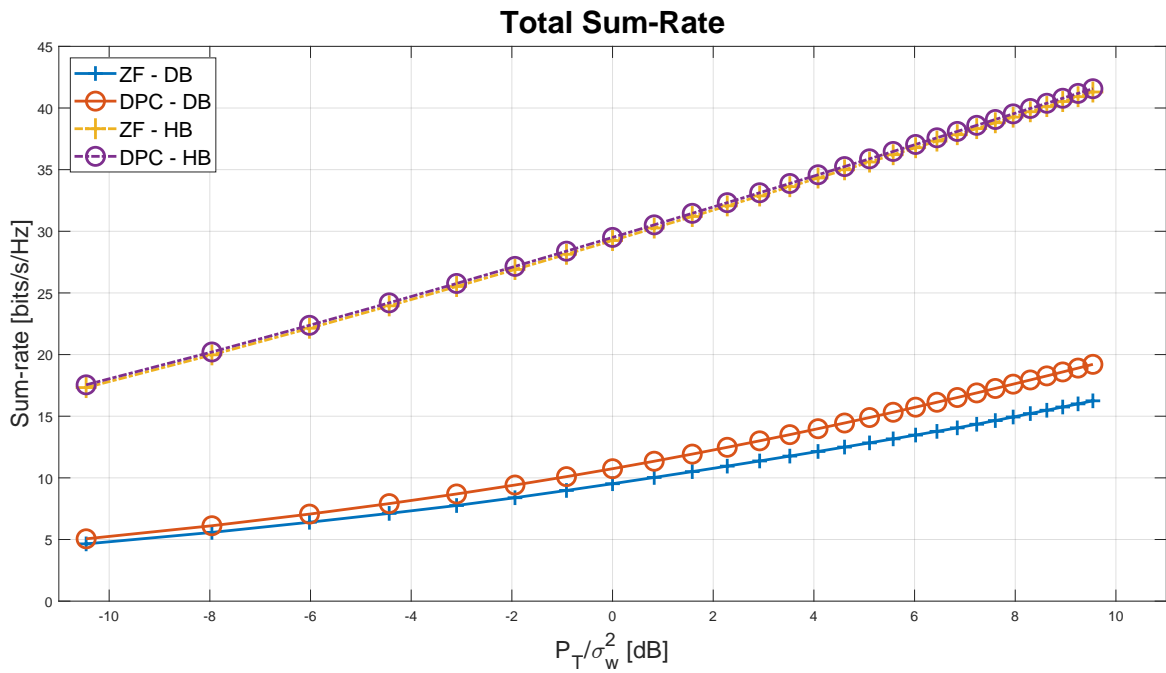


FIGURE 6.9: Comparison of the total achievable rate between digital and hybrid beamforming using ULA ( $N_t^{RF} = 8$ ,  $N_u = 100$ )

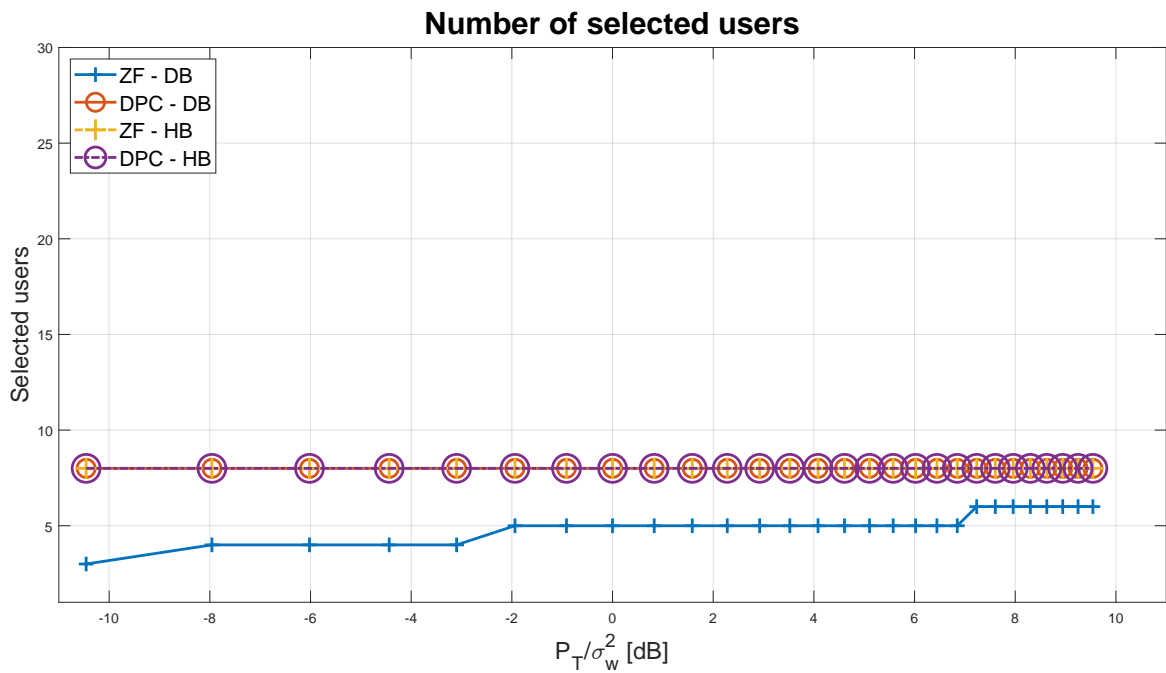


FIGURE 6.10: Comparison of the number of selected users between digital and hybrid beamforming using ULA ( $N_t^{RF} = 8$ ,  $N_u = 100$ )

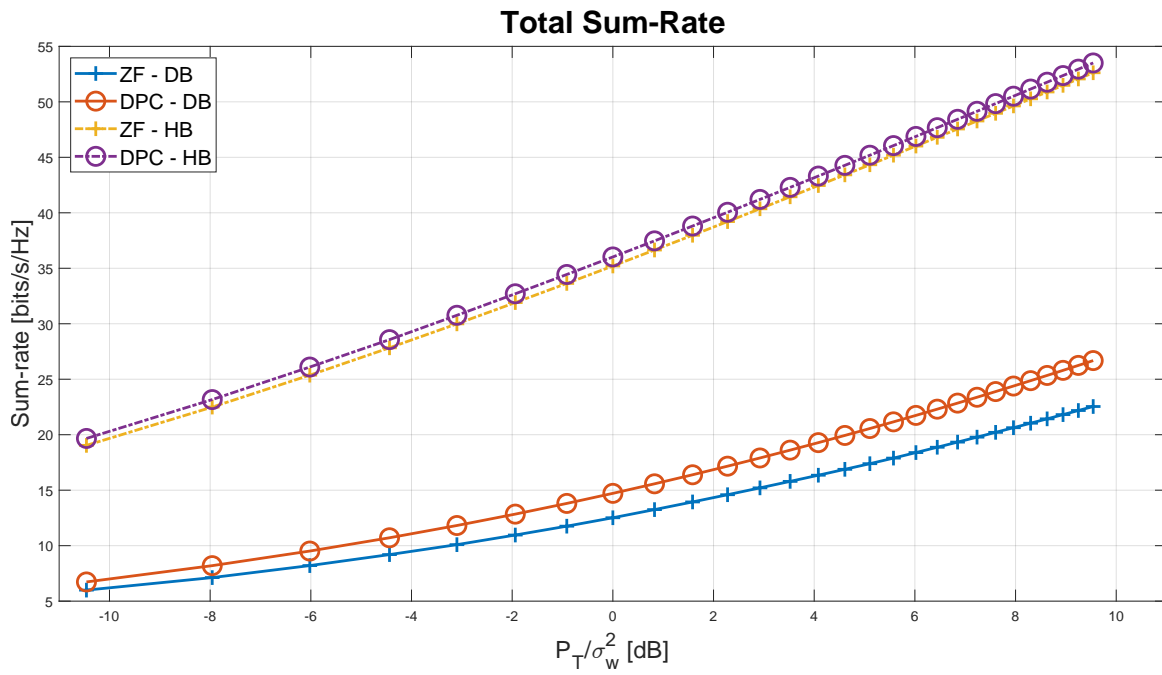


FIGURE 6.11: Comparison of the total achievable rate between digital and hybrid beamforming using ULA ( $N_t^{RF} = 12, N_u = 100$ )

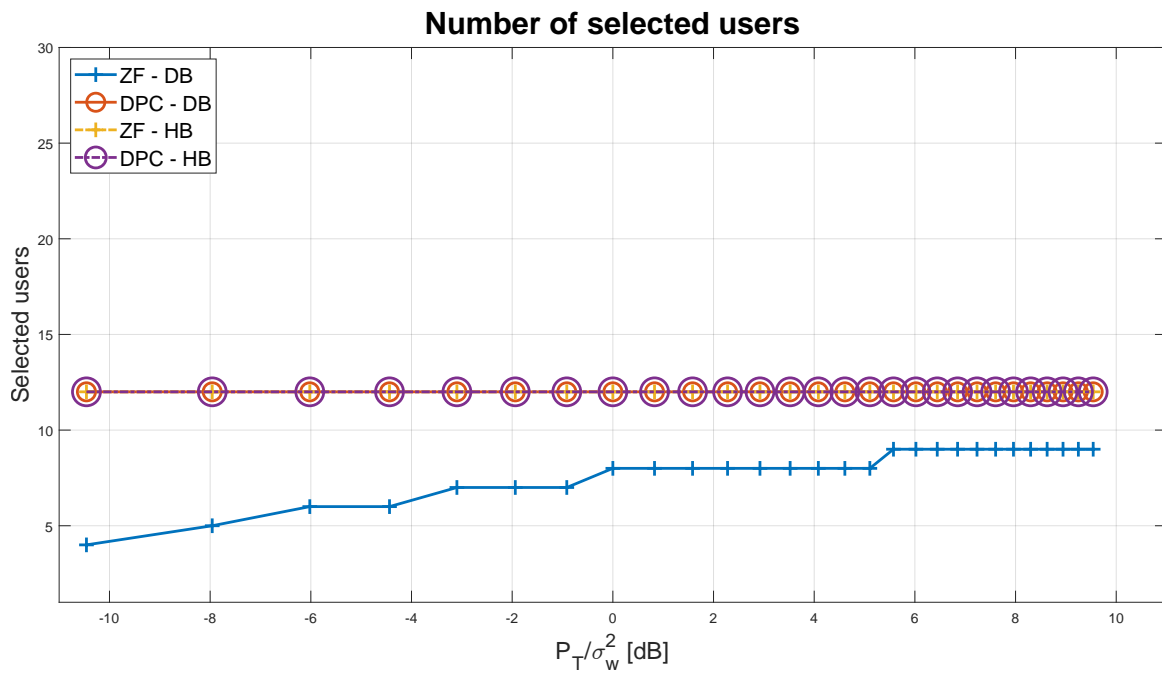


FIGURE 6.12: Comparison of the number of selected users between digital and hybrid beamforming using ULA ( $N_t^{RF} = 12, N_u = 100$ )

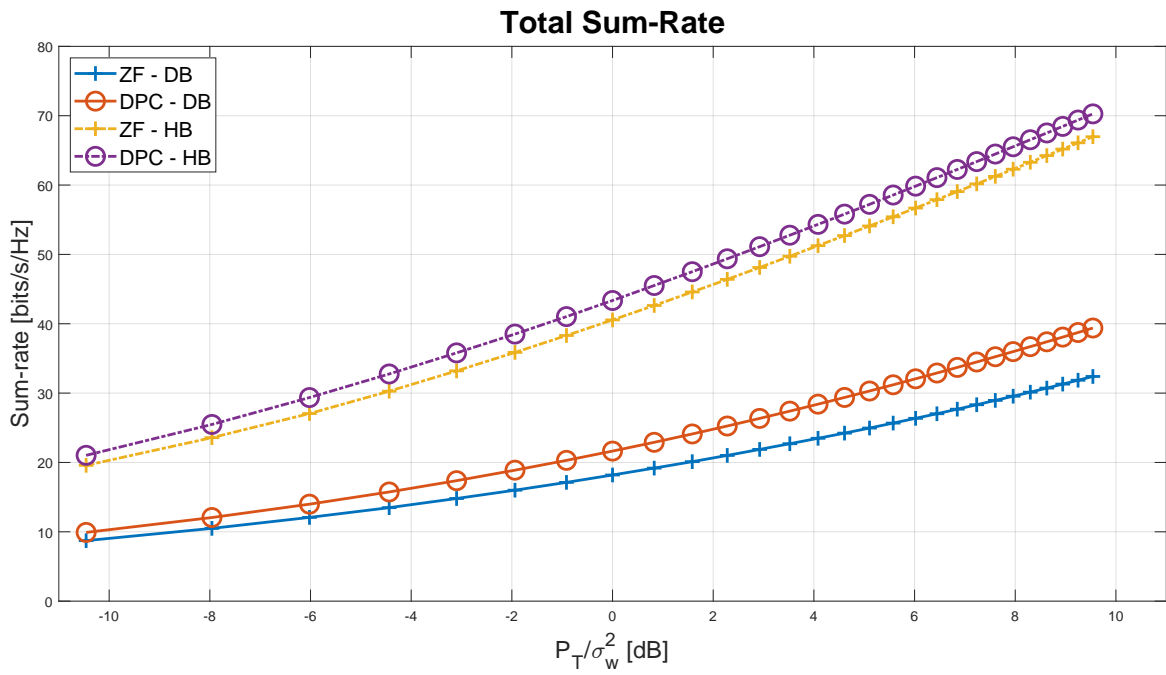


FIGURE 6.13: Comparison of the total achievable rate between digital and hybrid beamforming using ULA ( $N_t^{RF} = 20$ ,  $N_u = 100$ )

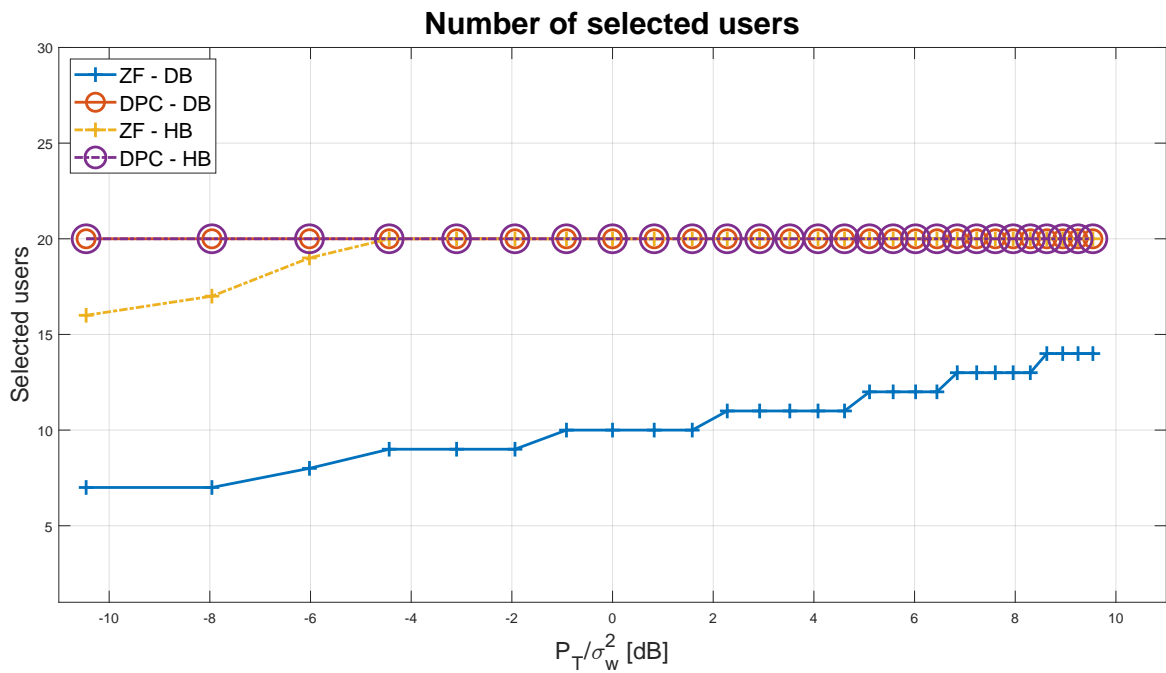


FIGURE 6.14: Comparison of the number of selected users between digital and hybrid beamforming using ULA ( $N_t^{RF} = 20$ ,  $N_u = 100$ )

## Chapter 7

# Conclusions and Future Developments

To make possible new applications, future wireless networks will need to transfer much greater amount of data at much higher speed. In this thesis, the problem of downlink transmission scheduling for MU-MIMO is investigated: multiple users need to receive data from a BS, thus this procedure is required to increase the total achievable rate.

By considering 5G wireless network, fully digital precoding scheme is not feasible because of the great amount of antenna exploited, hence, to limit the energy consumption, I studied the hybrid-beamforming architecture based on DPC.

From the results shown in Chapter 6 it is possible to observe that the algorithm proposed in 5.4 manages to provide a higher total sum-rate than the analogous algorithm based on ZF.

The difference in terms of performance is more significant when users are not uniformly distributed over  $360^\circ$  and when more RF chains are used.

This solution has low hardware-complexity since it is based on hybrid beamforming, thus a limited number of RF chains are employed.

The algorithm proposed has also low computation-complexity because the most critical task, for this problem, is the scheduling of users that has been solved using a greedy algorithm studied in [24].

Future developments are necessary for THz transmissions (6G), because communicate using this frequency band requires arrays of a much higher dimension to overcome the even stronger path loss compared to mmWave communications (5G).

Thus, because of the high dimensionality of the antenna arrays, in [28] a dynamic analog precoder is studied to design the hybrid beamforming.

Hence, instead of using a fully connected system (FC) (as in the mmWave) in which each RF chain is connected to each antenna, it seems more convenient to employ adaptive connections between RF chains and antennas, the so called dynamic array of subarray (DAoSA).

Moreover, as stated in [29], reducing the computational complexity of hybrid beamforming algorithms is an important direction for the future research.

Recently, in [15] a beamformer neural network (BFNN) has been proposed: it can be trained to learn how to optimize the beamformer for maximizing the spectral efficiency with hardware limitation.

Future developments could also address the problem of interaction between different layers of the protocol stack for the next generations of wireless networks. Indeed, future applications will be based on heterogeneous networks, thus the analysis of only the PHY layer does not lead to an optimal user experience.

The end-to-end performance analysis of the transmissions in a complex network is necessary and it depends in complex ways on the interactions of all the layers of the protocol stack, thus, to increase the overall quality of service (QoS), different protocols are required.

So far, most of the studies on the interaction between higher layers and the PHY layer for mmWave, consider the simpler case of analog beamforming, hence future studies can contemplate hybrid beamforming.

# Appendix A

## Review of Algebra

### A.1 Determinant properties

The determinant of a square matrix is a scalar value that is a function of the entries of the matrix.

For instance, the determinant of a  $2 \times 2$  matrix can be easily computed as:

$$\det \left( \begin{bmatrix} a & b \\ c & d \end{bmatrix} \right) = ad - cb$$

#### A.1.1 Basic properties

The determinant of the transpose of  $\mathbf{A}$  is equal to the determinant of  $\mathbf{A}$ :

$$\det(\mathbf{A}) = \det(\mathbf{A}^T) \quad (\text{A.1})$$

The determinant of the Hermitian transpose of  $\mathbf{A}$  is equal to the complex conjugated of the determinant of  $\mathbf{A}$ :

$$\det(\mathbf{A}^H) = \det(\mathbf{A})^* \quad (\text{A.2})$$

**Theorem A.1.1** (Binet's Theorem). *Let  $\mathbf{A}$  and  $\mathbf{B}$  be two square matrices, then the determinant of the product can be written as the product of the determinants:*

$$\det(\mathbf{AB}) = \det(\mathbf{A}) \det(\mathbf{B}) \quad (\text{A.3})$$

A square matrix is invertible if its determinant is not equal to 0, in this case the determinant of the inverse matrix can be written as:

$$\det(\mathbf{A}^{-1}) = \frac{1}{\det(\mathbf{A})} \quad (\text{A.4})$$

*Proof.* It follows from Binet's theorem:

$$\begin{aligned}\det(\mathbf{A}\mathbf{A}^{-1}) &= \det(\mathbf{I}) = 1 \\ &= \det(\mathbf{A}) \det(\mathbf{A}^{-1})\end{aligned}$$

thus,

$$\det(\mathbf{A}) = \frac{1}{\det(\mathbf{A}^{-1})}$$

□

The determinant is related to the eigenvalues of the matrix. Let  $\mathbf{A}$  be a  $N \times N$  square matrix with eigenvalues  $\lambda_1, \lambda_2, \dots, \lambda_k$  with algebraic multiplicity  $\mu_1, \mu_2, \dots, \mu_k$ , thus  $k \leq N$ . The case in which  $k = N$  happens when all the eigenvalues are different to each other, thus the multiplicity is equal to 1.

The determinant of  $\mathbf{A}$  can be computed as sum of the products of the eigenvalues by their algebraic multiplicity:

$$\det \mathbf{A} = \sum_{i=1}^k \lambda_i \mu_i \quad (\text{A.5})$$

## A.2 Trace properties

The trace of a  $n \times n$  square matrix  $\mathbf{A}$  is defined as:

$$\text{tr}(\mathbf{A}) = \sum_{i=1}^n a_{i,i} \quad (\text{A.6})$$

where  $a_{i,i}$  denotes the entry of the matrix in position  $(i, i)$

### A.2.1 Basic properties

It is a linear mapping:

$$\text{tr}(a\mathbf{A} + b\mathbf{B}) = a\text{tr}(\mathbf{A}) + b\text{tr}(\mathbf{B}) \quad (\text{A.7})$$

for all the square matrices  $\mathbf{A}$ ,  $\mathbf{B}$  and the scalars  $a$ ,  $b$ .

The transpose transformation is invariant for the trace, because the elements in the diagonal do not change:

$$\text{tr}(\mathbf{A}) = \text{tr}(\mathbf{A}^T) \quad (\text{A.8})$$



The trace of the Hermitian transpose of  $\mathbf{A}$  is equal to the complex conjugated of the trace of  $\mathbf{A}$ :

$$\text{tr}(\mathbf{A}^H) = \text{tr}(\mathbf{A})^* \quad (\text{A.9})$$

**Theorem A.2.1.** Let  $\mathbf{A}$  be a  $M \times N$  matrix and  $\mathbf{B}$  be a  $N \times M$  matrix, then:

$$\text{tr}(\mathbf{AB}) = \text{tr}(\mathbf{BA}) \quad (\text{A.10})$$

*Proof.*

$$\begin{aligned} \text{tr}(\mathbf{AB}) &= \sum_{m=1}^M (\mathbf{AB})_{m,m} \\ &= \sum_{m=1}^M \sum_{n=1}^N A_{m,n} B_{n,m} \\ &= \sum_{n=1}^N \sum_{m=1}^M B_{n,m} A_{m,n} \\ &= \sum_{n=1}^N (\mathbf{BA})_{n,n} \\ &= \text{tr}(\mathbf{BA}) \end{aligned}$$

□

In general, it can be shown that the trace is invariant under cyclic permutations:

$$\text{tr}(\mathbf{ABCD}) = \text{tr}(\mathbf{BCDA}) = \text{tr}(\mathbf{CDAB}) = \text{tr}(\mathbf{DABC}) \quad (\text{A.11})$$



# Bibliography

- [1] Mustafa Riza Akdeniz et al. “Millimeter Wave Channel Modeling and Cellular Capacity Evaluation”. In: *IEEE Journal on Selected Areas in Communications* 32.6 (2014), pp. 1164–1179. DOI: [10.1109/JSAC.2014.2328154](https://doi.org/10.1109/JSAC.2014.2328154).
- [2] Omar El Ayach et al. “Spatially Sparse Precoding in Millimeter Wave MIMO Systems”. In: *IEEE Transactions on Wireless Communications* 13.3 (2014), pp. 1499–1513. DOI: [10.1109/TWC.2014.011714.130846](https://doi.org/10.1109/TWC.2014.011714.130846).
- [3] Mingming Cai. “Modeling and Mitigating Beam Squint in Millimeter Wave Wireless Communication”. PhD thesis. University of Notre Dame, Mar. 2018.
- [4] G. Caire and S. Shamai. “On the achievable throughput of a multiantenna Gaussian broadcast channel”. In: *IEEE Transactions on Information Theory* 49.7 (2003), pp. 1691–1706. DOI: [10.1109/TIT.2003.813523](https://doi.org/10.1109/TIT.2003.813523).
- [5] Yong Soo Cho et al. “MultiUser MIMO”. In: *MIMO-OFDM Wireless Communications with MATLAB®*. 2010, pp. 395–417. DOI: [10.1002/9780470825631.ch13](https://doi.org/10.1002/9780470825631.ch13).
- [6] M. Costa. “Writing on dirty paper (Corresp.)” In: *IEEE Transactions on Information Theory* 29.3 (1983), pp. 439–441. DOI: [10.1109/TIT.1983.1056659](https://doi.org/10.1109/TIT.1983.1056659).
- [7] G. Dimic and N.D. Sidiropoulos. “On downlink beamforming with greedy user selection: performance analysis and a simple new algorithm”. In: *IEEE Transactions on Signal Processing* 53.10 (2005), pp. 3857–3868. DOI: [10.1109/TSP.2005.855401](https://doi.org/10.1109/TSP.2005.855401).
- [8] U. Erez, S. Shamai, and R. Zamir. “Capacity and lattice strategies for canceling known interference”. In: *IEEE Transactions on Information Theory* 51.11 (2005), pp. 3820–3833. DOI: [10.1109/TIT.2005.856935](https://doi.org/10.1109/TIT.2005.856935).
- [9] Ericsson. “Ericsson Mobility Report”. In: (Nov. 2020). URL: <https://www.ericsson.com/4adc87/assets/local/mobility-report/documents/2020-november-2020-ericsson-mobility-report.pdf>.
- [10] A. Goldsmith. “Capacity of Wireless Channels”. In: *Wireless Communications*. 2005, pp. 99–125. DOI: [10.1017/CB09780511841224.005](https://doi.org/10.1017/CB09780511841224.005).

- [11] Simon Haykin and K. J. Ray Liu. "Wireless Communication and Sensing in Multipath Environments Using Multiantenna Transceivers". In: *Handbook on Array Processing and Sensor Networks*. 2009, pp. 115–170. DOI: [10.1002/9780470487068.ch5](https://doi.org/10.1002/9780470487068.ch5).
- [12] Robert W. Heath et al. "An Overview of Signal Processing Techniques for Millimeter Wave MIMO Systems". In: *IEEE Journal of Selected Topics in Signal Processing* 10.3 (2016), pp. 436–453. DOI: [10.1109/JSTSP.2016.2523924](https://doi.org/10.1109/JSTSP.2016.2523924).
- [13] N. Jindal, S. Vishwanath, and A. Goldsmith. "On the duality of Gaussian multiple-access and broadcast channels". In: *IEEE Transactions on Information Theory* 50.5 (2004), pp. 768–783. DOI: [10.1109/TIT.2004.826646](https://doi.org/10.1109/TIT.2004.826646).
- [14] Jhe-Yi Lin et al. "Low Complexity Hybrid Precoder Design for mmWave Multi-User MIMO Systems: A Non-Iterative Approach". In: (2019), pp. 1–7. DOI: [10.1109/VTCFall.2019.8891355](https://doi.org/10.1109/VTCFall.2019.8891355).
- [15] Tian Lin and Yu Zhu. "Beamforming Design for Large-Scale Antenna Arrays Using Deep Learning". In: *CoRR abs/1904.03657* (2019). arXiv: [1904.03657](https://arxiv.org/abs/1904.03657). URL: <http://arxiv.org/abs/1904.03657>.
- [16] Yuan-Pei Lin. "On the Quantization of Phase Shifters for Hybrid Precoding Systems". In: *IEEE Transactions on Signal Processing* 65.9 (2017), pp. 2237–2246. DOI: [10.1109/TSP.2016.2646659](https://doi.org/10.1109/TSP.2016.2646659).
- [17] G. R. Mohammad-Khani, S. Lasaulce, and J Dumont. "About the Performance of Practical Dirty Paper Coding Schemes in Gaussian MIMO Broadcast Channels". In: (2006), pp. 1–5. DOI: [10.1109/SPAWC.2006.346428](https://doi.org/10.1109/SPAWC.2006.346428).
- [18] C.B. Peel. "On "Dirty-Paper coding"". In: *IEEE Signal Processing Magazine* 20.3 (2003), pp. 112–113. DOI: [10.1109/MSP.2003.1203214](https://doi.org/10.1109/MSP.2003.1203214).
- [19] Zhao Qingling and Jin Li. "Rain Attenuation in Millimeter Wave Ranges". In: *2006 7th International Symposium on Antennas, Propagation EM Theory*. 2006, pp. 1–4. DOI: [10.1109/ISAPE.2006.353538](https://doi.org/10.1109/ISAPE.2006.353538).
- [20] Sundeep Rangan, Theodore S. Rappaport, and Elza Erkip. "Millimeter-Wave Cellular Wireless Networks: Potentials and Challenges". In: *Proceedings of the IEEE* 102.3 (2014), pp. 366–385. DOI: [10.1109/JPROC.2014.2299397](https://doi.org/10.1109/JPROC.2014.2299397).
- [21] Theodore S. Rappaport et al. "Wireless Communications and Applications Above 100 GHz: Opportunities and Challenges for 6G and Beyond". In: *IEEE Access* 7 (2019), pp. 78729–78757. DOI: [10.1109/ACCESS.2019.2921522](https://doi.org/10.1109/ACCESS.2019.2921522).
- [22] H. Sato. "An outer bound to the capacity region of broadcast channels (Corresp.)" In: *IEEE Transactions on Information Theory* 24.3 (1978), pp. 374–377. DOI: [10.1109/TIT.1978.1055883](https://doi.org/10.1109/TIT.1978.1055883).

- [23] Q.H. Spencer et al. "An introduction to the multi-user MIMO downlink". In: *IEEE Communications Magazine* 42.10 (2004), pp. 60–67. DOI: [10.1109/MCOM.2004.1341262](https://doi.org/10.1109/MCOM.2004.1341262).
- [24] Zhenyu Tu and R.S. Blum. "Multiuser diversity for a dirty paper approach". In: *IEEE Communications Letters* 7.8 (2003), pp. 370–372. DOI: [10.1109/LCOMM.2003.815652](https://doi.org/10.1109/LCOMM.2003.815652).
- [25] P. Viswanath and D.N.C. Tse. "Sum capacity of the vector Gaussian broadcast channel and uplink–downlink duality". In: *IEEE Transactions on Information Theory* 49.8 (2003), pp. 1912–1921. DOI: [10.1109/TIT.2003.814483](https://doi.org/10.1109/TIT.2003.814483).
- [26] Cheng-Xiang Wang et al. "Cellular architecture and key technologies for 5G wireless communication networks". In: *IEEE Communications Magazine* 52.2 (2014), pp. 122–130. DOI: [10.1109/MCOM.2014.6736752](https://doi.org/10.1109/MCOM.2014.6736752).
- [27] Gary A. Thiele Warren L. Stutzman. "Antenna Theory and Design". In: (2012).
- [28] Longfei Yan, Chong Han, and Jinhong Yuan. "A Dynamic Array of Sub-Array Architecture for Hybrid Precoding in the Millimeter Wave and Terahertz Bands". In: *2019 IEEE International Conference on Communications Workshops (ICC Workshops)*. 2019, pp. 1–5. DOI: [10.1109/ICCW.2019.8756936](https://doi.org/10.1109/ICCW.2019.8756936).
- [29] Jun Zhang, Xianghao Yu, and Khaled B. Letaief. "Hybrid Beamforming for 5G and Beyond Millimeter-Wave Systems: A Holistic View". In: *IEEE Open Journal of the Communications Society* 1 (2020), pp. 77–91. DOI: [10.1109/OJCOMS.2019.2959595](https://doi.org/10.1109/OJCOMS.2019.2959595).